ALICE Status Report

Alexander Kalweit, CERN
on behalf of the ALICE collaboration

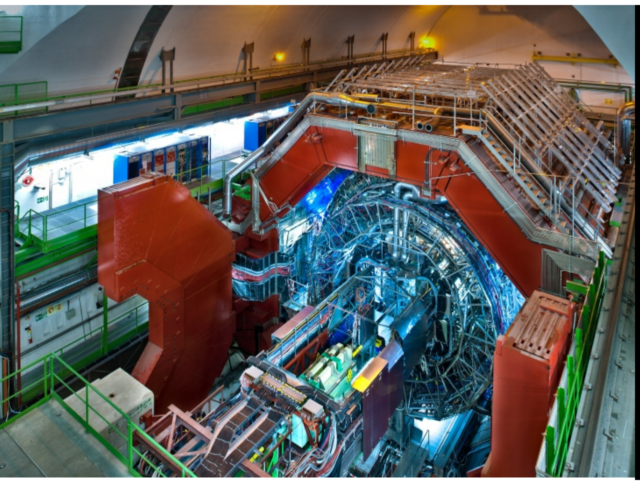
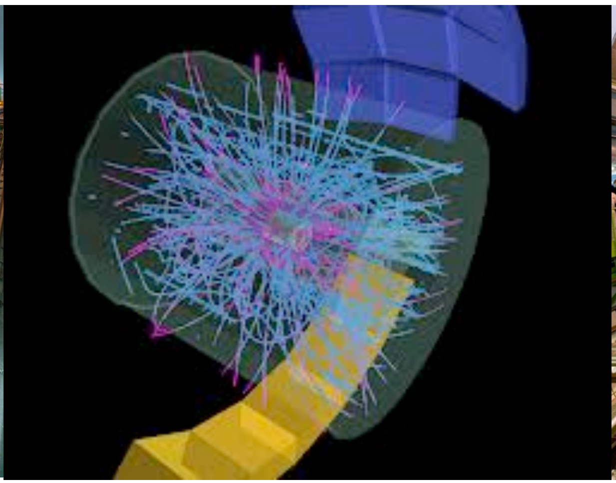


ALICE

CERN

Outline

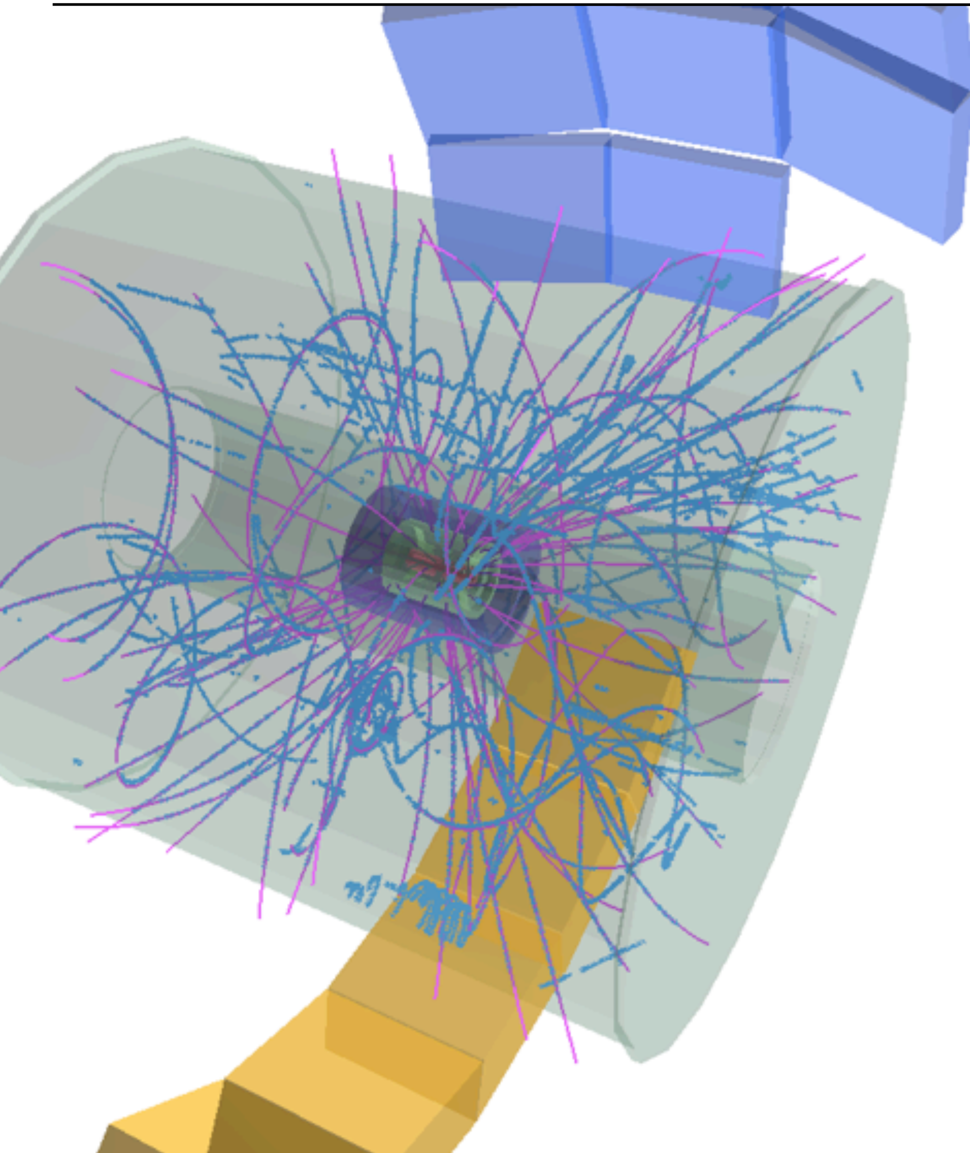

(A.) New Physics Results

(B.) Detector Status (LS1 Activities)

(C.) Short Summary of Upgrade

Recently submitted publications

Recently submitted:

- “Multi-strange baryon production at mid-rapidity in Pb-Pb collisions at $\sqrt{s_{NN}}$ = 2.76 TeV”, **arXiv:1307.5543**
- “K^0_S and Λ production in Pb-Pb collisions at $\sqrt{s_{NN}}$ = 2.76 TeV”, **arXiv:1307.5530**
- “Multiplicity dependence of the average transverse momentum in pp, p-Pb, and Pb-Pb collisions at the LHC”, **arXiv:1307.1094**
- “Multiplicity dependence of $\pi^\pm$, $K^\pm$, K^0_S, p, and Λ in p-Pb collisions at $\sqrt{s_{NN}}$ = 5.02 TeV”, **arXiv:1307.6796**
- “J/ψ production and nuclear effects in p-Pb collisions at $\sqrt{s_{NN}}$ = 5.02 TeV”, **arXiv:1308.6726**
- “Energy dependence of the Transverse Momentum Distributions of Charged Particles in pp Collisions with ALICE”, **arXiv:1307.1093**
- “Directed flow of charged particles at midrapidity relative to the spectator plane in Pb-Pb collisions at $\sqrt{s_{NN}}$ = 2.76 TeV”, **arXiv:1306.4145**
- “Long-range angular correlations of π, K, and p in p-Pb collisions at $\sqrt{s_{NN}}$ = 5.02 TeV”, **arXiv:1307.3237**

Recently published papers

Recently published:

- "D-meson elliptic flow in non-central Pb-Pb collisions at $\sqrt{s_{NN}}$ = 5.02 TeV",
  PRL 111, 102301 (2013)

- "Mid-rapidity anti-baryon to baryon ratios in pp collisions at $\sqrt{s_{NN}}$ = 0.9, 2.76 and 7 TeV measured by ALICE",
  EPJC (2013) 73:2496

- "Measurement of inelastic, single and double diffraction cross sections in pp collisions at the LHC with ALICE",
  EPJC (2013) 73:2456

- "Multiplicity dependence of two-particle azimuthal correlations in pp collisions at the LHC",
  JHEP 09 (2013) 049

ALICE contributions to summer conferences

HEP 2013
Stockholm
18-24 July 2013
(info@eps-hep2013.eu)

13 Parallel talks
1 Plenary talk

http://www.eps-hep2013.eu

IS2013

Special focus on pA collisions.

9 Parallel talks
10 Plenary talks

http://igfae.usc.es/is2013/

BIRMINGHAM SQM 2013

27 Parallel talks
6 Plenary talks

http://www.ep.ph.bham.ac.uk/SQM2013/

New Physics Results
(since last LHCC)

Global event properties: ⟨p_T⟩ vs. multiplicity

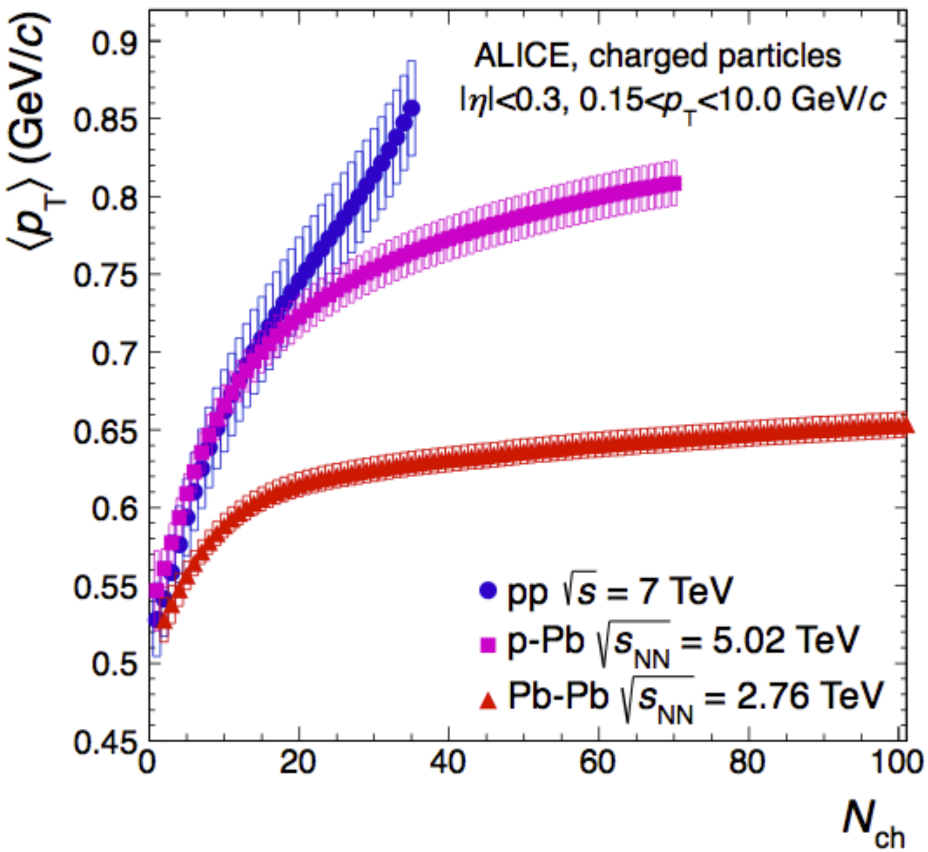

arXiv: 1307.1094

Global event properties: $\langle p_T \rangle$ vs. multiplicity

Much stronger increase in pp and p-Pb collisions than in PbPb.

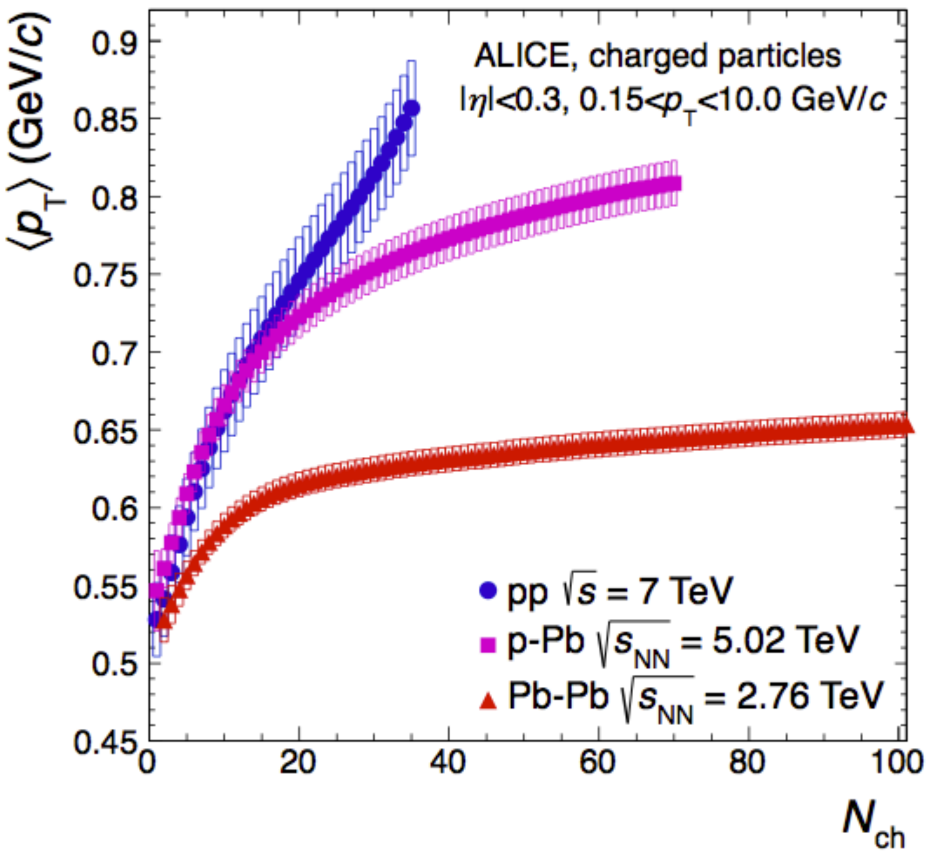

arXiv: 1307.1094

Global event properties: ⟨p_T⟩ vs. multiplicity

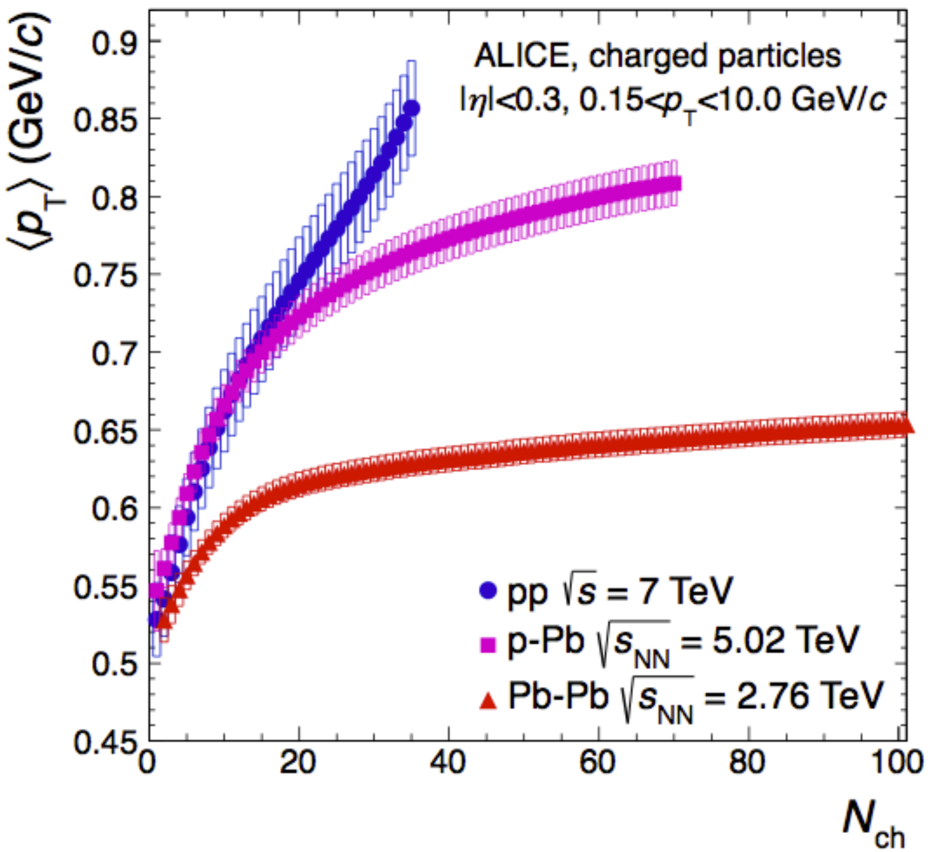

arXiv: 1307.1094

Much stronger increase in pp and p-Pb collisions than in PbPb.

pp and p-Pb follow the same trend up to N_{ch}≈15 (90% of pp and 50% of p-Pb x-section).

Global event properties: ⟨p_T⟩ vs. multiplicity

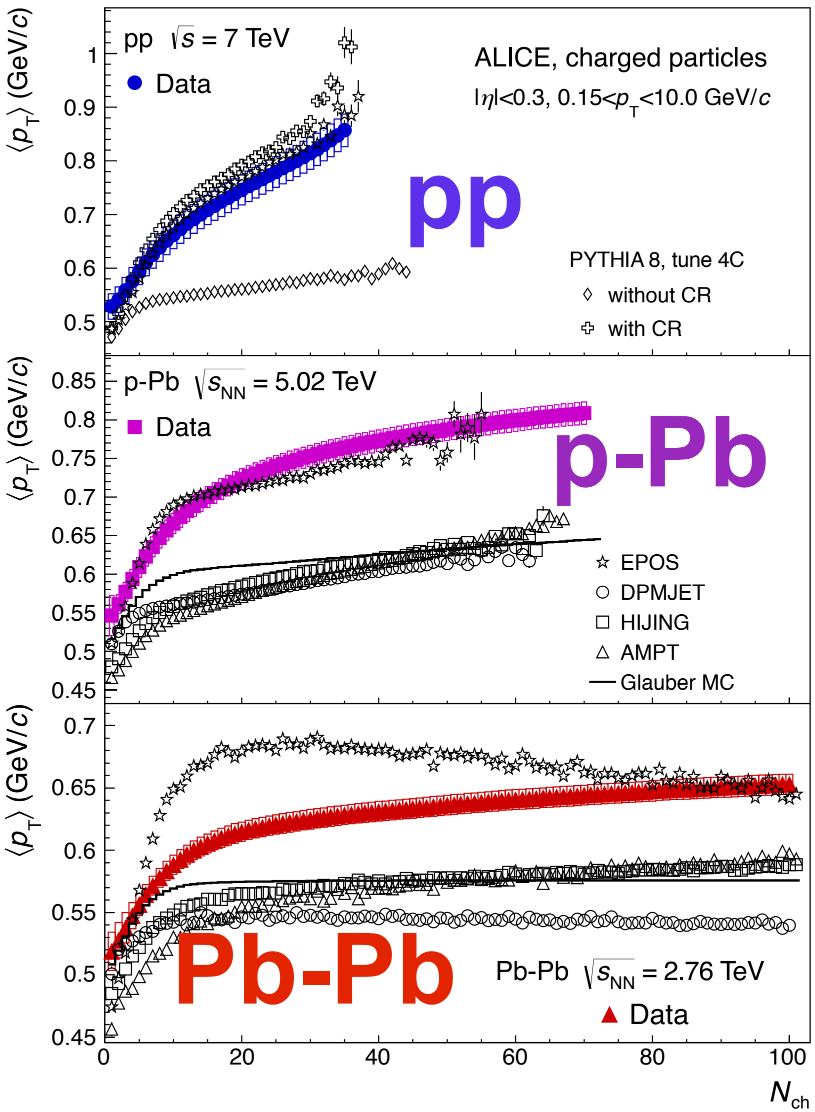

Much stronger increase in pp and p-Pb collisions than in PbPb.

pp and p-Pb follow the same trend up to N_{ch}≈15 (90% of pp and 50% of p-Pb x-section).

Global event properties: ⟨p_T⟩ vs. multiplicity

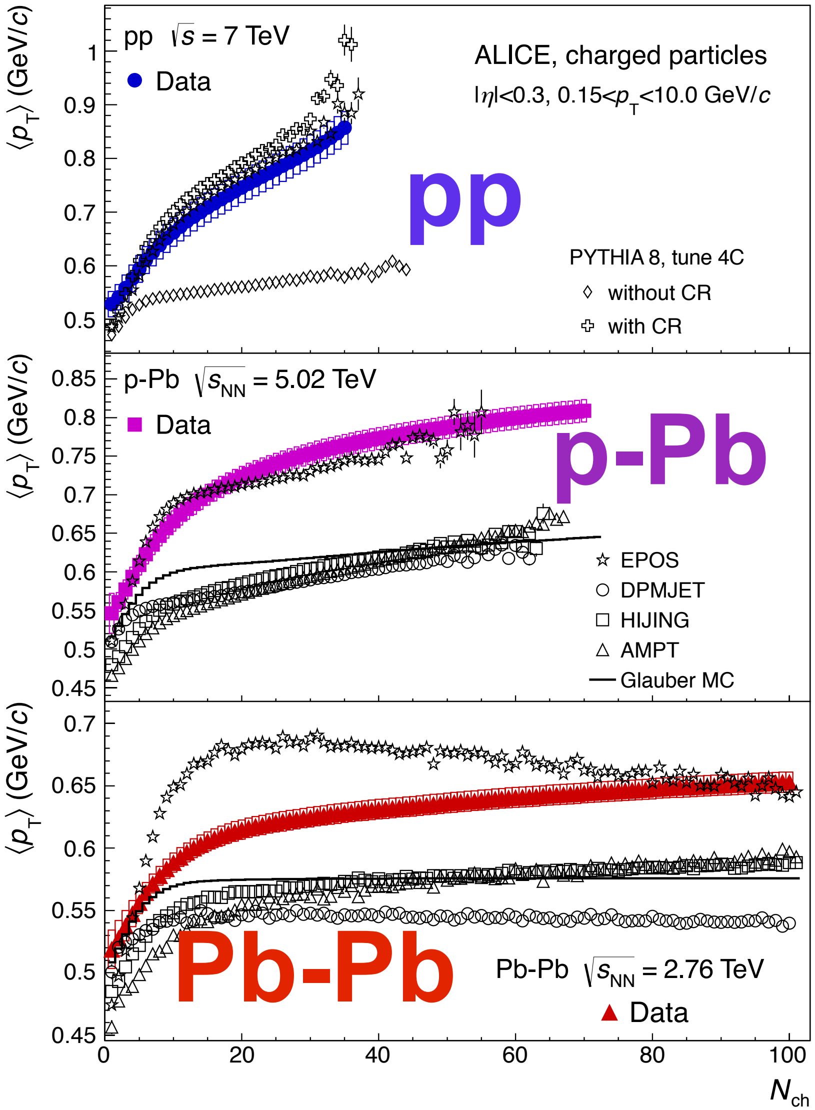

Much stronger increase in pp and p-Pb collisions than in PbPb.

pp and p-Pb follow the same trend up to N_{ch}≈15 (90% of pp and 50% of p-Pb x-section).

pp: strong increase can be attributed to color reconnections.

Global event properties: $\langle p_T \rangle$ vs. multiplicity

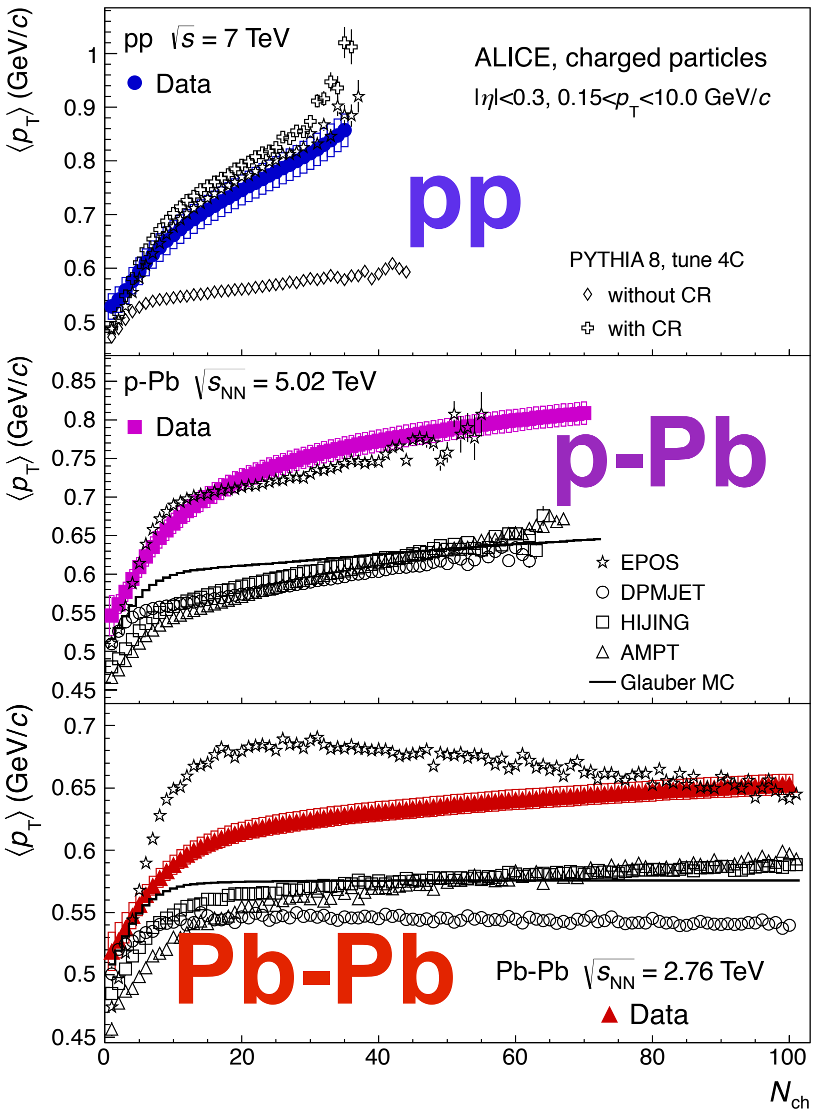

Much stronger increase in pp and p-Pb collisions than in PbPb.

pp and p-Pb follow the same trend up to $N_{ch}\approx15$ (90% of pp and 50% of p-Pb x-section).

pp: strong increase can be attributed to color reconnections.

p-Pb: superposition of *incoherent* p-N collisions (Glauber MC) does not explain the data. Coherent effects acting on strings from different p-N collisions?

Global event properties: ⟨p_T⟩ vs. multiplicity

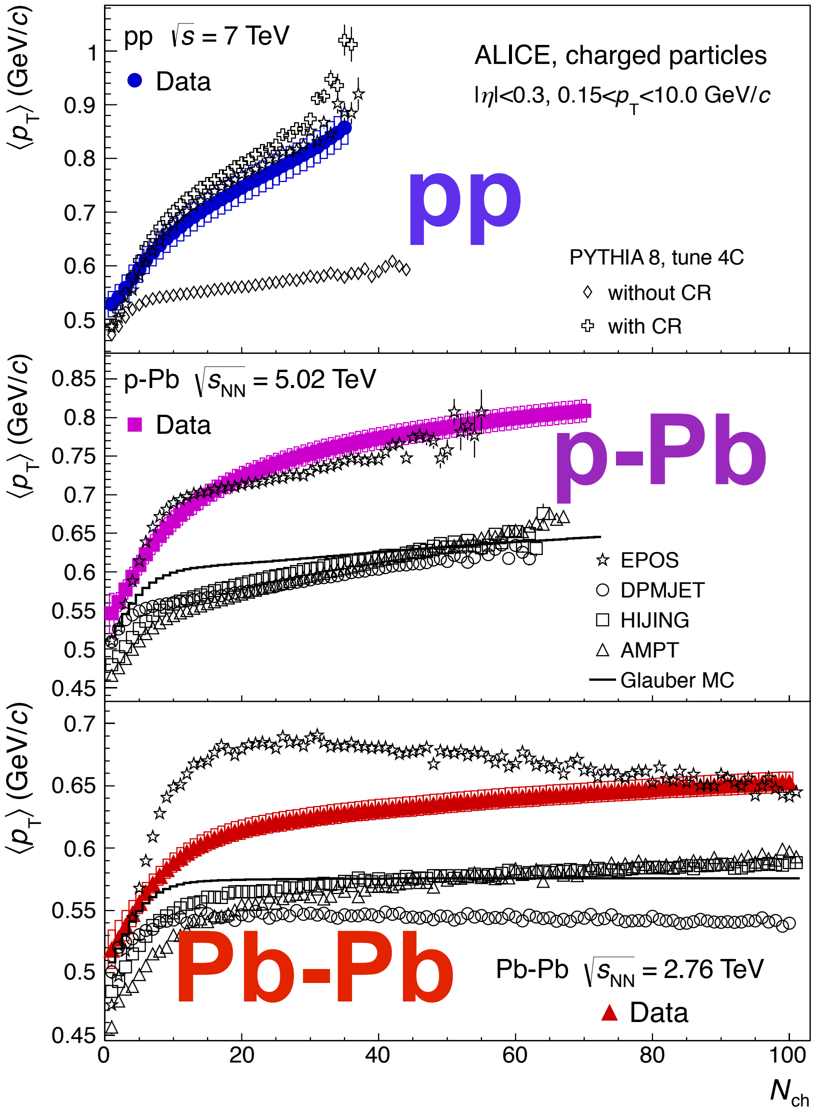

Much stronger increase in pp and p-Pb collisions than in PbPb.

pp and p-Pb follow the same trend up to N_{ch}≈15 (90% of pp and 50% of p-Pb x-section).

pp: strong increase can be attributed to color reconnections.

p-Pb: superposition of *incoherent* p-N collisions (Glauber MC) does not explain the data. Coherent effects acting on strings from different p-N collisions?

EPOS includes collective effects (hydrodynamic model).

Global event properties: ⟨p_T⟩ vs. multiplicity

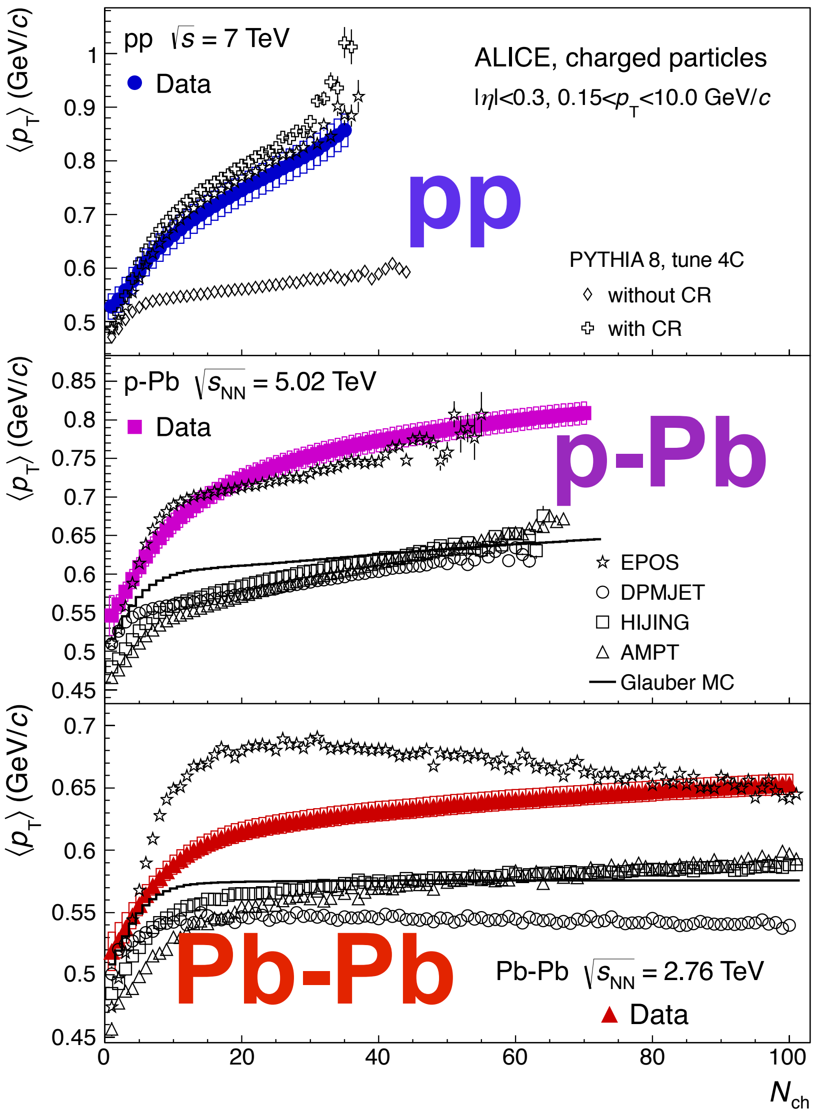

Much stronger increase in pp and p-Pb collisions than in PbPb.

pp and p-Pb follow the same trend up to N_{ch}≈15 (90% of pp and 50% of p-Pb x-section).

pp: strong increase can be attributed to color reconnections.

p-Pb: superposition of *incoherent* p-N collisions (Glauber MC) does not explain the data. Coherent effects acting on strings from different p-N collisions?

EPOS includes collective effects (hydrodynamic model).

Pb-Pb: DPMJET, AMPT describe trend correctly. EPOS shows different shape in peripheral collisions

Identified particles: p-Pb and Pb-Pb

How can we better differentiate if collective effects are present in a system?

➔ Hydrodynamic flow typically exhibits a characteristic mass ordering ($p = \beta_f \gamma_f \cdot m$).

➔ We look at identified particles.

Identified particles: p-Pb and Pb-Pb

How can we better differentiate if collective effects are present in a system?

➔ Hydrodynamic flow typically exhibits a characteristic mass ordering ($p = \beta_f \gamma_f \cdot m$).

➔ We look at identified particles.

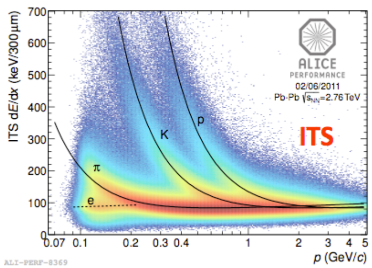

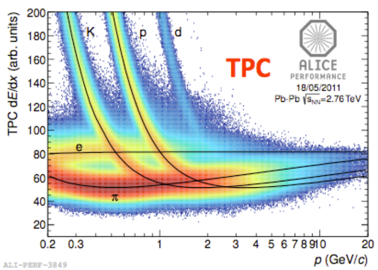

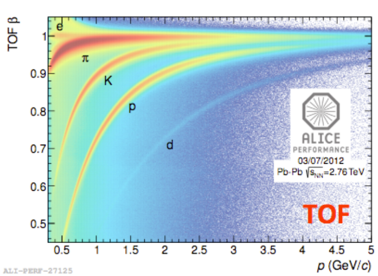

Identified particles: p-Pb and Pb-Pb

How can we better differentiate if collective effects are present in a system?

➔ Hydrodynamic flow typically exhibits a characteristic mass ordering ($p = \beta_f \gamma_f \cdot m$).

➔ We look at identified particles.

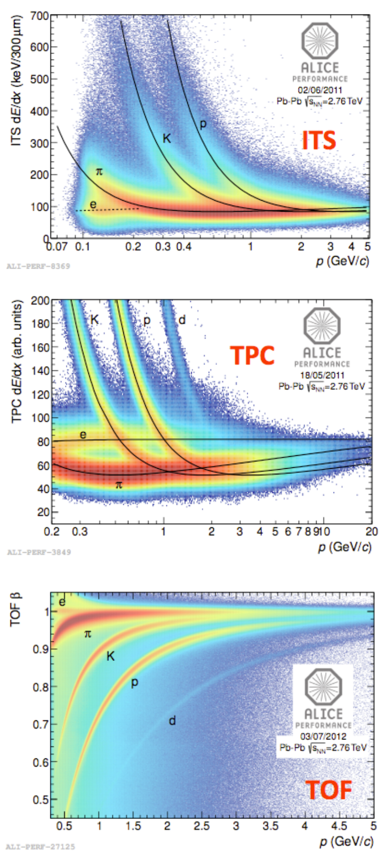

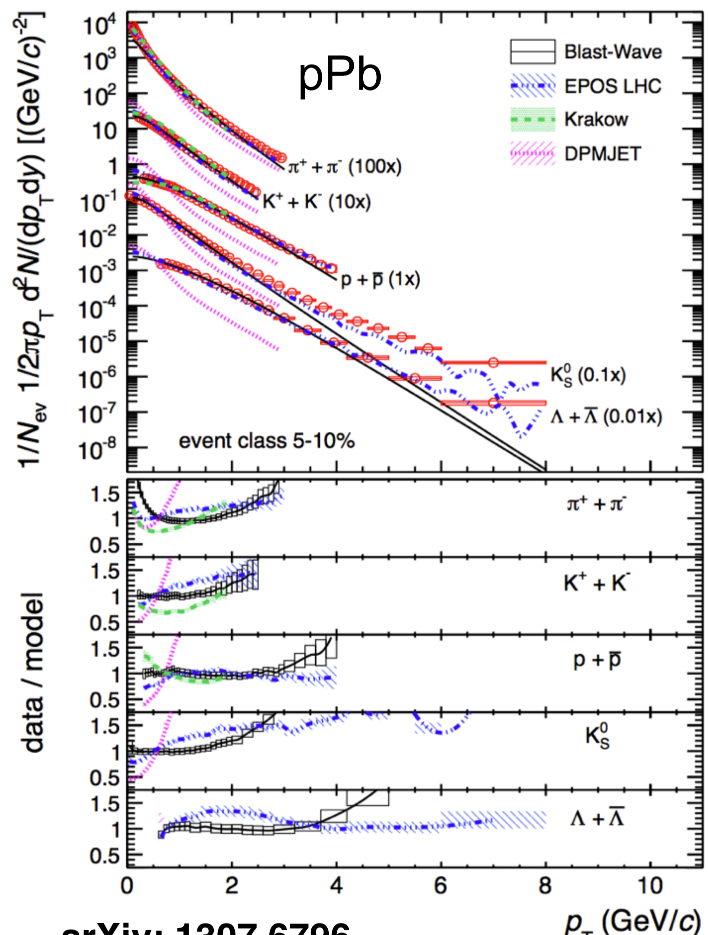

arXiv: 1307.6796

Identified particles: p-Pb and Pb-Pb

How can we better differentiate if collective effects are present in a system?

➔ Hydrodynamic flow typically exhibits a characteristic mass ordering ($p = \beta_f \gamma_f \cdot m$).

➔ We look at identified particles.

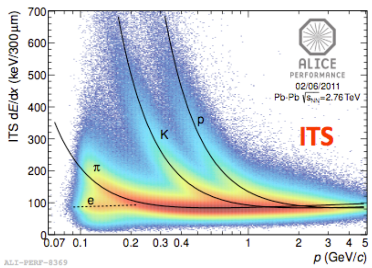

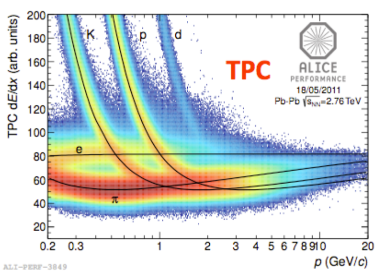

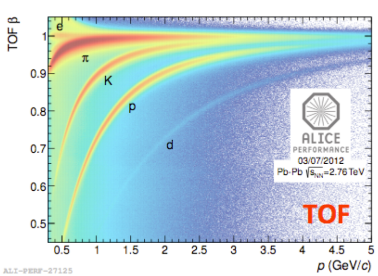

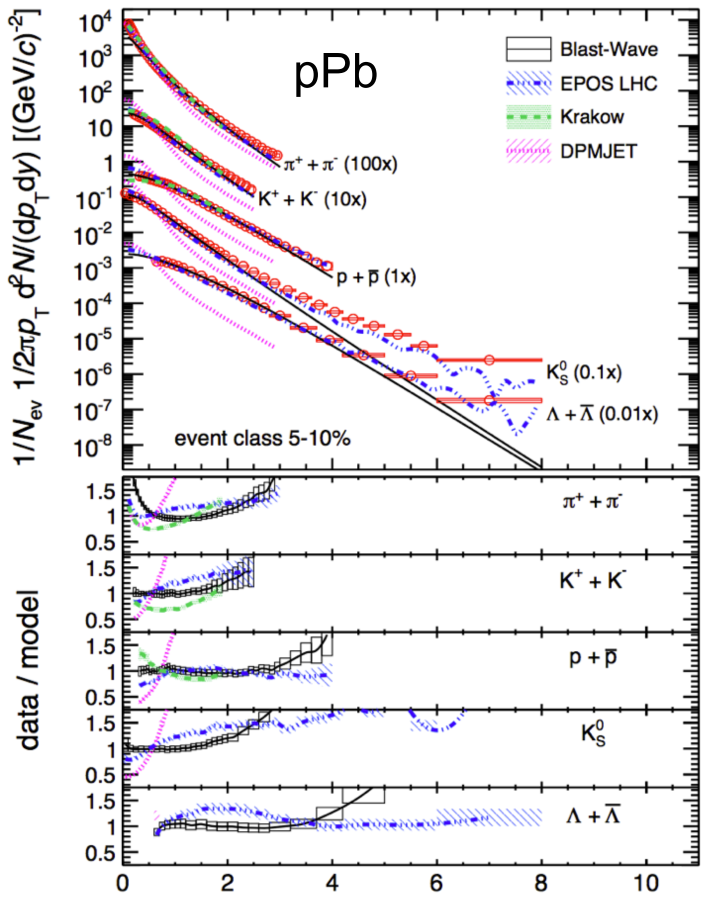

arXiv: 1307.6796

QCD inspired models (DPMJET) cannot describe the data.

Identified particles: p-Pb and Pb-Pb

How can we better differentiate if collective effects are present in a system?

➔ Hydrodynamic flow typically exhibits a characteristic mass ordering ($p = \beta_f \gamma_f \cdot m$).

➔ We look at identified particles.

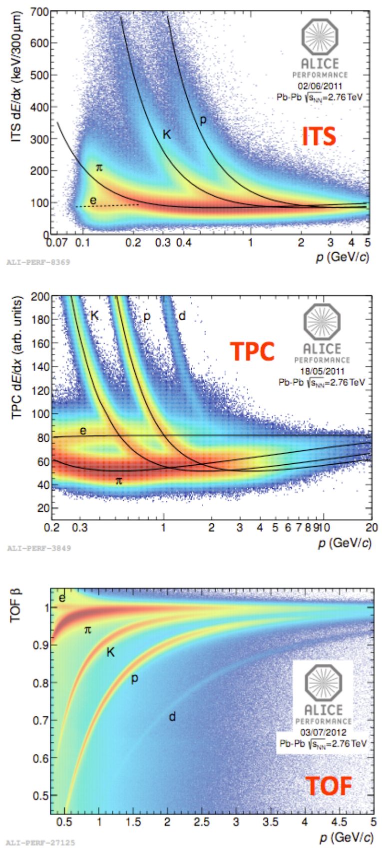

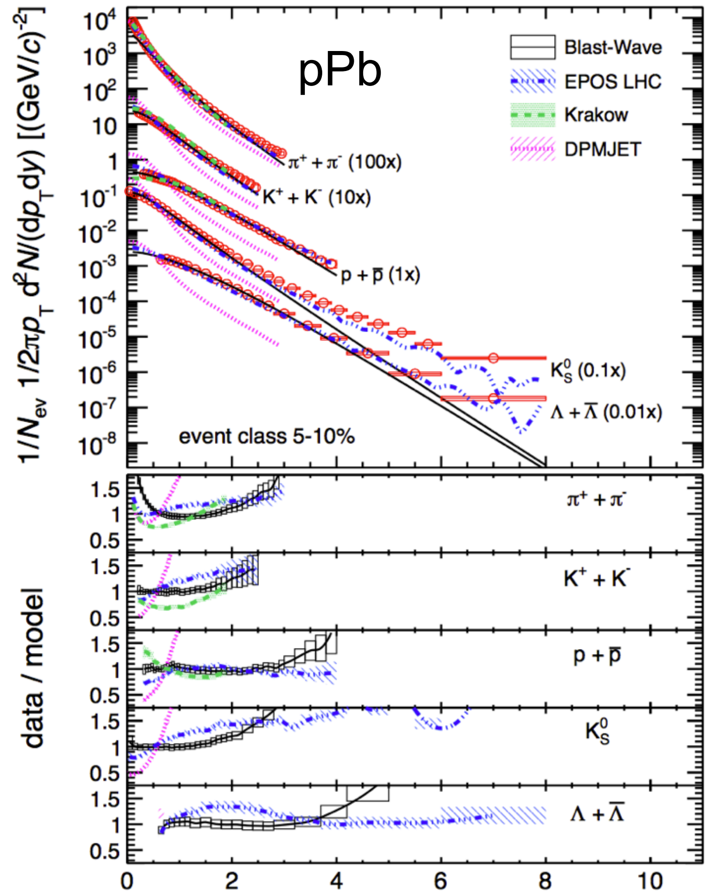

arXiv: 1307.6796

QCD inspired models (DPMJET) cannot describe the data.

Hydrodynamic models (EPOS, Krakow) show a better agreement.

Identified particles: p-Pb and Pb-Pb

How can we better differentiate if collective effects are present in a system?

➔ Hydrodynamic flow typically exhibits a characteristic mass ordering ($p = \beta_f \gamma_f \cdot m$).

➔ We look at identified particles.

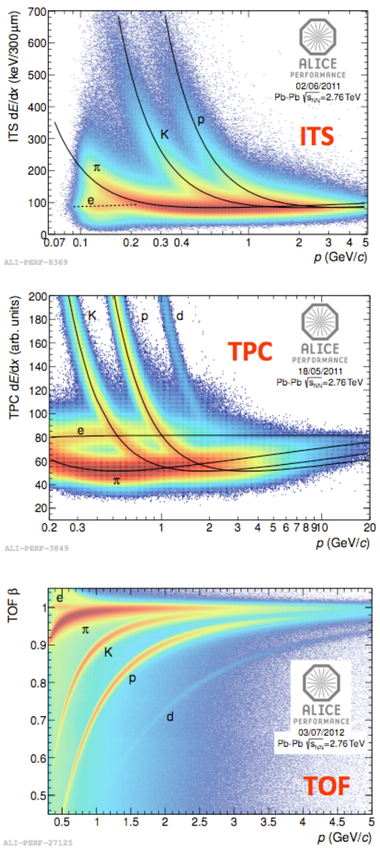

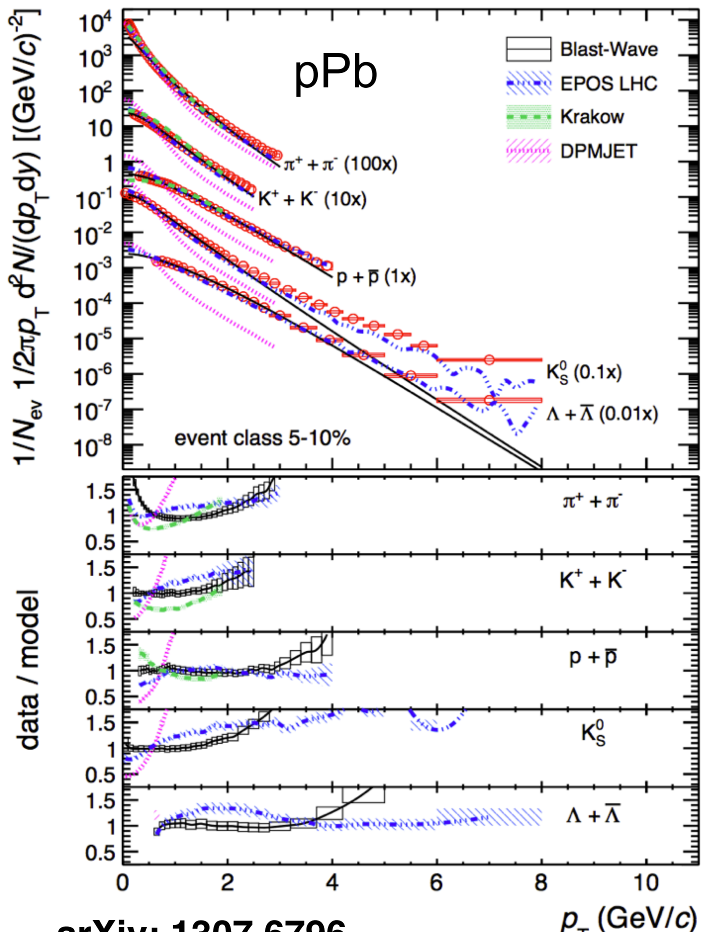

arXiv: 1307.6796

QCD inspired models (DPMJET) cannot describe the data.

Hydrodynamic models (EPOS, Krakow) show a better agreement.

A combined blast-wave fit to the data (simplified hydro model) gives a reasonable description.

Systematic blast-wave study: pp, p-Pb, Pb-Pb

- The hydro-motivated blast-wave parametrization assumes a locally thermalized medium, expanding collectively with a common velocity field β and an instantaneous common freeze-out at a temperature T_{kin}.
- Systematic description of spectral shape with two fit parameters as a function centrality/multiplicity.

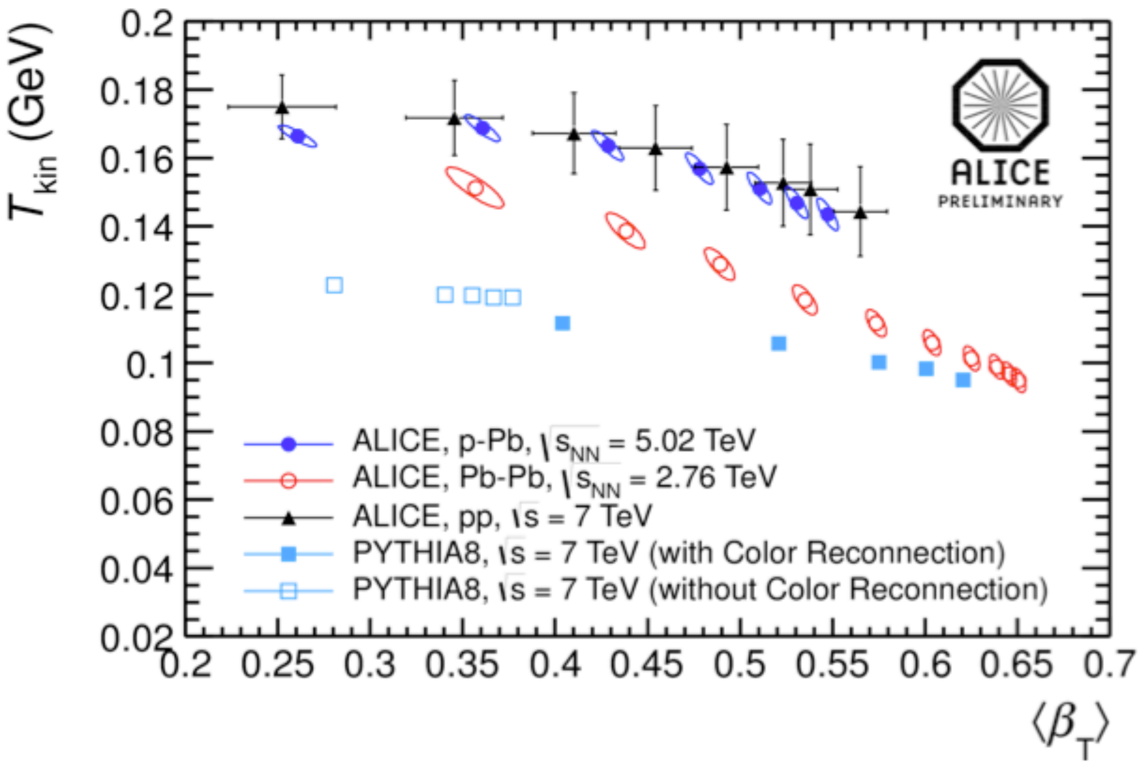

Systematic blast-wave study: pp, p-Pb, Pb-Pb

- The hydro-motivated blast-wave parametrization assumes a locally thermalized medium, expanding collectively with a common velocity field β and an instantaneous common freeze-out at a temperature T_{kin}.
- Systematic description of spectral shape with two fit parameters as a function centrality/multiplicity.

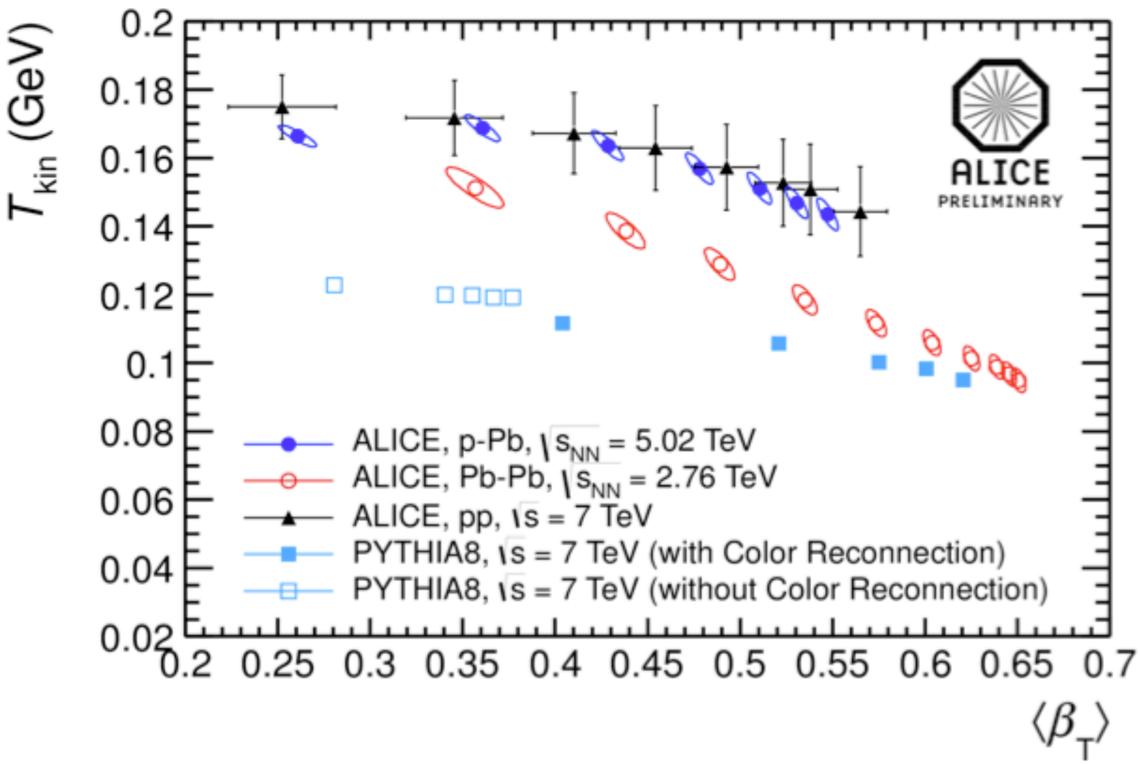

p-Pb and Pb-Pb data follow the same trend → consistent with a collective expansion.

Systematic blast-wave study: pp, p-Pb, Pb-Pb

- The hydro-motivated blast-wave parametrization assumes a locally thermalized medium, expanding collectively with a common velocity field β and an instantaneous common freeze-out at a temperature T_{kin}.
- Systematic description of spectral shape with two fit parameters as a function centrality/multiplicity.

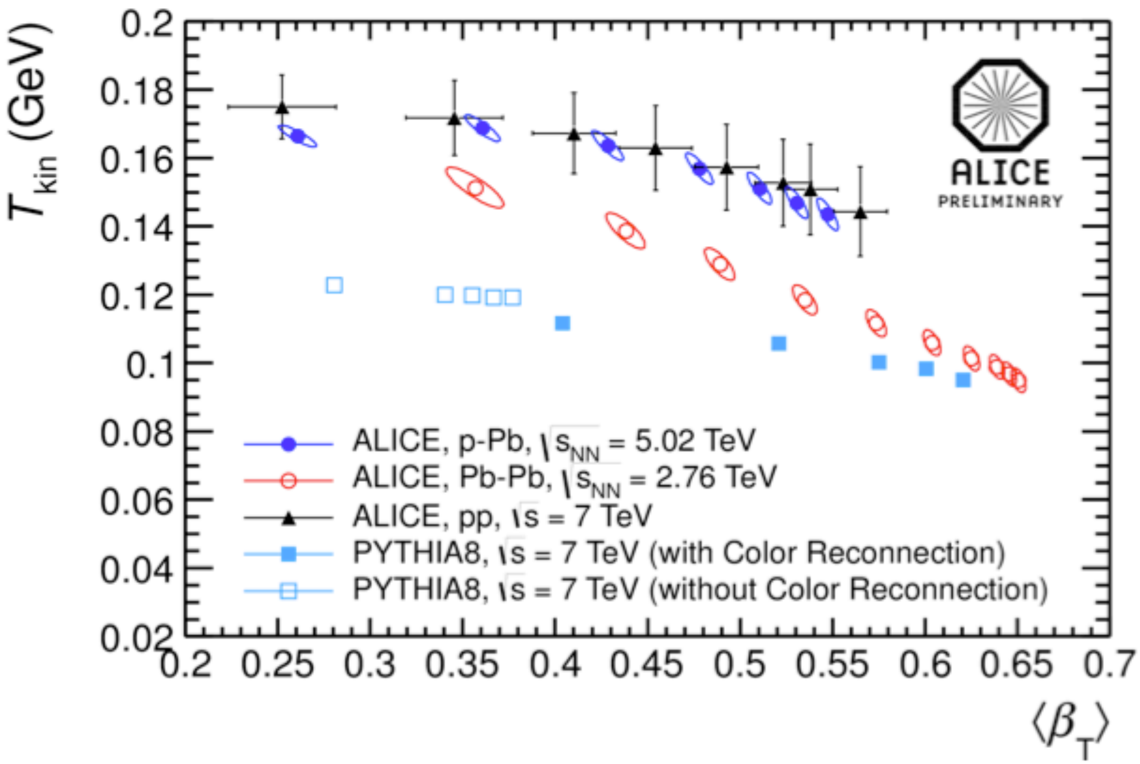

p-Pb and Pb-Pb data follow the same trend → consistent with a collective expansion.

PYTHIA 8 with color reconnection shows a similar trend (without including hydrodynamic flow).

Systematic blast-wave study: pp, p-Pb, Pb-Pb

- The hydro-motivated blast-wave parametrization assumes a locally thermalized medium, expanding collectively with a common velocity field β and an instantaneous common freeze-out at a temperature T_{kin}.
- Systematic description of spectral shape with two fit parameters as a function centrality/multiplicity.

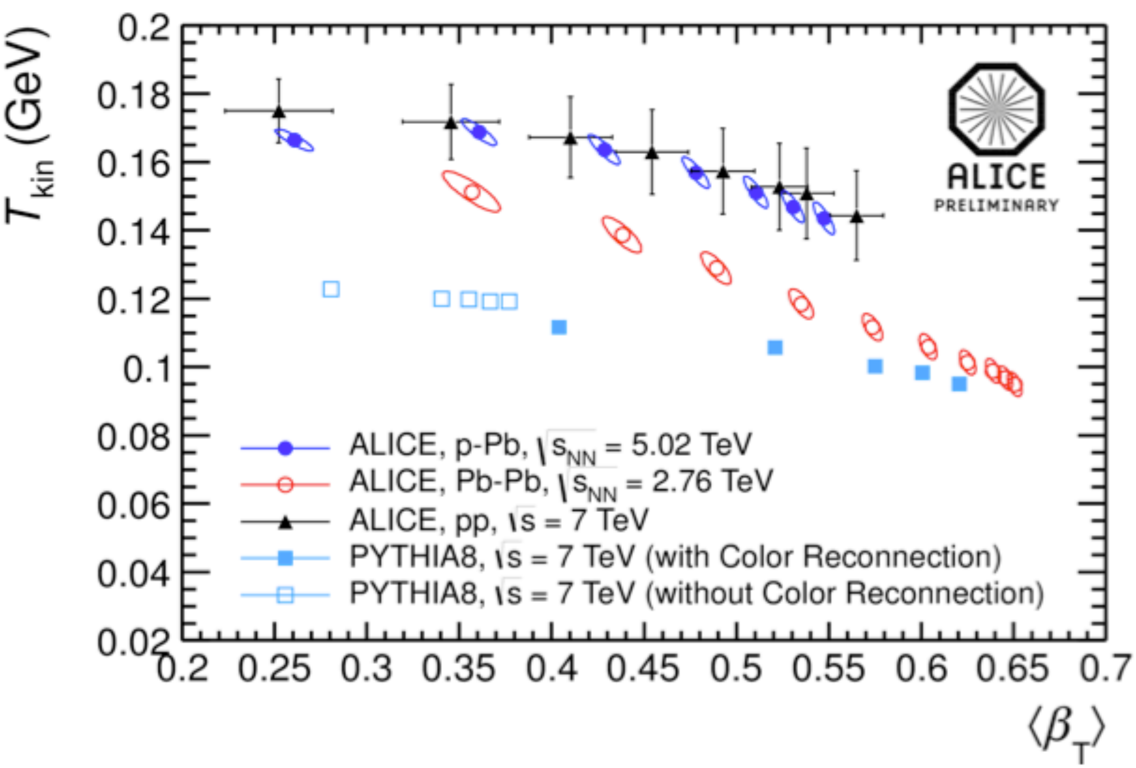

p-Pb and Pb-Pb data follow the same trend → consistent with a collective expansion.

PYTHIA 8 with color reconnection shows a similar trend (without including hydrodynamic flow).

Other effects can mimic flow-like patterns.

Systematic blast-wave study: pp, p-Pb, Pb-Pb

- The hydro-motivated blast-wave parametrization assumes a locally thermalized medium, expanding collectively with a common velocity field β and an instantaneous common freeze-out at a temperature T_{kin}.
- Systematic description of spectral shape with two fit parameters as a function centrality/multiplicity.

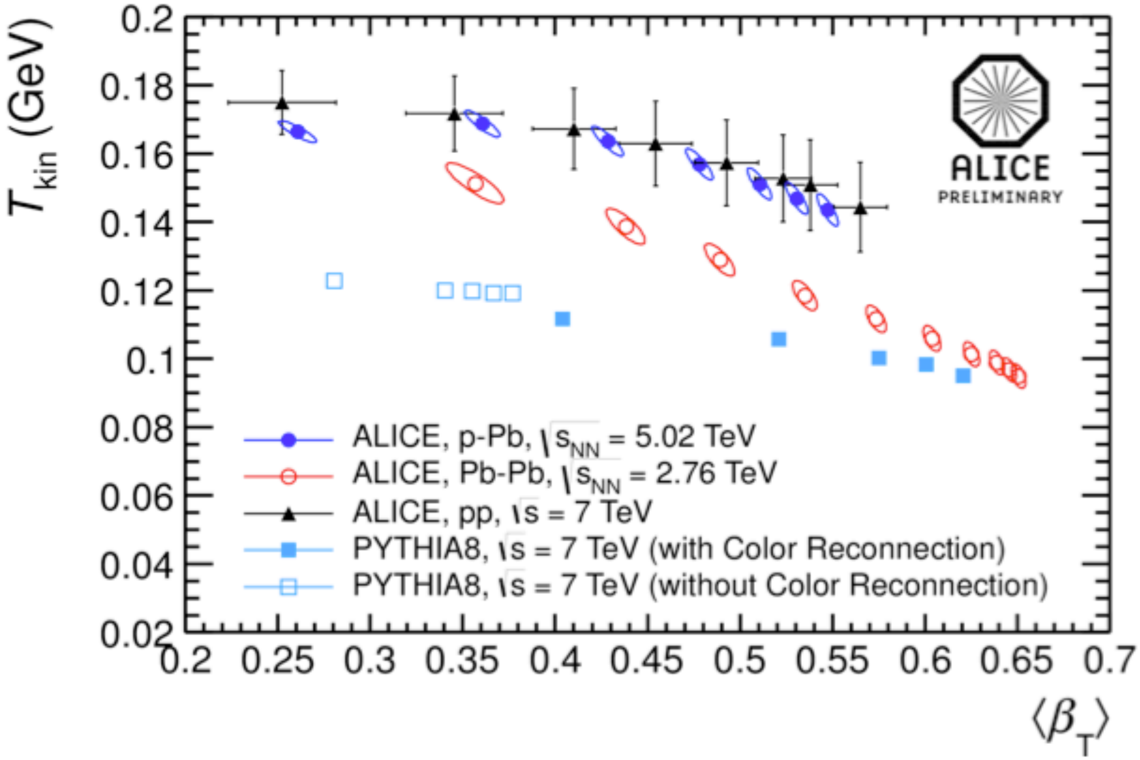

p-Pb and Pb-Pb data follow the same trend → consistent with a collective expansion.

PYTHIA 8 with color reconnection shows a similar trend (without including hydrodynamic flow).

Other effects can mimic flow-like patterns.

Also pp *data* shows a similar trend.

Λ/K^0_s ratio in p-Pb and Pb-Pb

Pb-Pb

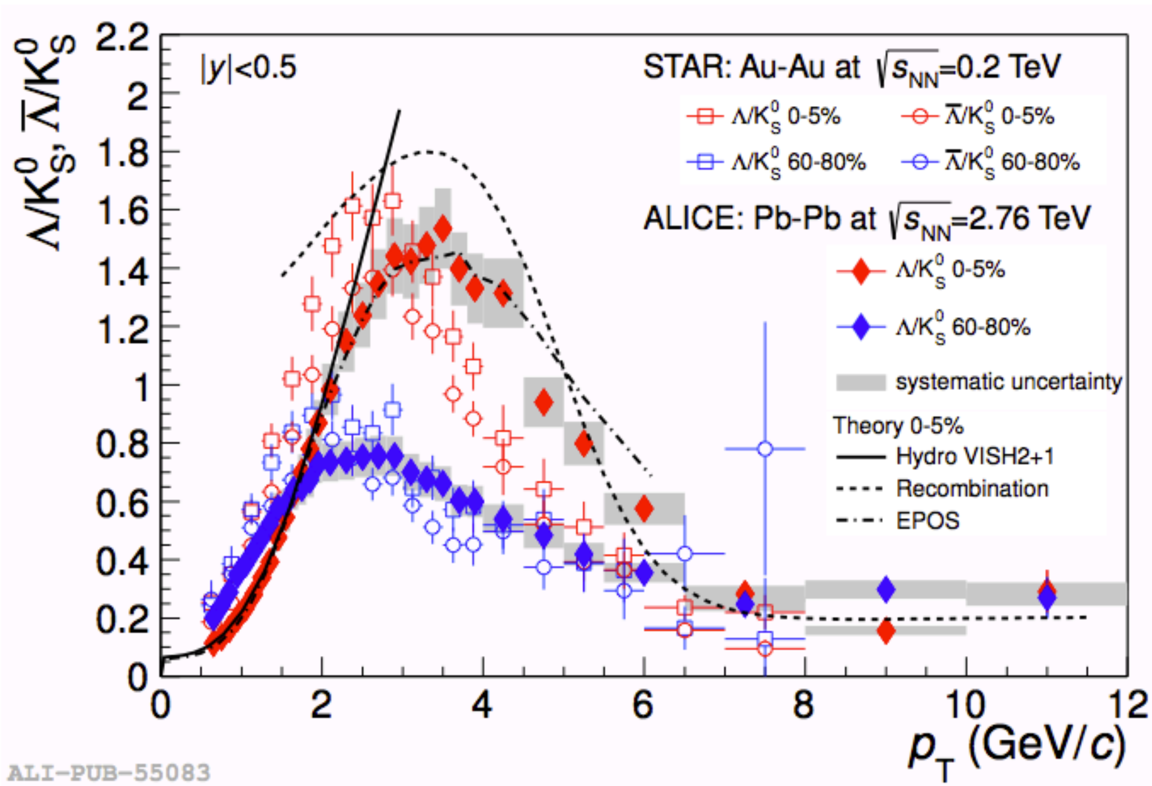

arXiv: 1307.5530

Λ/K^0_s ratio in p-Pb and Pb-Pb

Pb-Pb

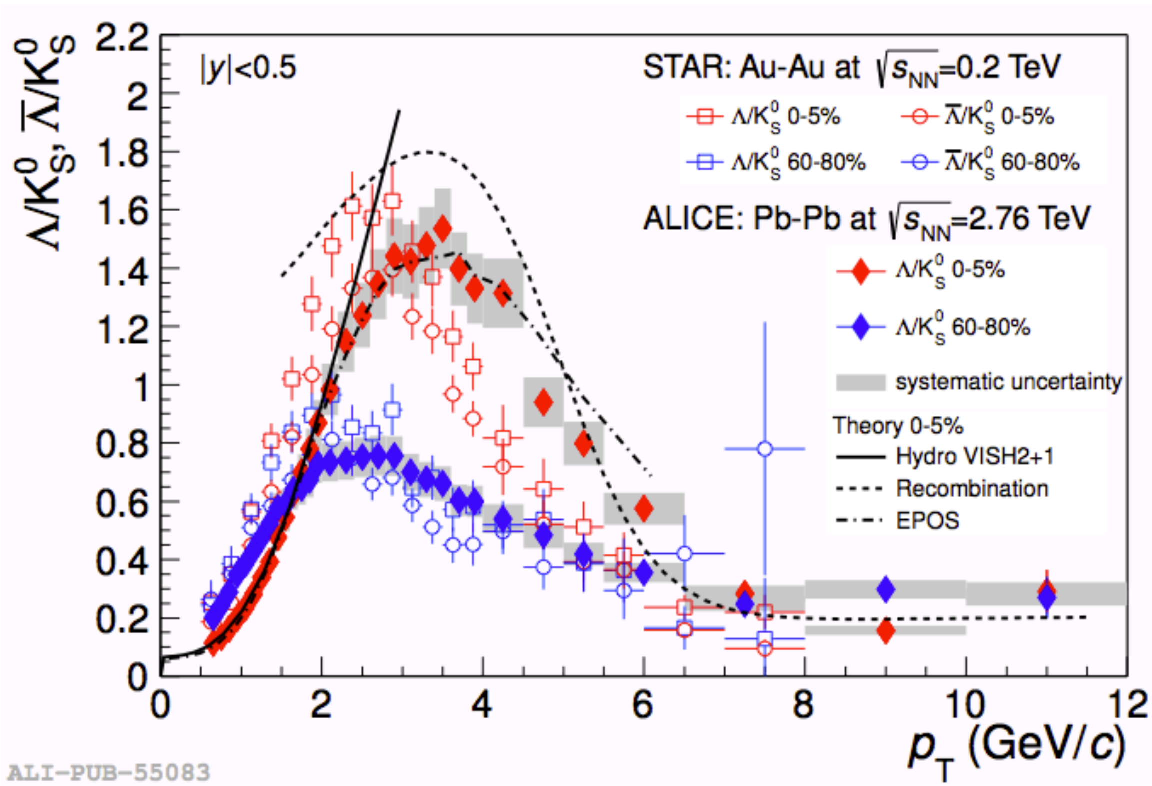

arXiv: 1307.5530

Pb-Pb: Integrated ratio independent of centrality (Λ/K^0_s ≈ 0.25)

Λ/K^0_s ratio in p-Pb and Pb-Pb

Pb-Pb

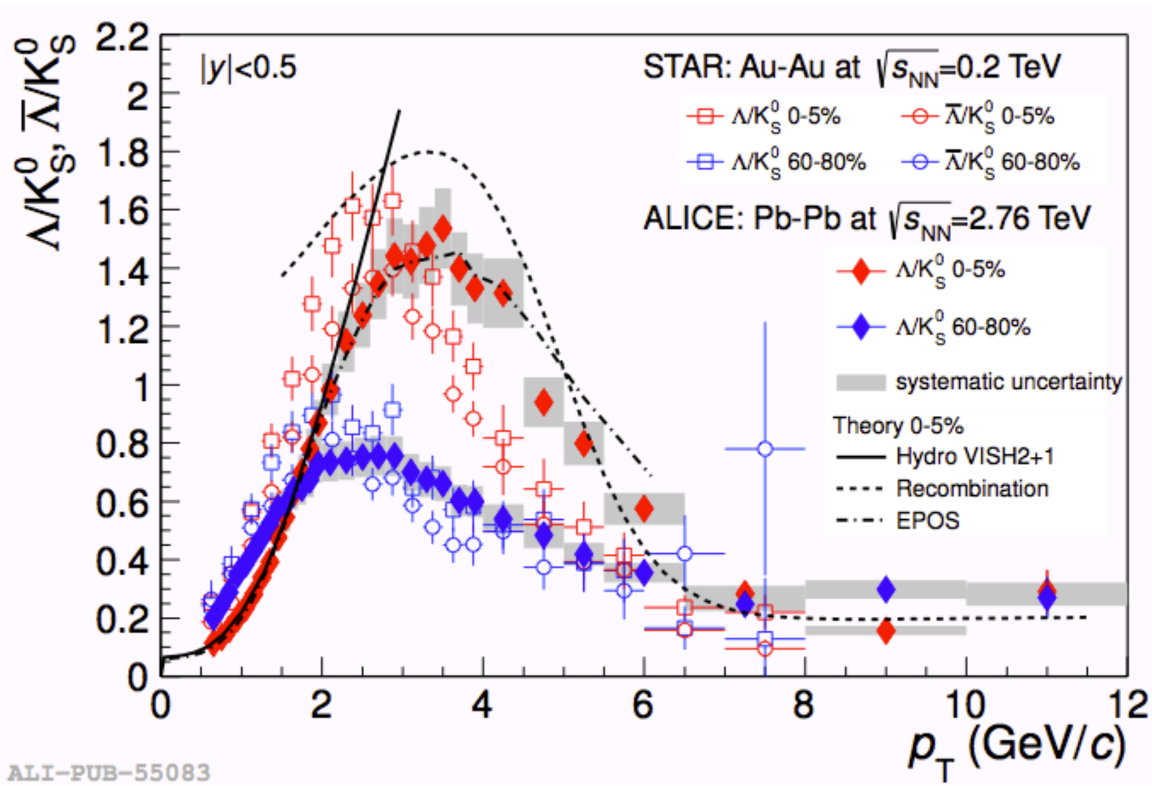

arXiv: 1307.5530

Pb-Pb: Integrated ratio independent of centrality ($\Lambda/K^0_s \approx 0.25$)

Pb-Pb: enhancement at intermediate p_T in central collisions, consistent with radial flow

Λ/K^0_s ratio in p-Pb and Pb-Pb

Pb-Pb

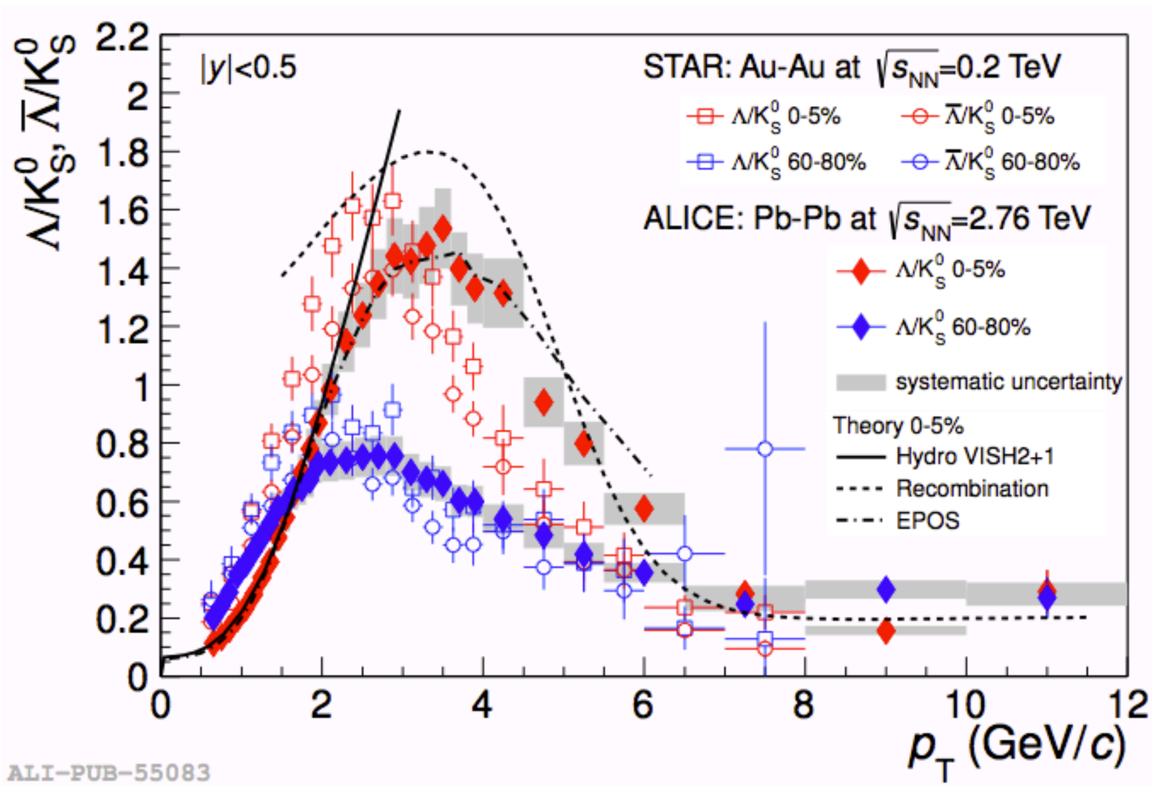

arXiv: 1307.5530

Pb-Pb: Integrated ratio independent of centrality ($\Lambda/K^0_s \approx 0.25$)

Pb-Pb: enhancement at intermediate p_T in central collisions, consistent with radial flow

Pb-Pb: at high p_T consistent with a vacuum-like fragmentation

Λ/K^0_s ratio in p-Pb and Pb-Pb

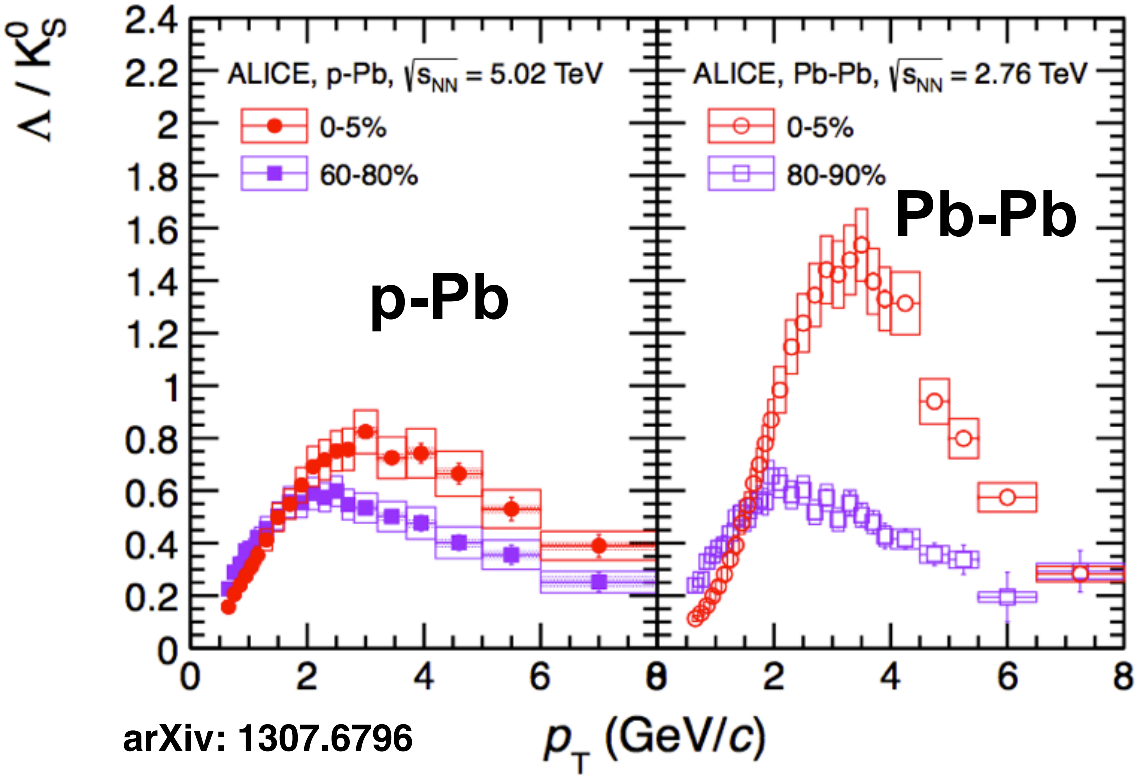

arXiv: 1307.6796

Pb-Pb: Integrated ratio independent of centrality ($\Lambda/K^0_s \approx 0.25$)

Pb-Pb: enhancement at intermediate p_T in central collisions, consistent with radial flow

Pb-Pb: at high p_T consistent with a vacuum-like fragmentation

Λ/K^0_s ratio in p-Pb and Pb-Pb

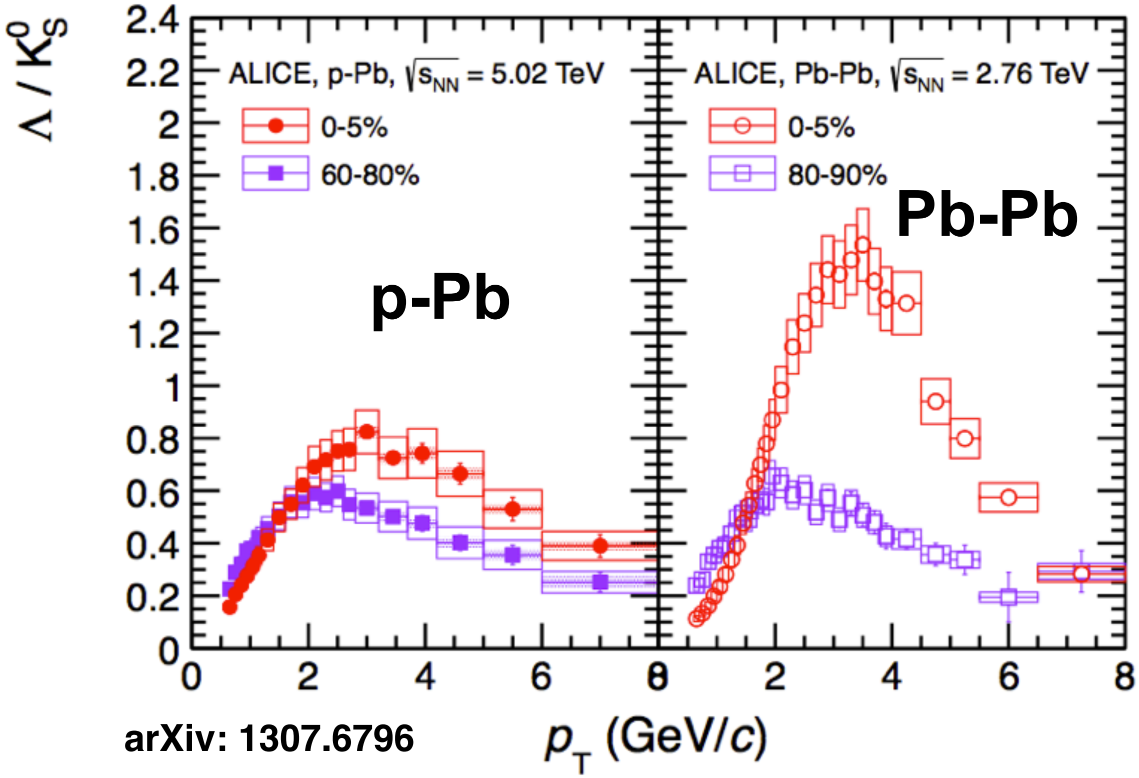

arXiv: 1307.6796

Pb-Pb: Integrated ratio independent of centrality ($\Lambda/K^0_s \approx 0.25$)

Pb-Pb: enhancement at intermediate p_T in central collisions, consistent with radial flow

Pb-Pb: at high p_T consistent with a vacuum-like fragmentation

Behavior in p-Pb collisions is reminiscent of the trends observed in Pb-Pb.

From radial to elliptic flow...

- Two particle correlations in p-Pb: from the high-multiplicity yield subtract the jet yield obtained in low-multiplicity events (no ridge) → *double ridge*.
- New: correlations of identified particles.

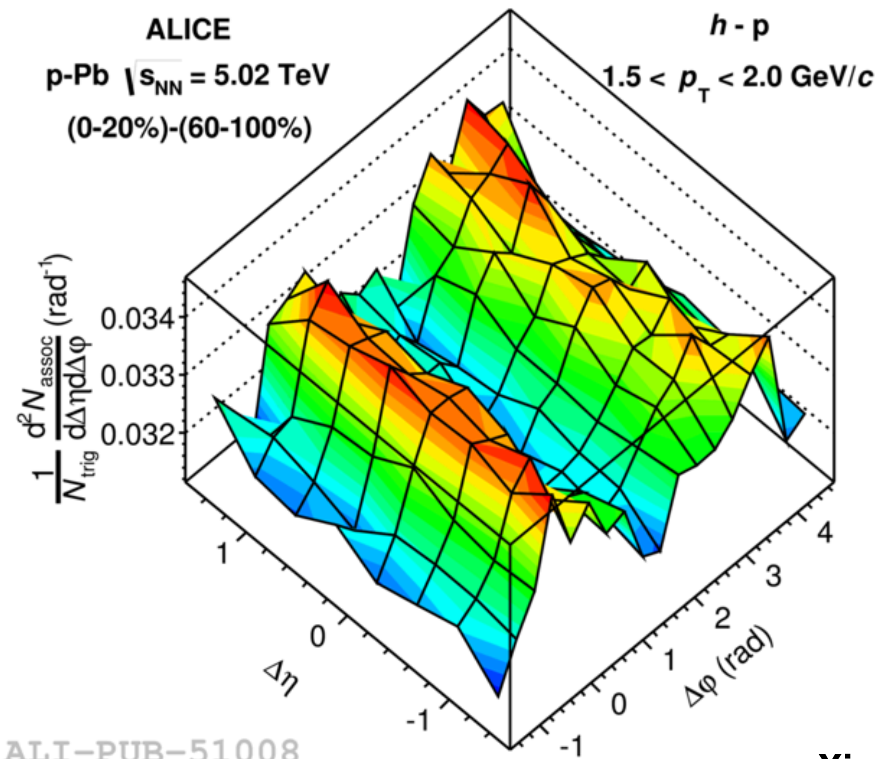

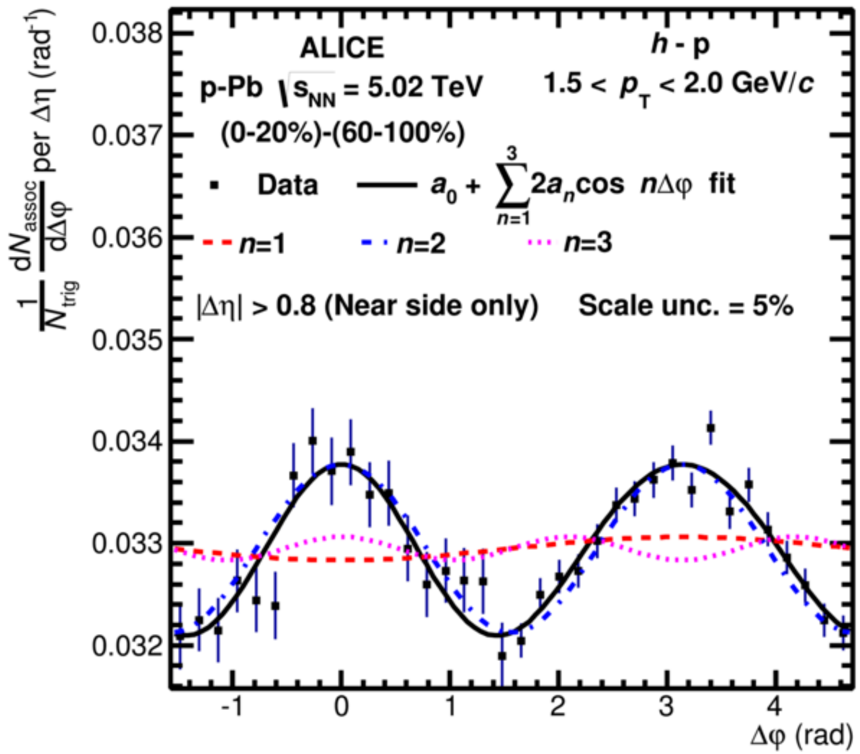

arXiv: 1307.3237

From radial to elliptic flow...

- Two particle correlations in p-Pb: from the high-multiplicity yield subtract the jet yield obtained in low-multiplicity events (no ridge) → *double ridge*.
- New: correlations of identified particles.

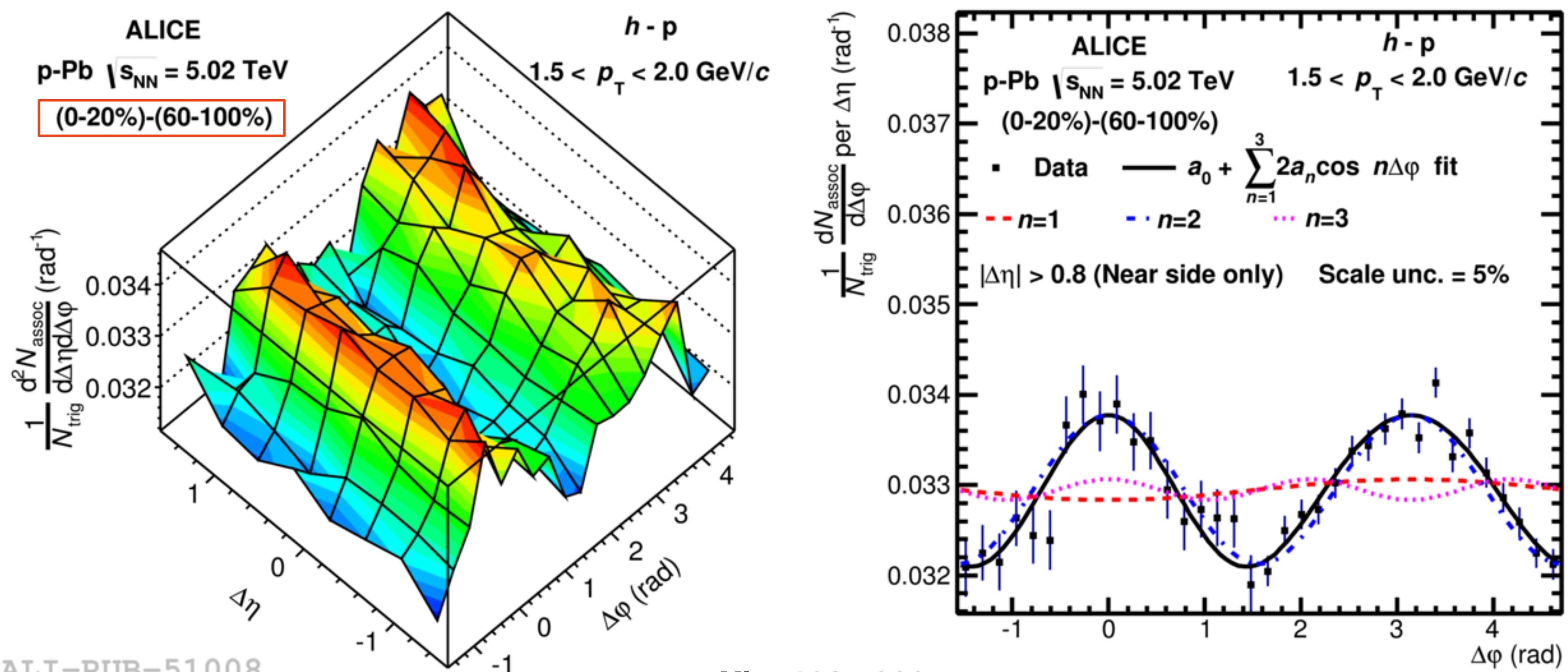

arXiv: 1307.3237

From radial to elliptic flow...

- Two particle correlations in p-Pb: from the high-multiplicity yield subtract the jet yield obtained in low-multiplicity events (no ridge) → *double ridge*.
- New: correlations of identified particles.

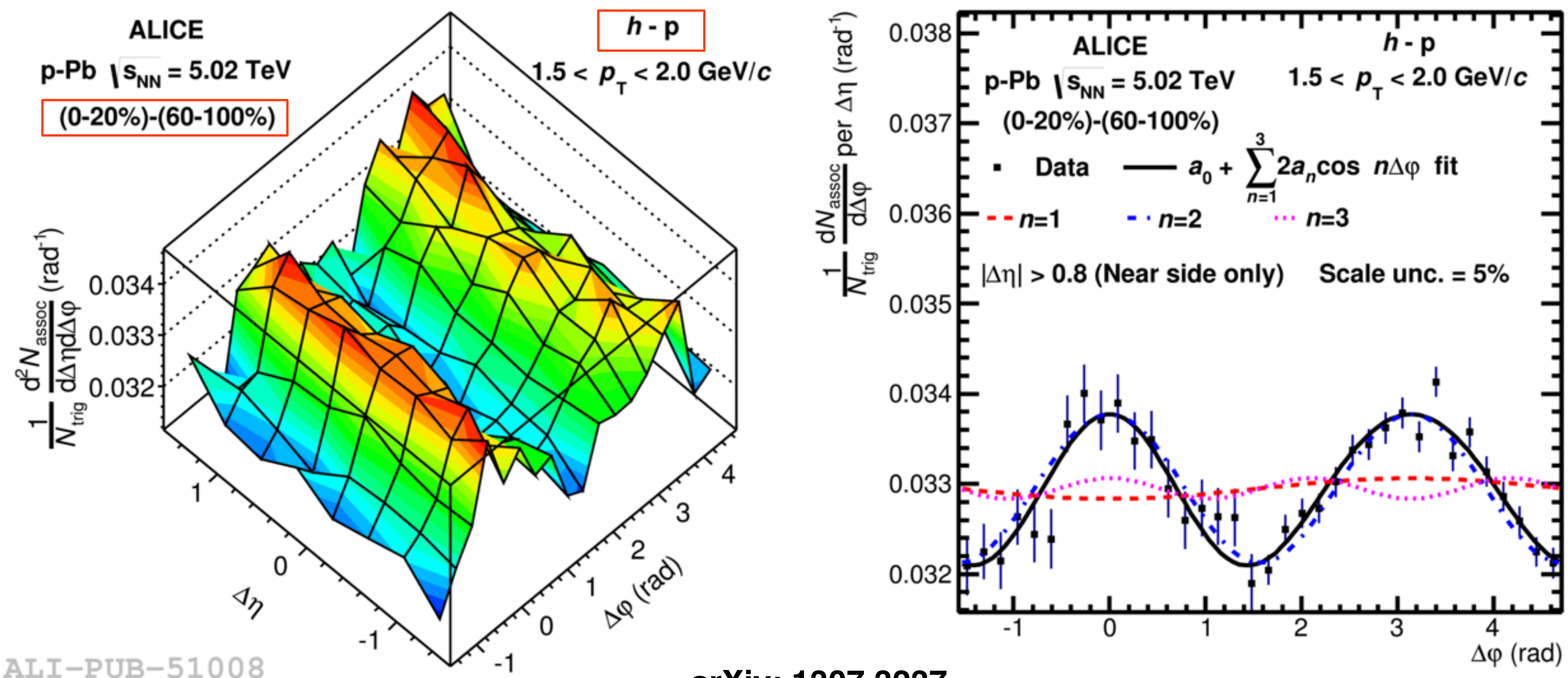

arXiv: 1307.3237

v_2 coefficient in p-Pb

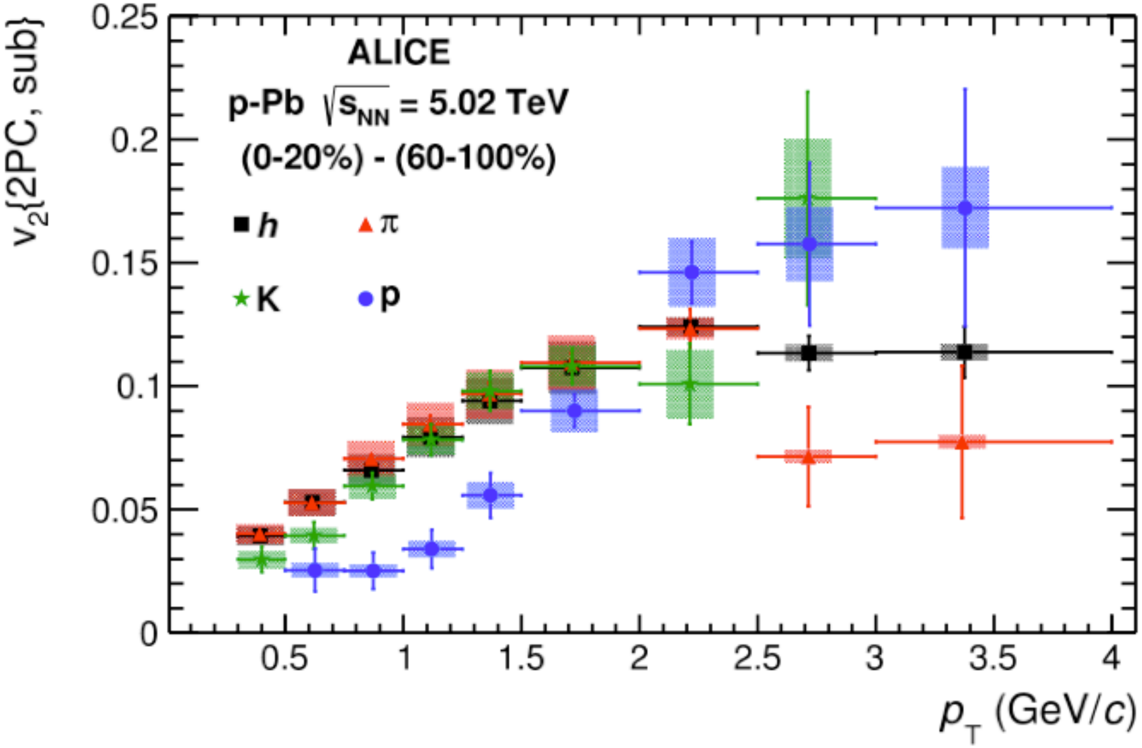

arXiv: 1307.3237

v_2 coefficient in p-Pb

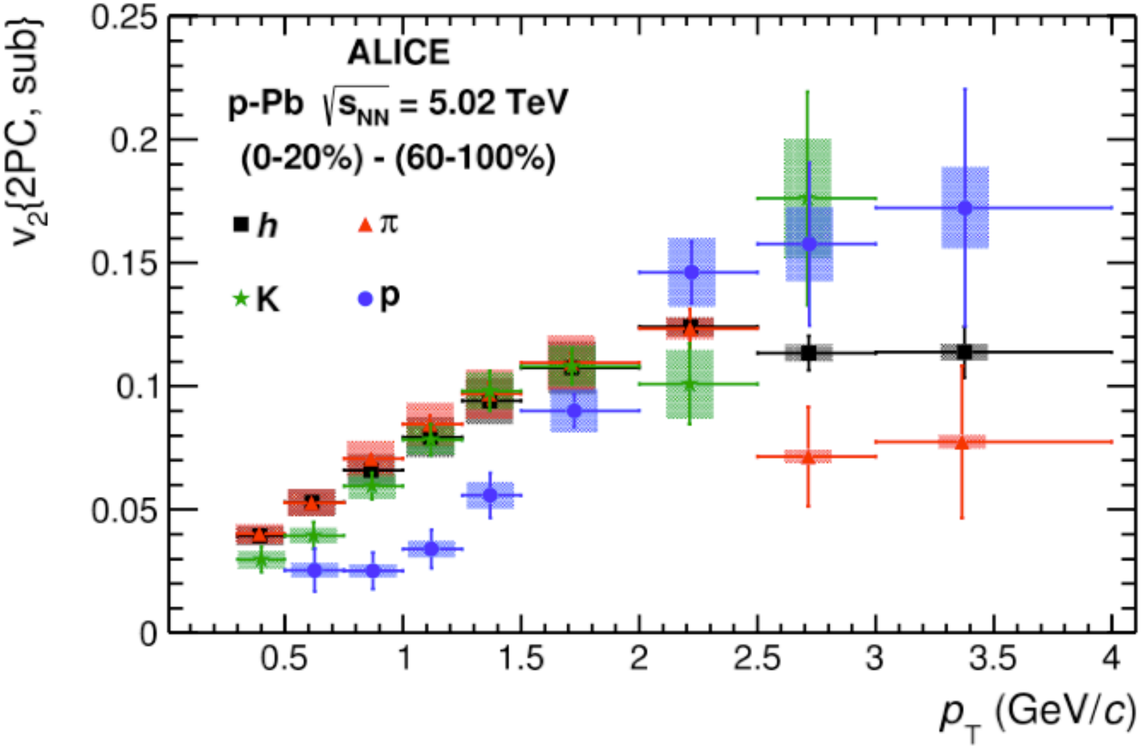

arXiv: 1307.3237

Number of explanations of the double ridge put forward: from hydrodynamic flow to color glass condensate formalism.

v_2 coefficient in p-Pb

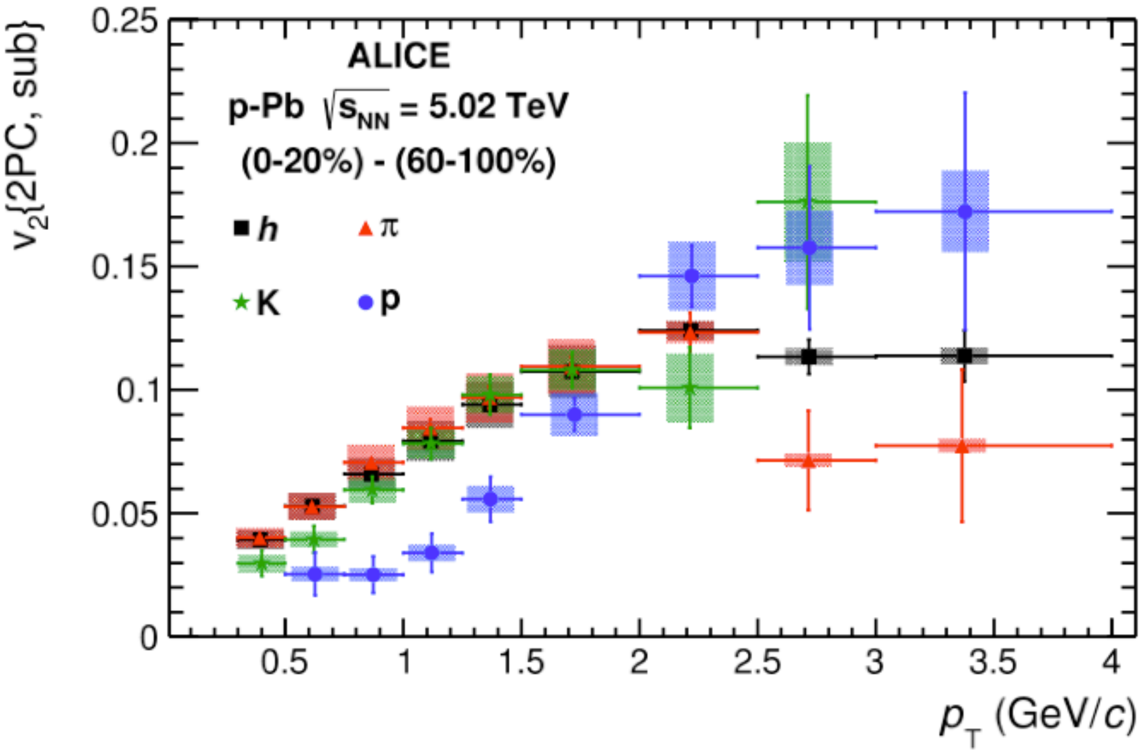

arXiv: 1307.3237

Number of explanations of the double ridge put forward: from hydrodynamic flow to color glass condensate formalism.

Identical to the identified p_T-spectra: characteristic mass ordering observed.

v_2 coefficient in p-Pb

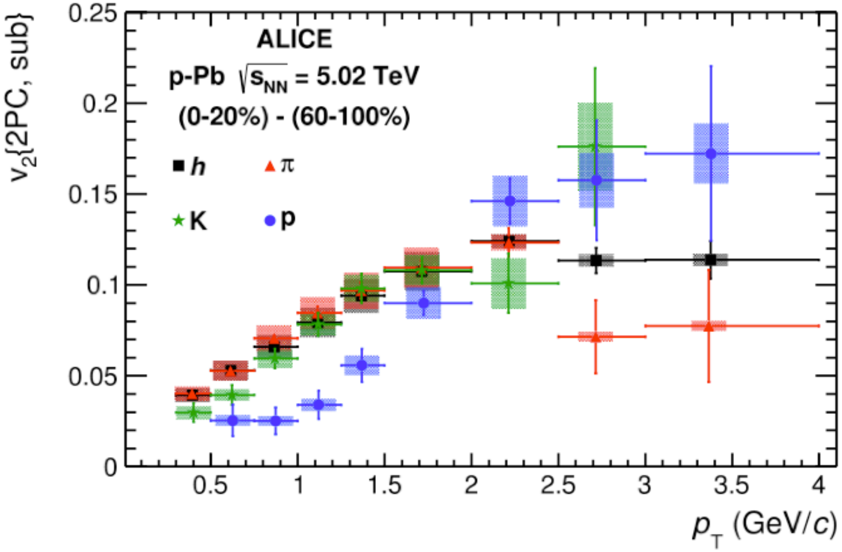

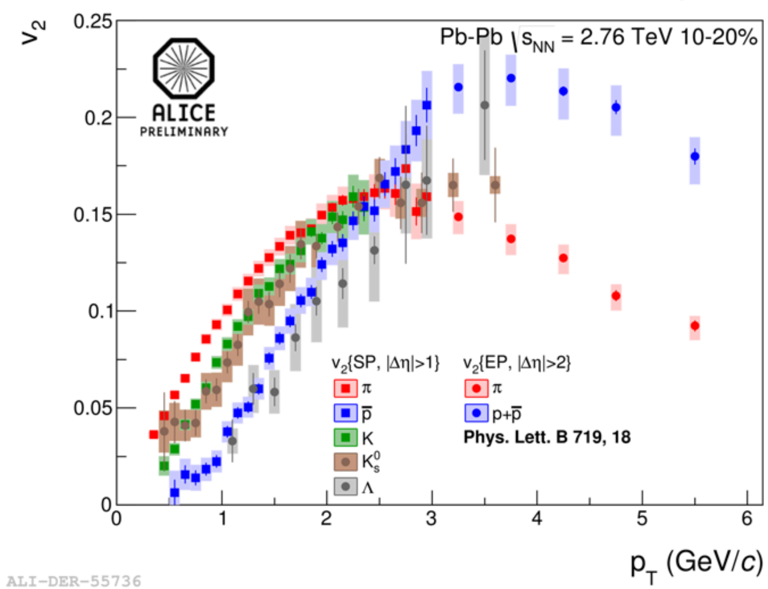

Number of explanations of the double ridge put forward: from hydrodynamic flow to color glass condensate formalism.

Identical to the identified p_T-spectra: characteristic mass ordering observed.

v_2 coefficient in p-Pb

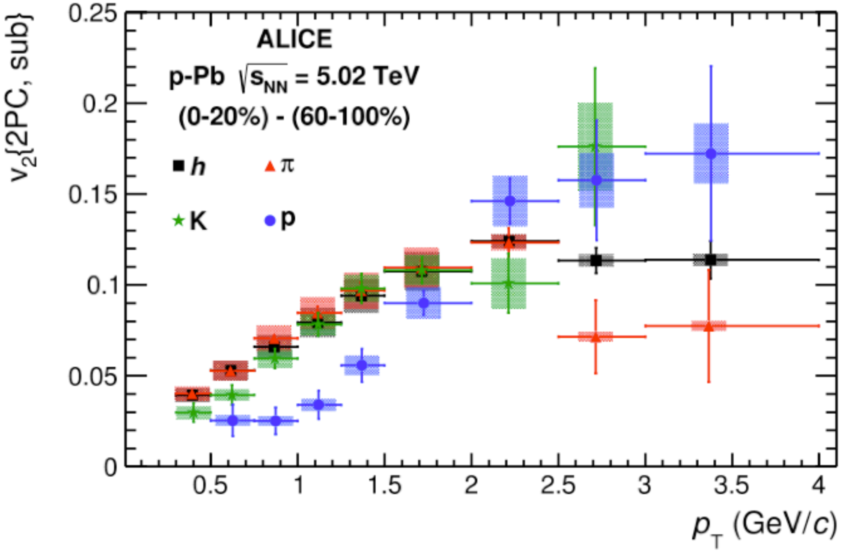

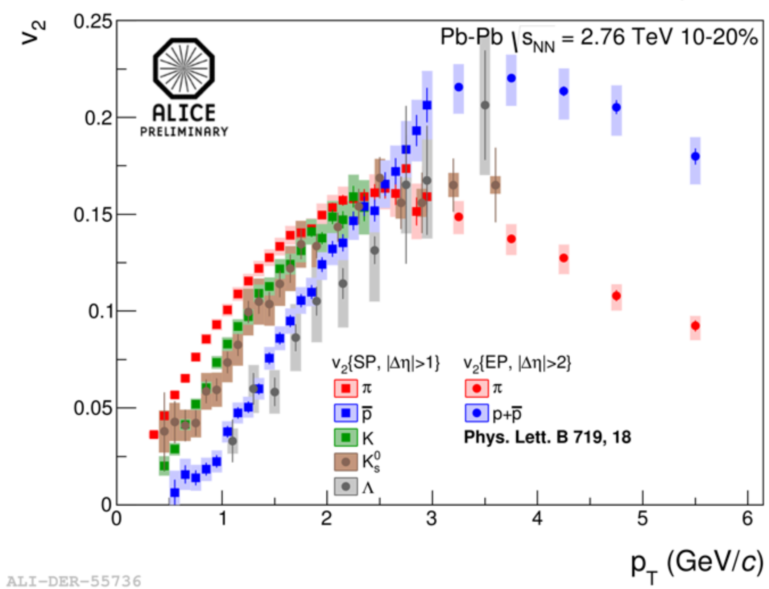

Number of explanations of the double ridge put forward: from hydrodynamic flow to color glass condensate formalism.

Identical to the identified p_T-spectra: characteristic mass ordering observed.

Phenomenologically reminiscent of the same features observed in Pb-Pb collisions.

v_2 coefficient in p-Pb

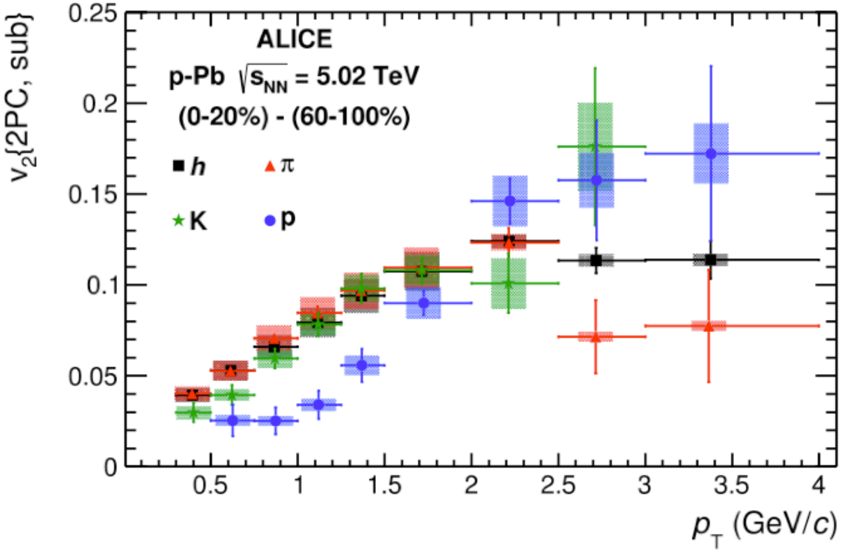

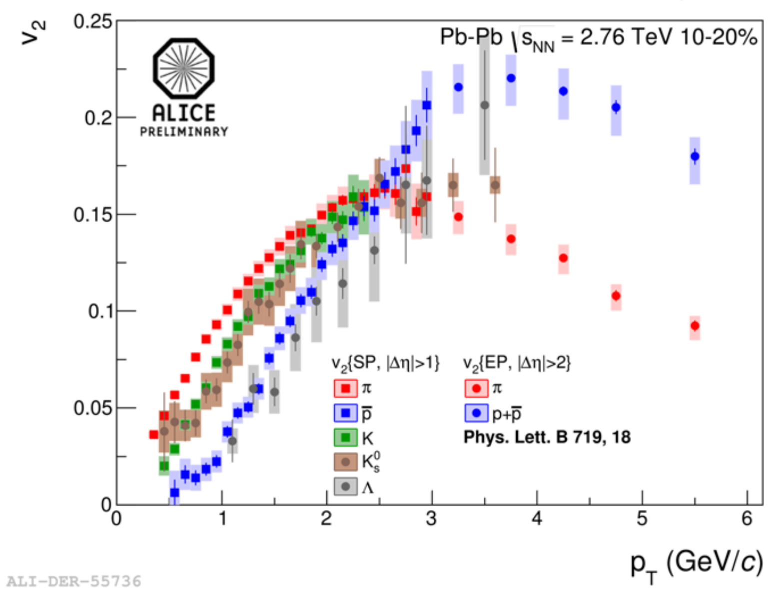

Number of explanations of the double ridge put forward: from hydrodynamic flow to color glass condensate formalism.

Identical to the identified p_T-spectra: characteristic mass ordering observed.

Phenomenologically reminiscent of the same features observed in Pb-Pb collisions.

In Pb-Pb collisions: ascribed to hydrodynamics. In p-Pb?

(Anti-)nuclei and hyper-nuclei

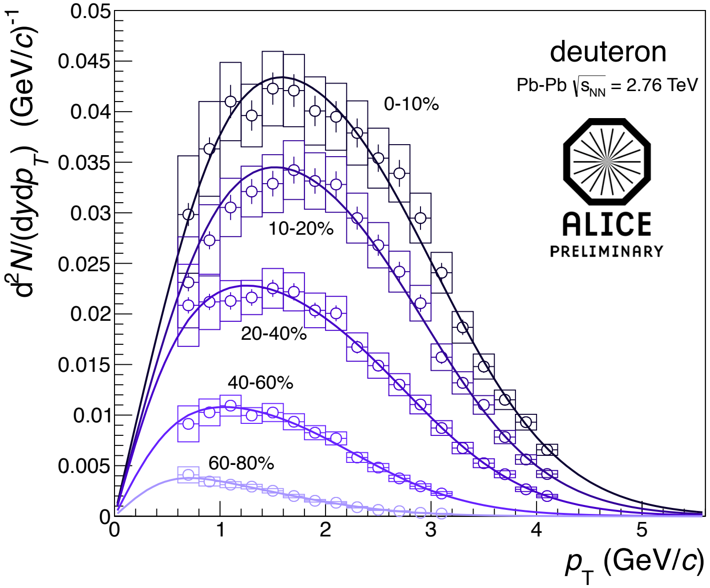

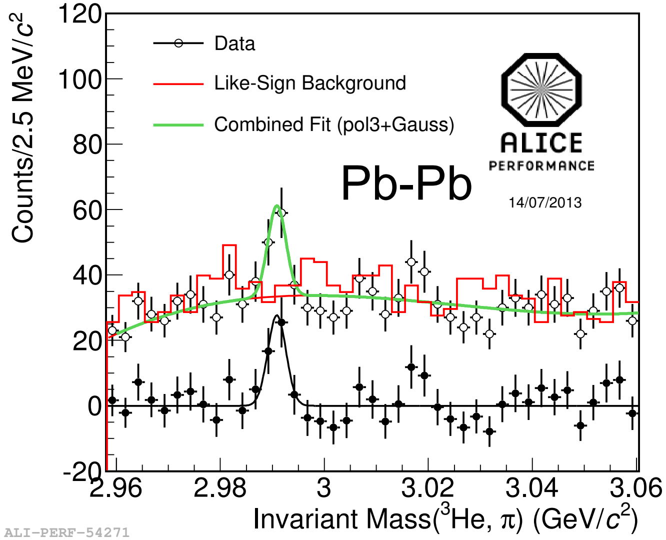

(Anti-)nuclei and hyper-nuclei

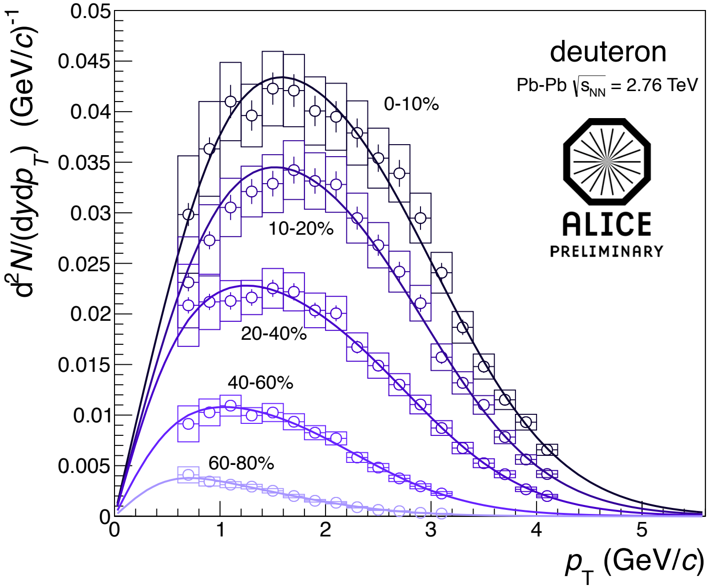

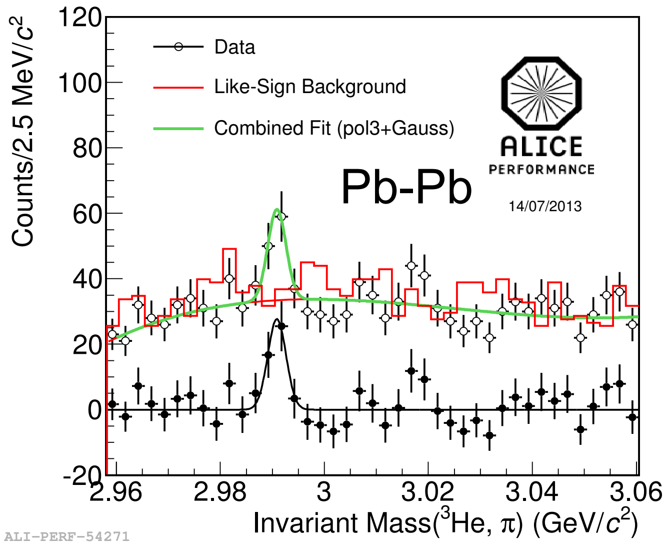

Deuteron spectra show characteristic hardening of the spectrum with increasing centrality (radial flow).

(Anti-)nuclei and hyper-nuclei

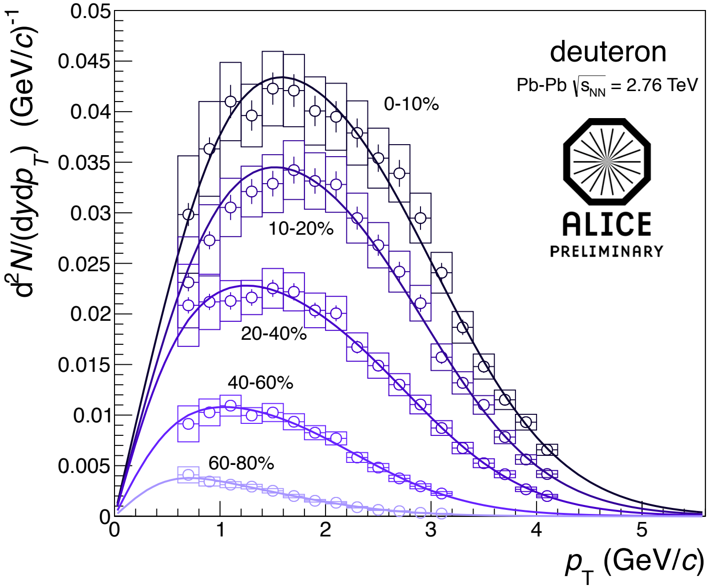

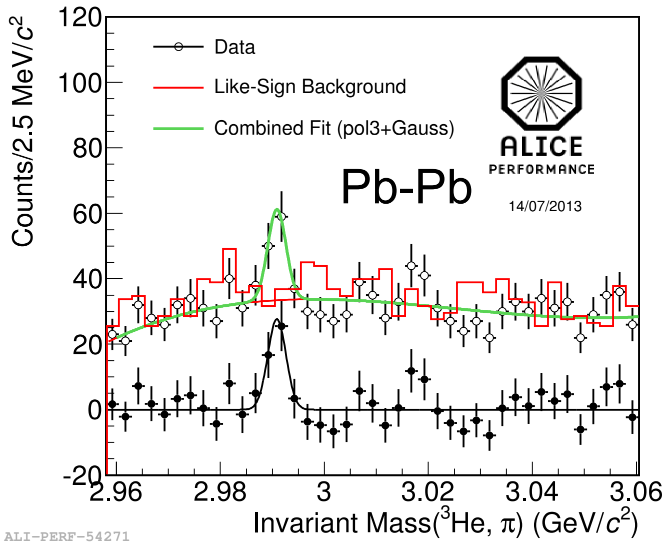

Deuteron spectra show characteristic hardening of the spectrum with increasing centrality (radial flow).

Hypertriton (p,n,Λ) yield measured in the $^3_\Lambda H \rightarrow {}^3He\,\pi$ decay channel.

(Anti-)nuclei and hyper-nuclei

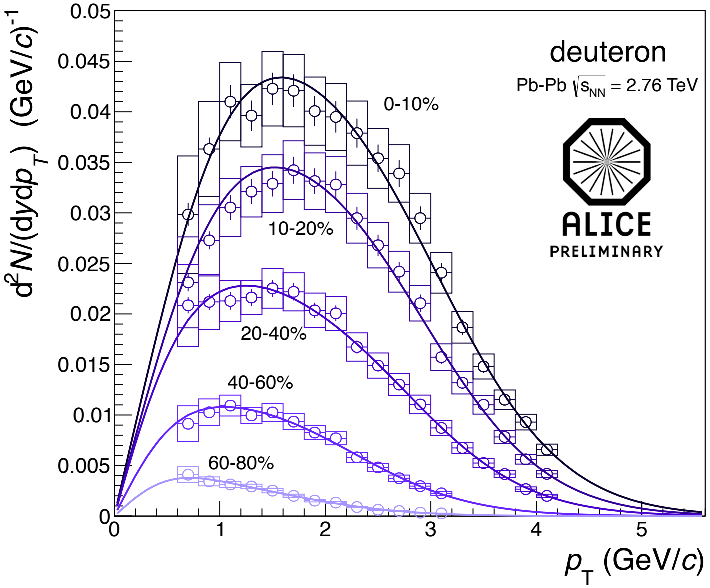

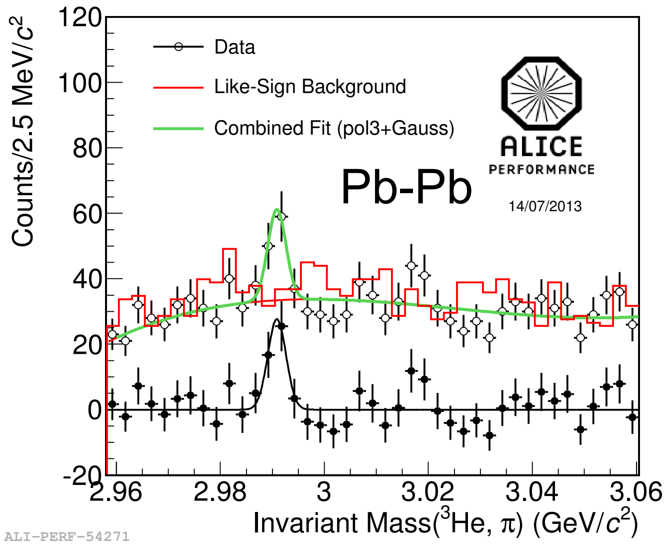

Deuteron spectra show characteristic hardening of the spectrum with increasing centrality (radial flow).

Hypertriton (p,n,Λ) yield measured in the $^3_\Lambda H \rightarrow {}^3He\ \pi$ decay channel.

Production rates of (hyper-)nuclei can be described in a thermal model approach.

(Anti-)nuclei and hyper-nuclei

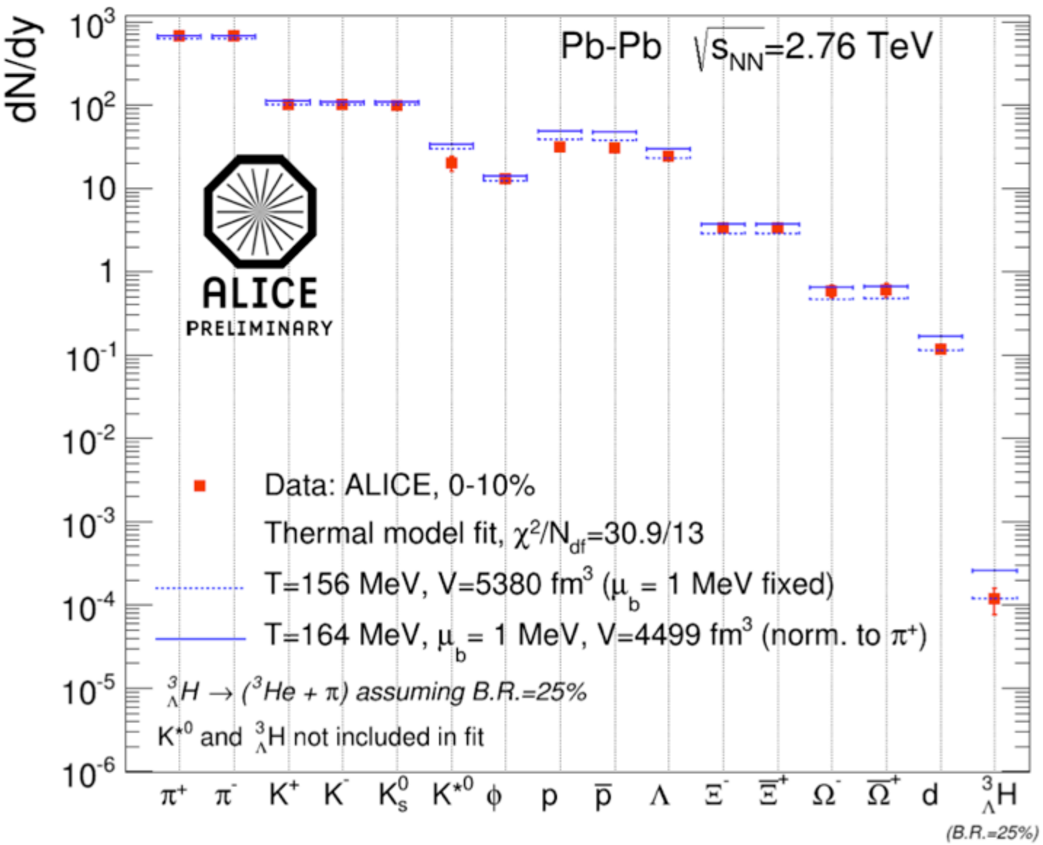

Deuteron spectra show characteristic hardening of the spectrum with increasing centrality (radial flow).

Hypertriton (p,n,Λ) yield measured in the $^3{}_\Lambda H \rightarrow {}^3He\ \pi$ decay channel.

Production rates of (hyper-)nuclei can be described in a thermal model approach.

Thermal model from:
A.Andronic, P. Braun-Munzinger, J. Stachel, Nucl. Phys.A 772 (2006) 167

(Anti-)nuclei and hyper-nuclei

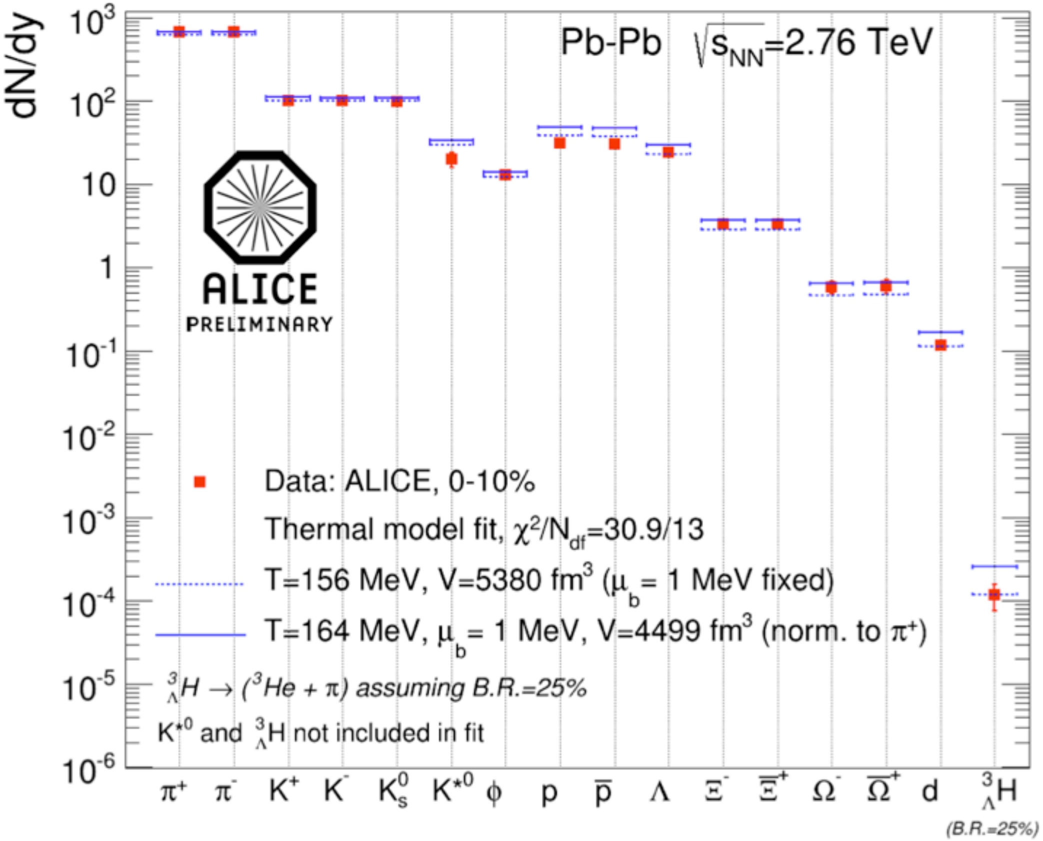

Deuteron spectra show characteristic hardening of the spectrum with increasing centrality (radial flow).

Hypertriton (p,n,Λ) yield measured in the $^3{}_\Lambda H \rightarrow {}^3He\ \pi$ decay channel.

Production rates of (hyper-)nuclei can be described in a thermal model approach.

In these models: very sensitive to the freeze-out temperature (large mass).

Thermal model from:
A.Andronic, P. Braun-Munzinger, J. Stachel, Nucl. Phys.A 772 (2006) 167

(Anti-)nuclei and hyper-nuclei

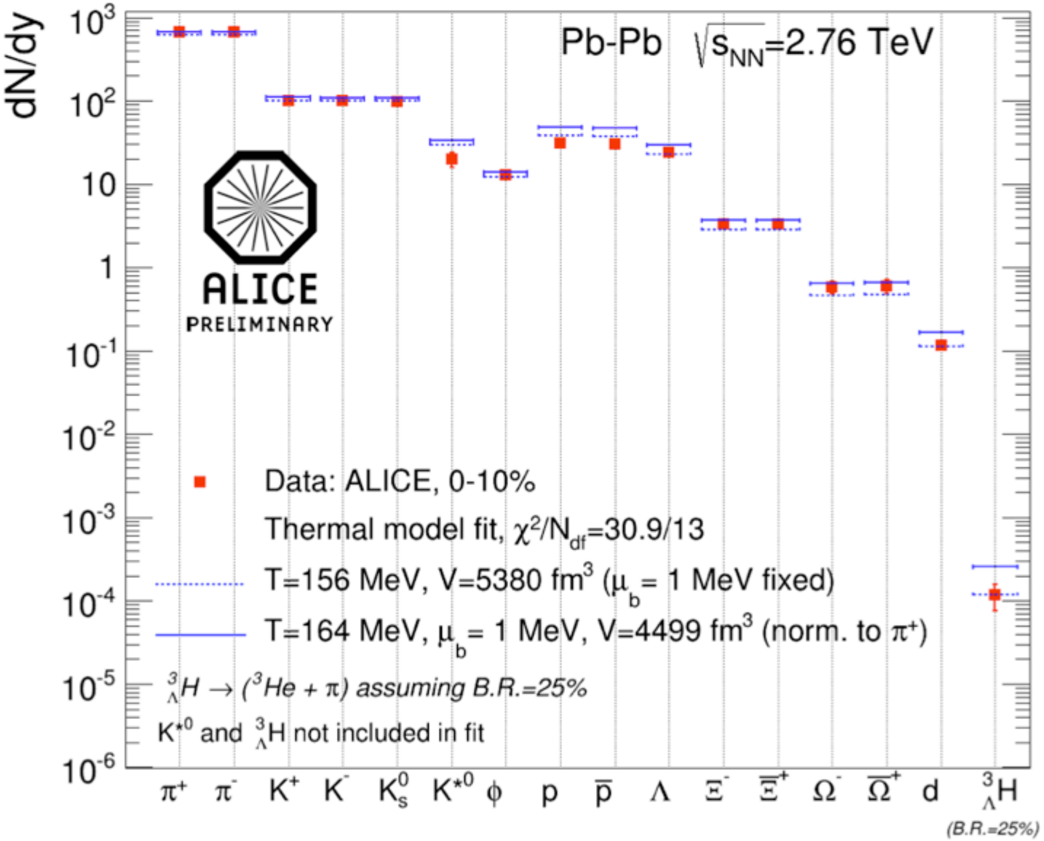

Deuteron spectra show characteristic hardening of the spectrum with increasing centrality (radial flow).

Hypertriton (p,n,Λ) yield measured in the $^3_\Lambda H \rightarrow {}^3He\ \pi$ decay channel.

Production rates of (hyper-)nuclei can be described in a thermal model approach.

In these models: very sensitive to the freeze-out temperature (large mass).

Observed nuclei yields are consistent with the currently best fit of $T_{ch} \approx$ 156 MeV. Remaining data-fit tension between protons (≈-2.9σ) and hyperons (for Xi ≈+2σ).

Thermal model from:
A.Andronic, P. Braun-Munzinger, J. Stachel, Nucl. Phys.A 772 (2006) 167

Hard probes

Flow and R_{AA} of heavy flavor decay muons/electrons (1)

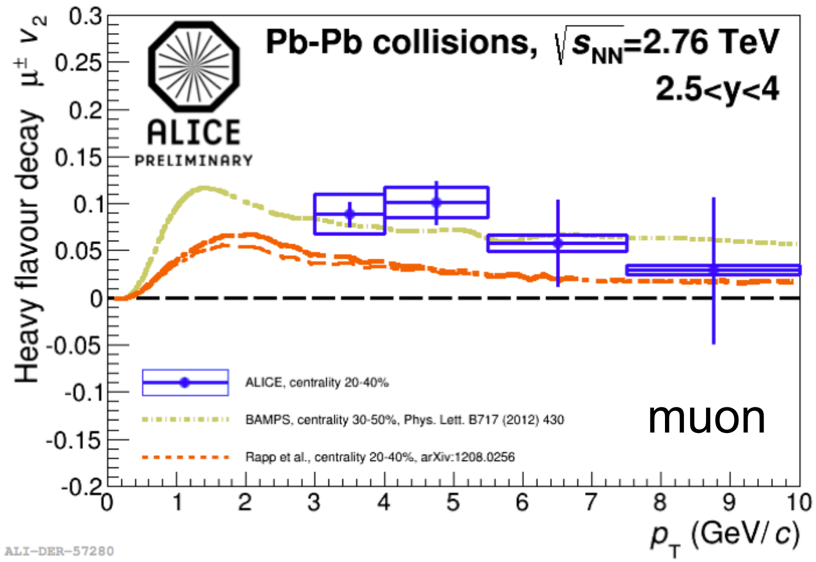

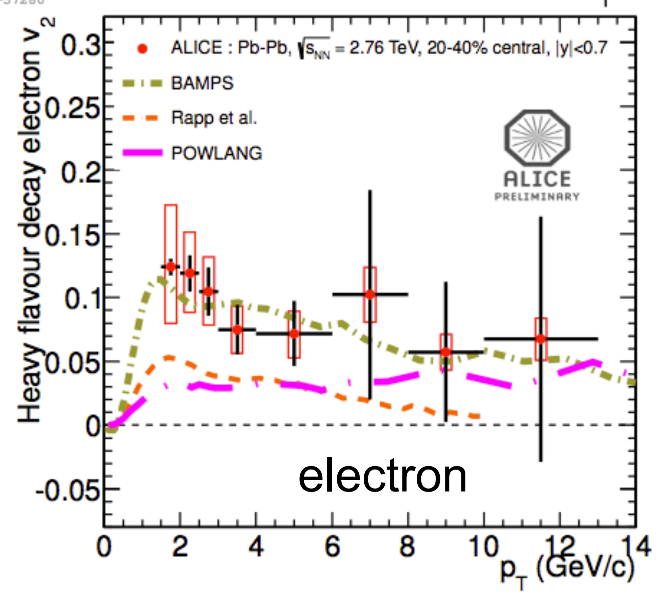

Flow and R_{AA} of heavy flavor decay muons/electrons (1)

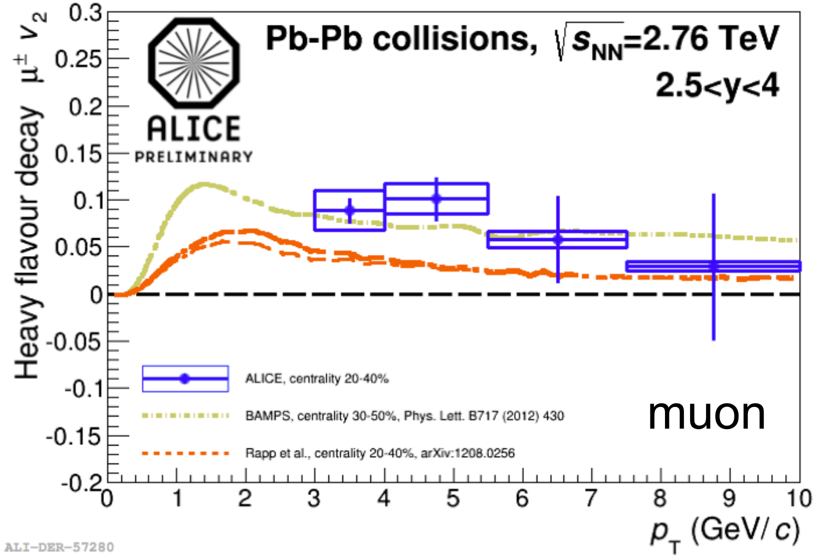

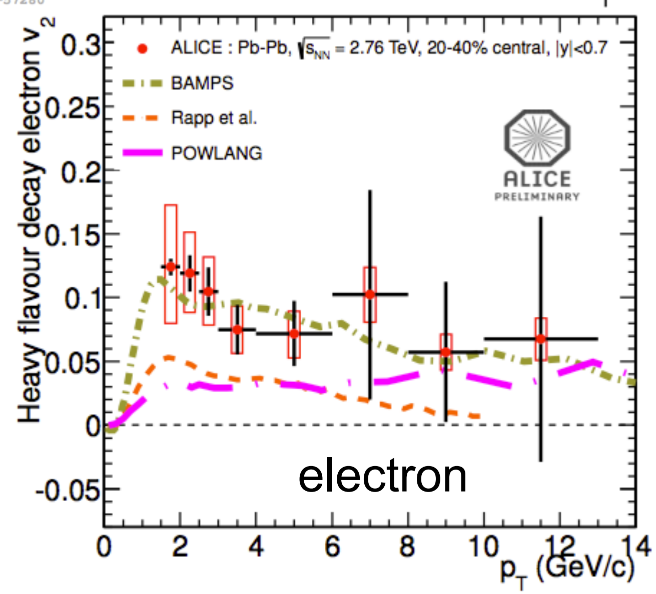

Heavy flavor particles show a non-zero elliptic flow.

Flow and R_{AA} of heavy flavor decay muons/electrons (1)

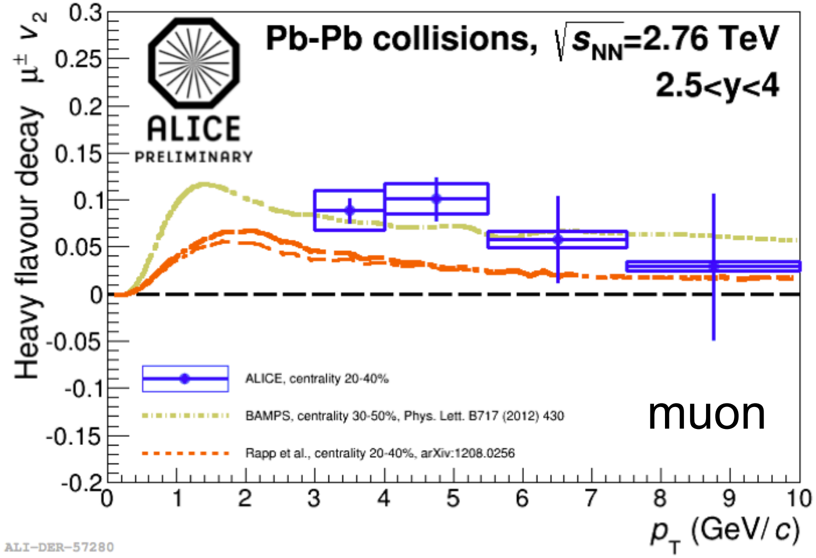

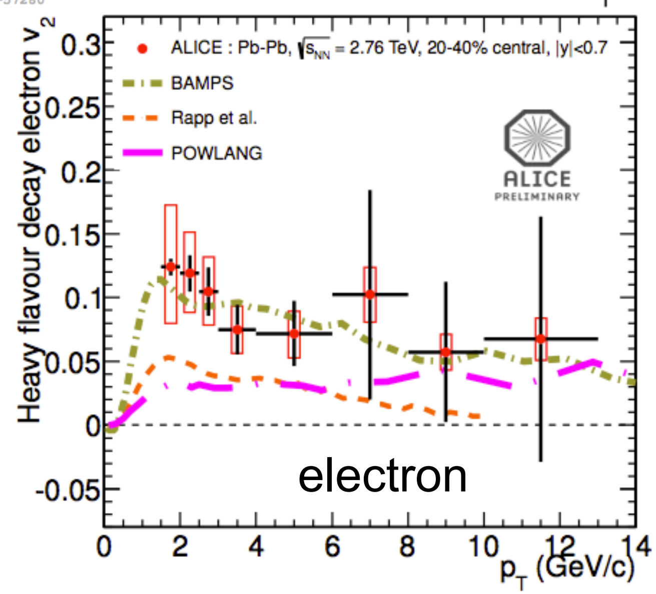

Heavy flavor particles show a non-zero elliptic flow.

v2 of HF → μ at forward rapidity similar as for heavy flavor electrons in central rapidity.

Flow and R_{AA} of heavy flavor decay muons/electrons (1)

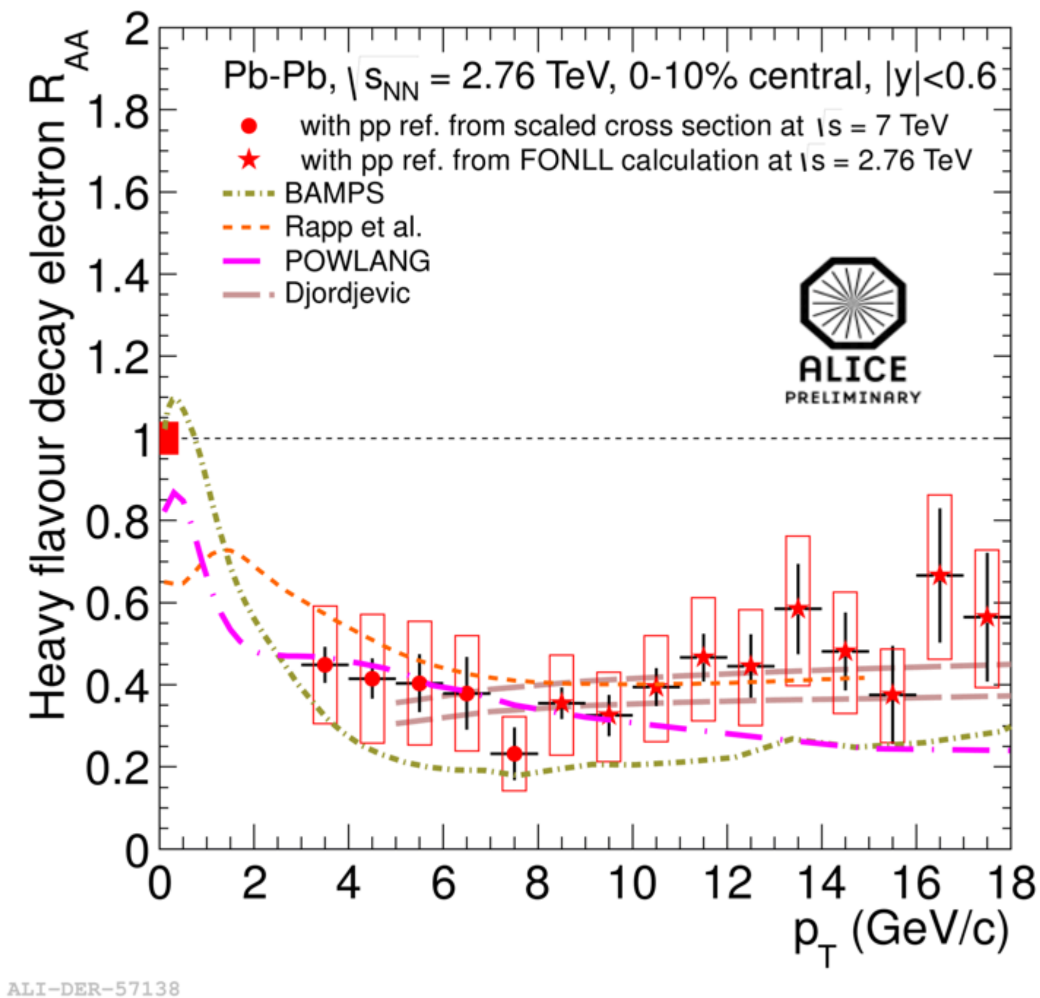

Heavy flavor particles show a non-zero elliptic flow.

v2 of HF → μ at forward rapidity similar as for heavy flavor electrons in central rapidity.

Flow and R_{AA} of heavy flavor decay muons/electrons (1)

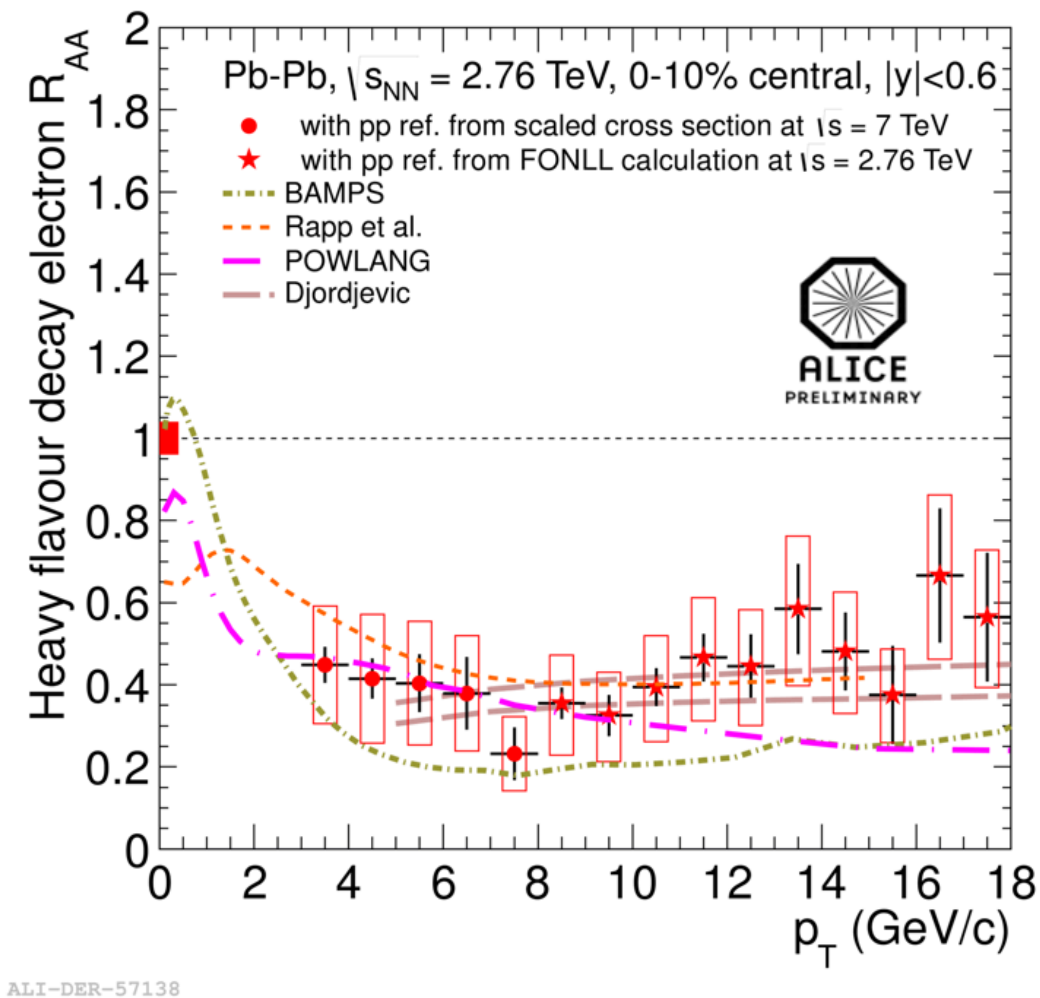

Heavy flavor particles show a non-zero elliptic flow.

v2 of HF → μ at forward rapidity similar as for heavy flavor electrons in central rapidity.

Simultaneous description of v_2 and R_{AA} poses a challenge to theoretical models (similar for the direct measurement of D mesons)

Flow and R_{AA} of heavy flavor decay muons/electrons (2)

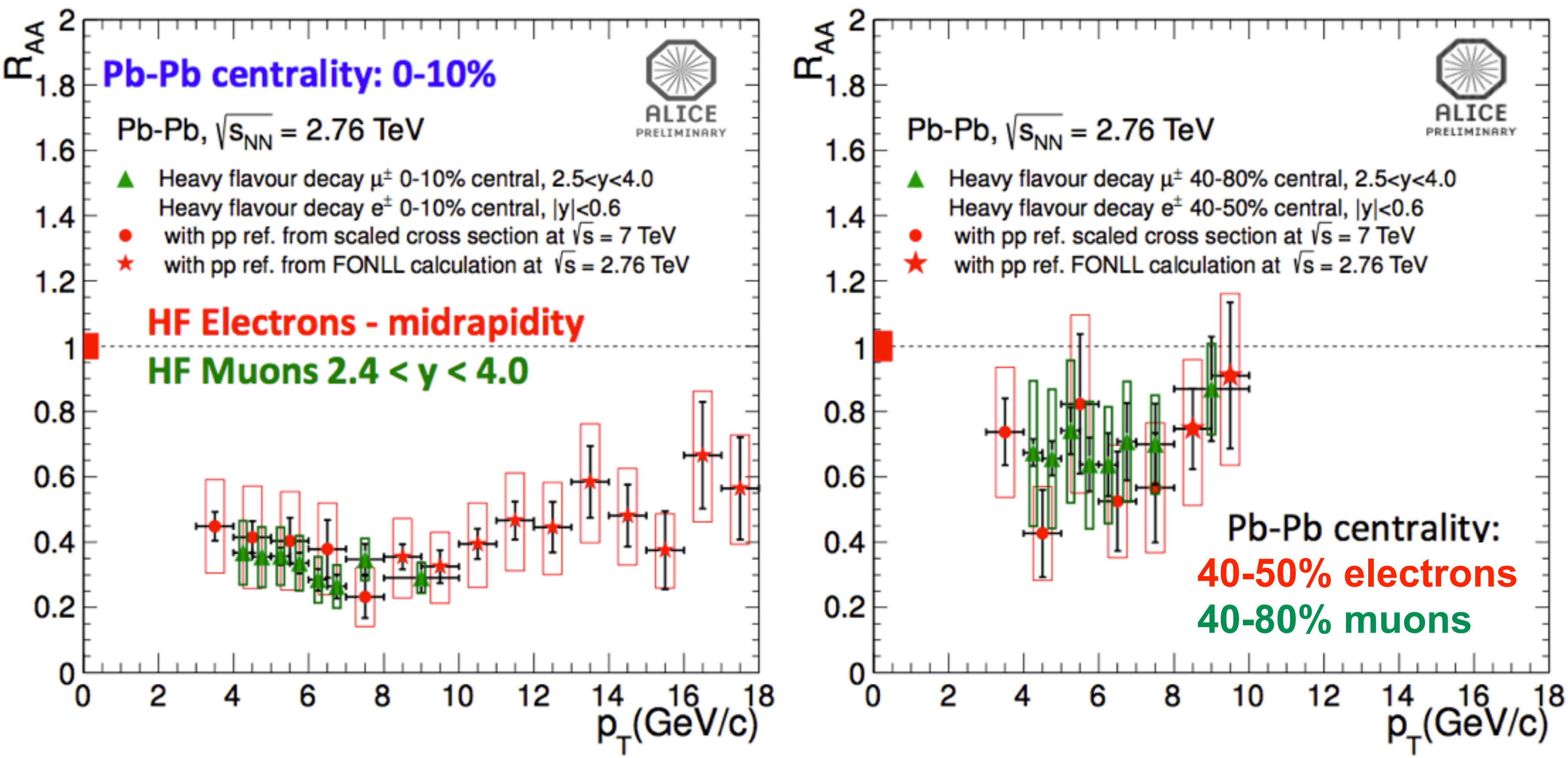

Flow and R_{AA} of heavy flavor decay muons/electrons (2)

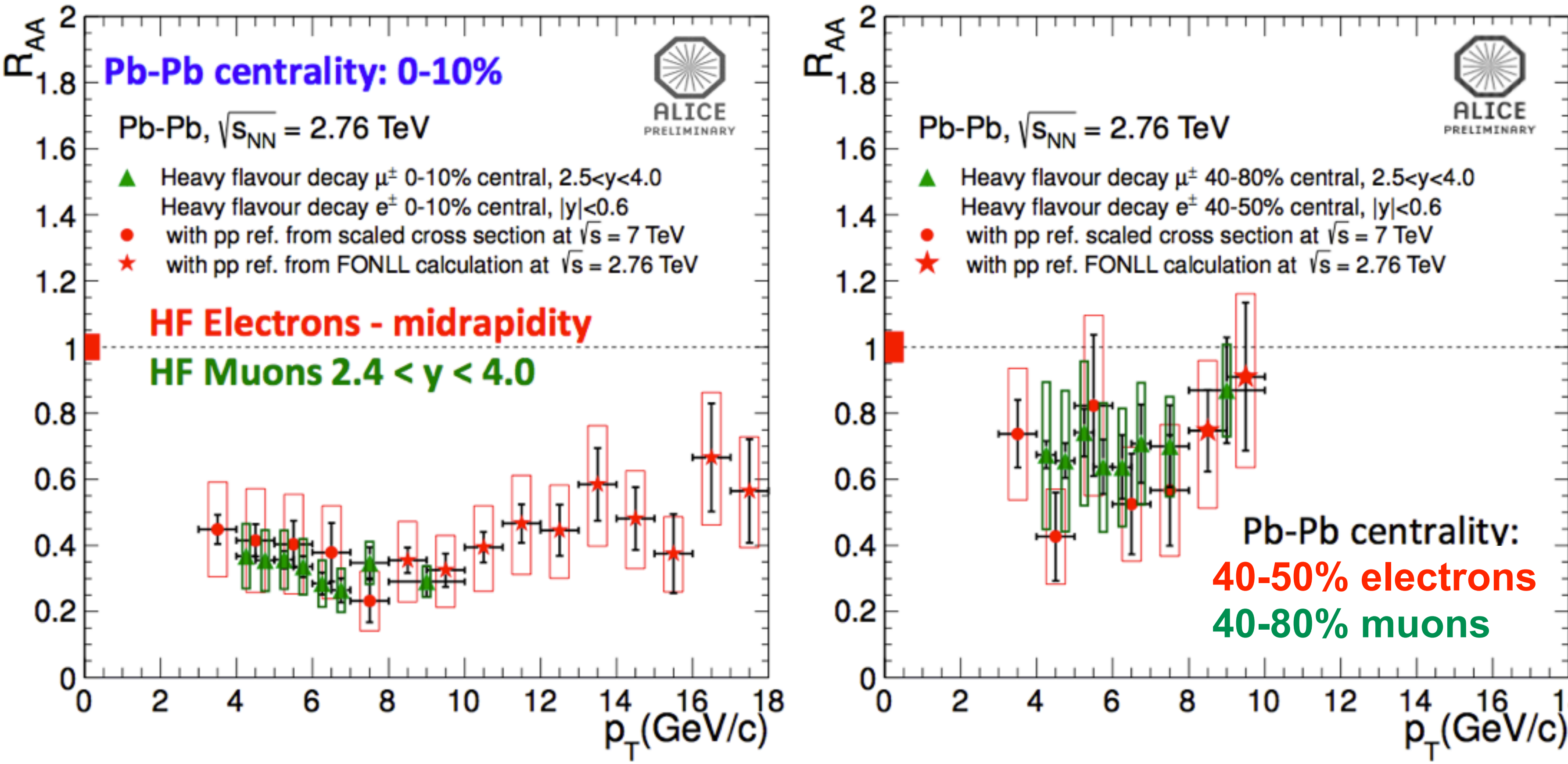

Similar suppression pattern and centrality dependence for muons (forward $2.4 < \eta < 5$) and electrons (central $|\eta| < 0.7$).

Heavy-flavor in p-Pb

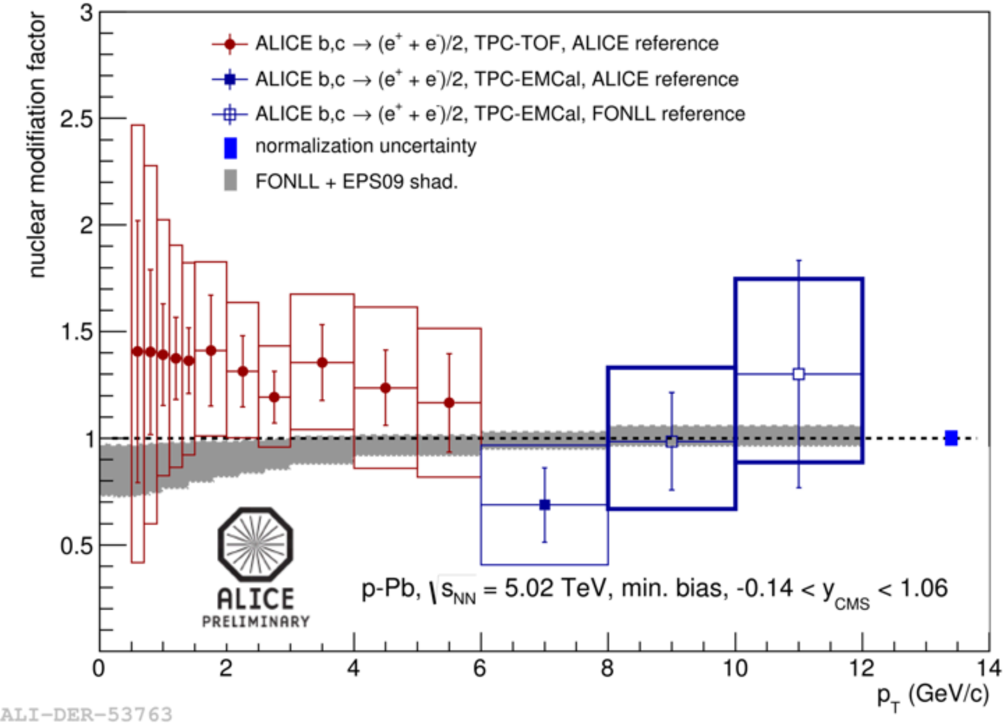

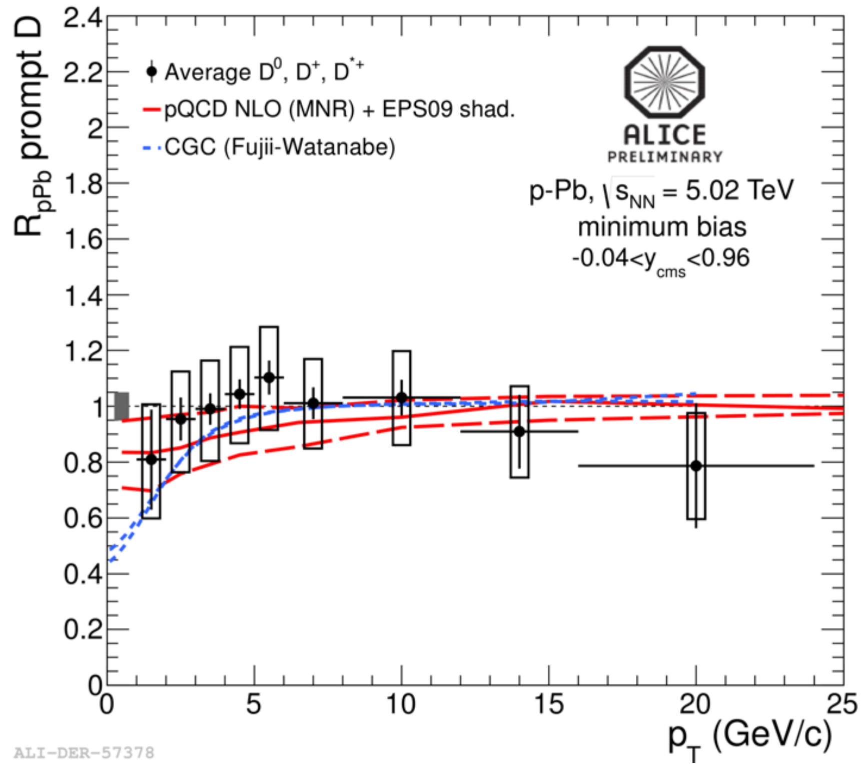

Heavy-flavor in p-Pb

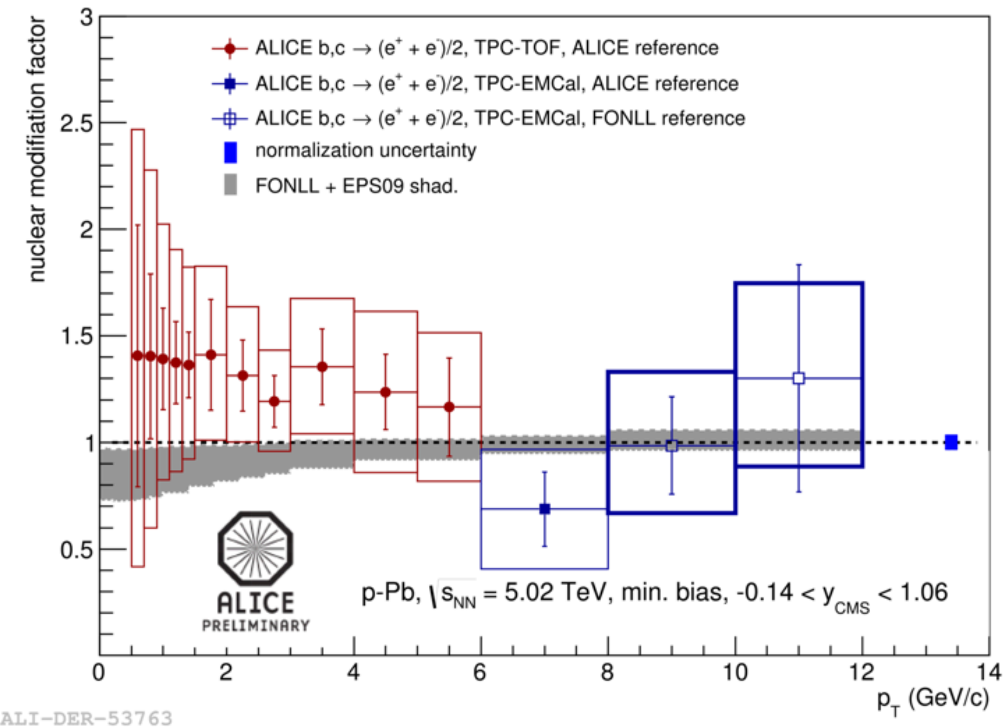

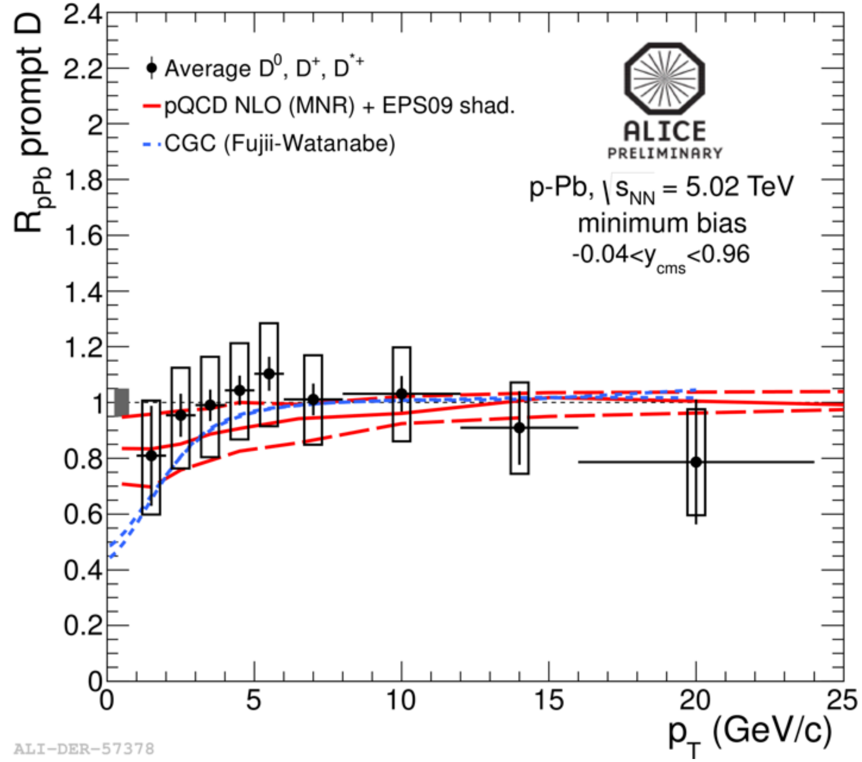

Nuclear modification factor R_{pPb} of HF→e at mid-rapidity is consistent with unity within uncertainties.

Heavy-flavor in p-Pb

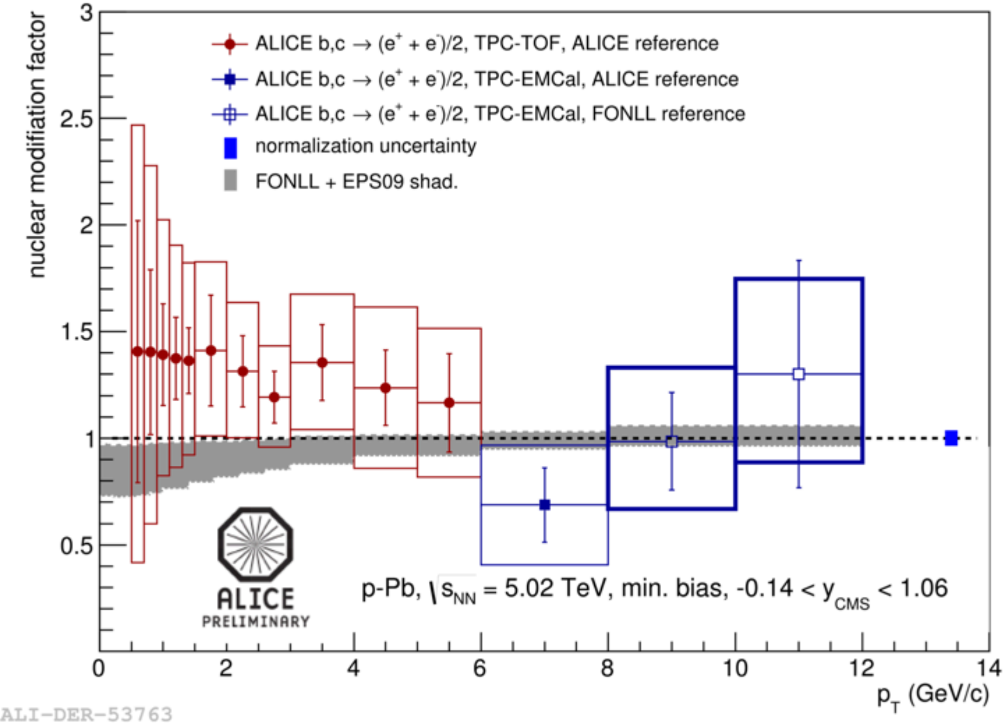

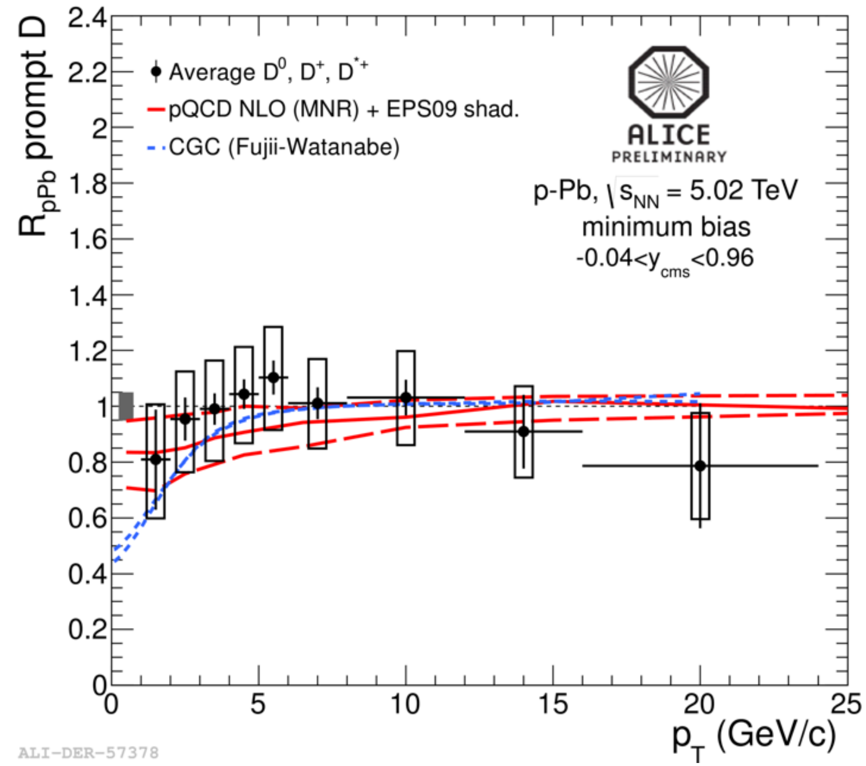

Nuclear modification factor R_{pPb} of HF→e at mid-rapidity is consistent with unity within uncertainties.

Pb-Pb suppression is not a cold nuclear matter effect. It is a final state effect.

Heavy-flavor in p-Pb

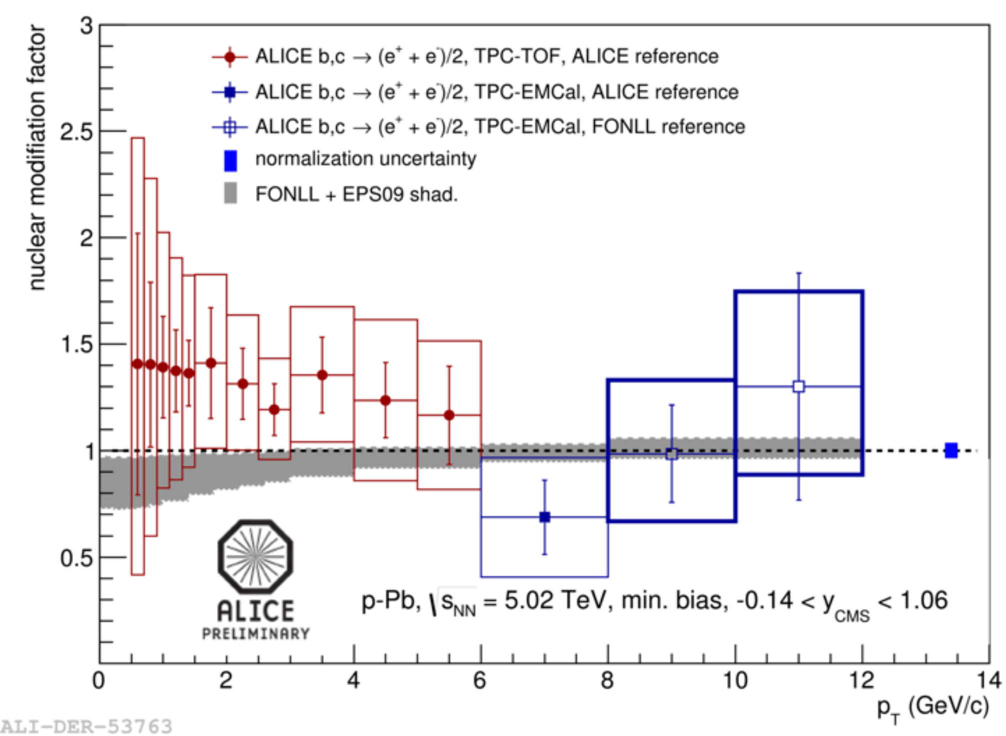

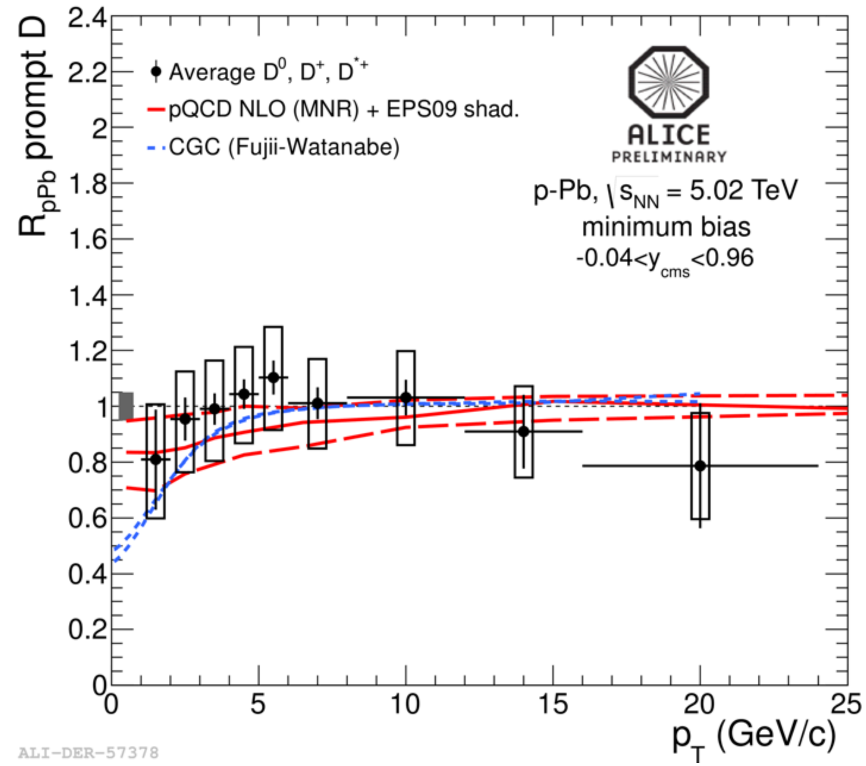

Nuclear modification factor R_{pPb} of HF→e at mid-rapidity is consistent with unity within uncertainties.

Pb-Pb suppression is not a cold nuclear matter effect.
It is a final state effect.

R_{pPb} of D-mesons is consistent with CGC and perturbative QCD MNR +EPS09 shadowing calculations.

Quarkonia in p-Pb

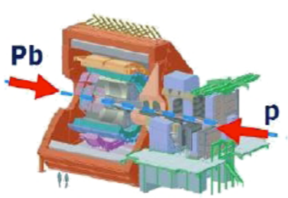

-4.46<y_{CMS}<-2.96

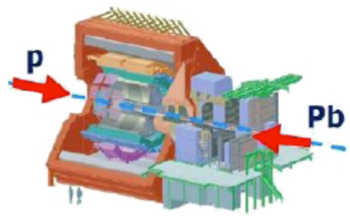

2.03<y_{CMS}<3.53

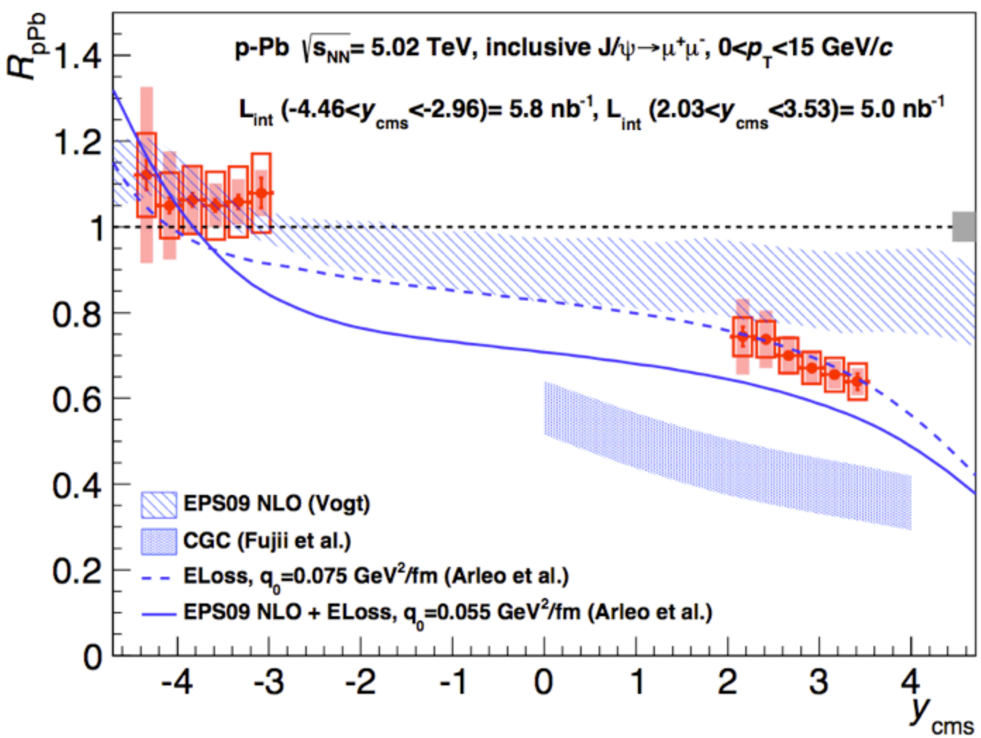

Quarkonia in p-Pb

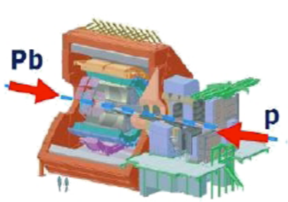

$-4.46<y_{CMS}<-2.96$

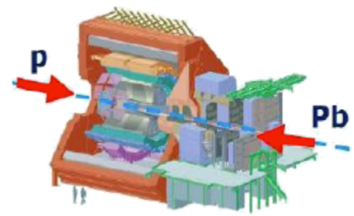

$2.03<y_{CMS}<3.53$

Nuclear absorption effects are small at the LHC. Data allows quantitative comparison with theory. New: measurement of Υ(1s)

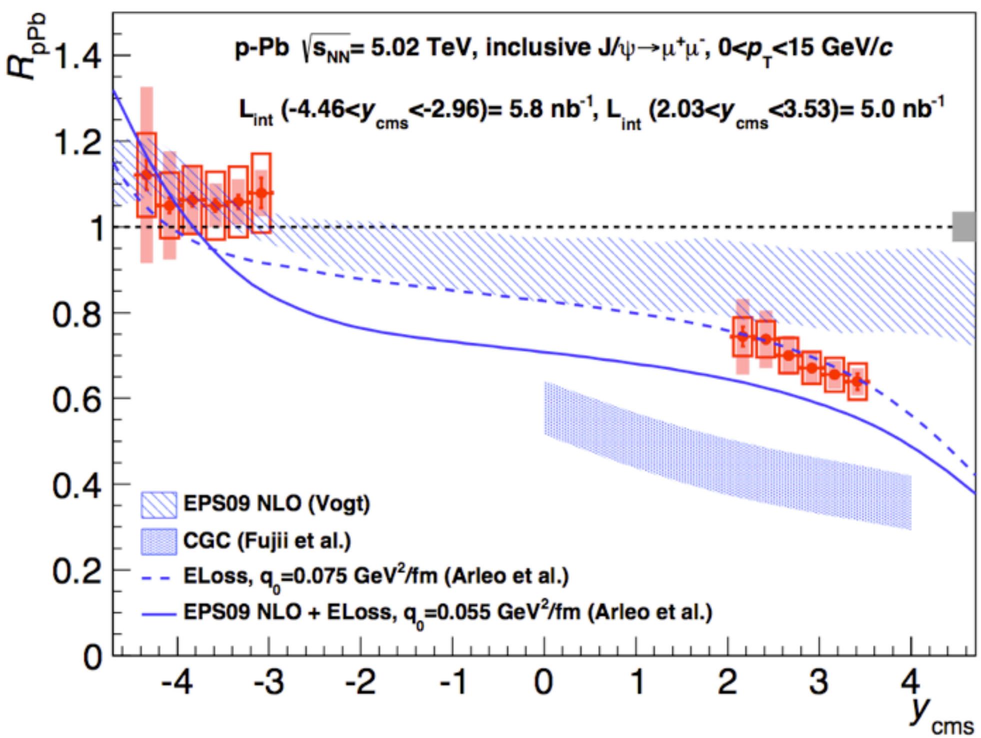

Quarkonia in p-Pb

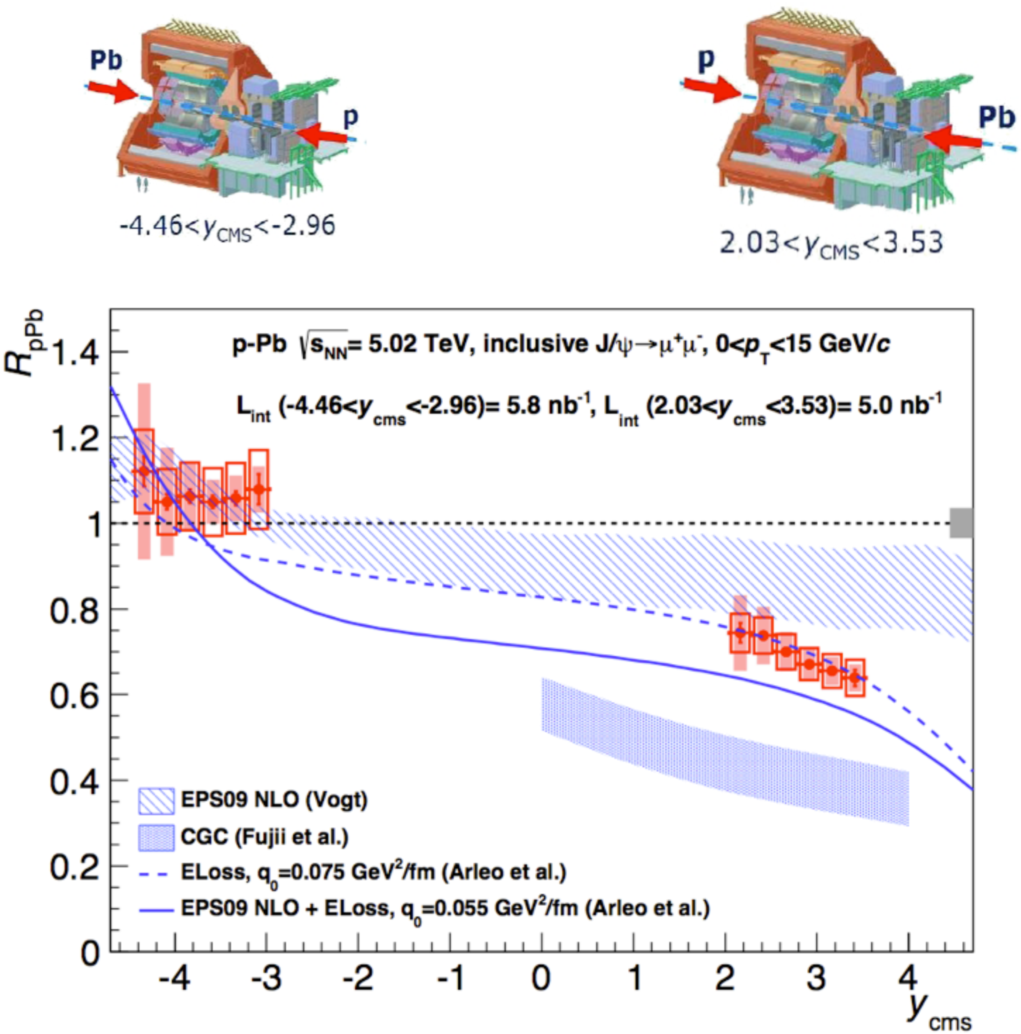

Nuclear absorption effects are small at the LHC. Data allows quantitative comparison with theory. New: measurement of Υ(1s)

Theoretical predictions based on nuclear shadowing (EPS09 + NLO by R. Vogt) are in fair agreement with the J/ψ data. They reproduces trend the for Υ(1s), but with slightly larger values.

Quarkonia in p-Pb

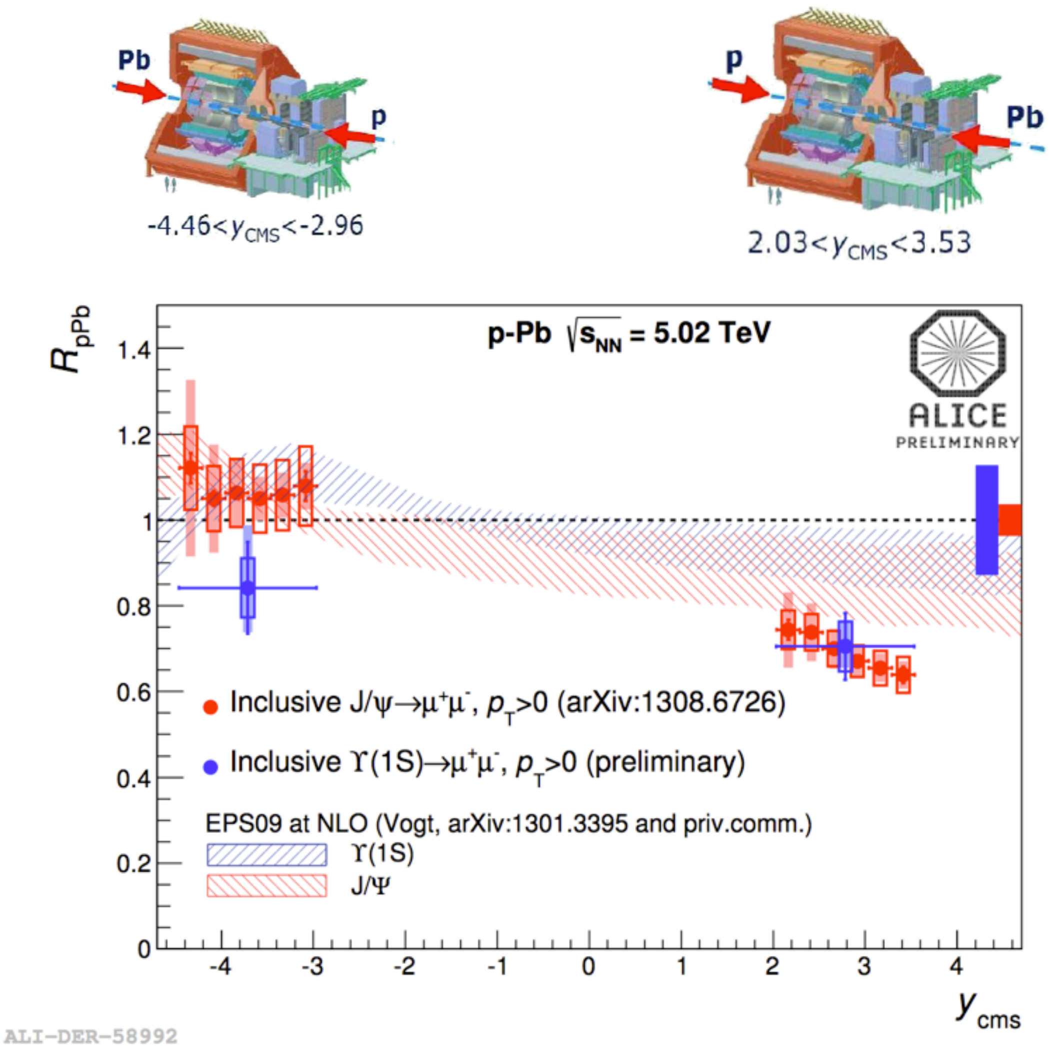

Nuclear absorption effects are small at the LHC. Data allows quantitative comparison with theory. New: measurement of Υ(1s)

Theoretical predictions based on nuclear shadowing (EPS09 + NLO by R. Vogt) are in fair agreement with the J/ψ data. They reproduces trend the for Υ(1s), but with slightly larger values.

Quarkonia in p-Pb

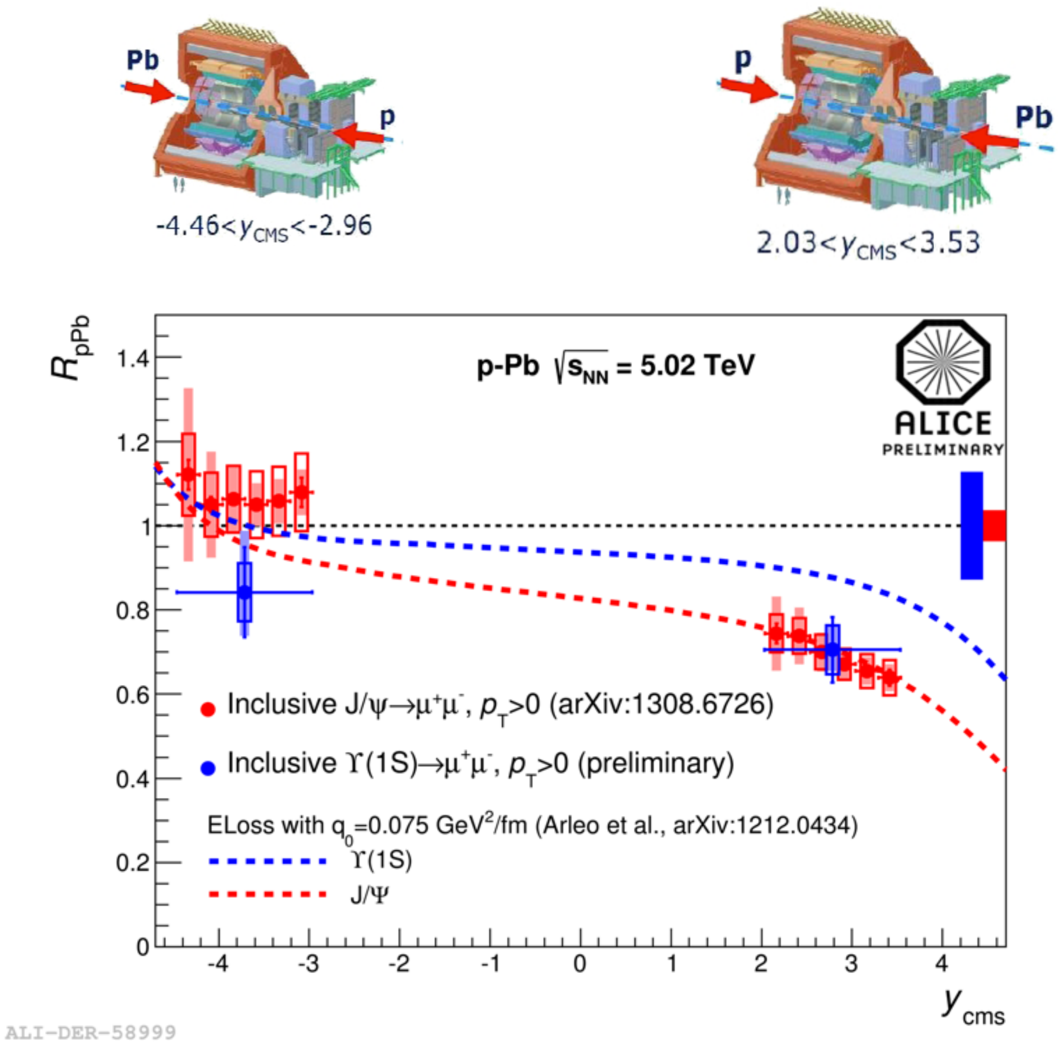

Nuclear absorption effects are small at the LHC. Data allows quantitative comparison with theory. New: measurement of Y(1s)

Theoretical predictions based on nuclear shadowing (EPS09 + NLO by R. Vogt) are in fair agreement with the J/ψ data. They reproduces trend the for Y(1s), but with slightly larger values.

Quarkonia in p-Pb

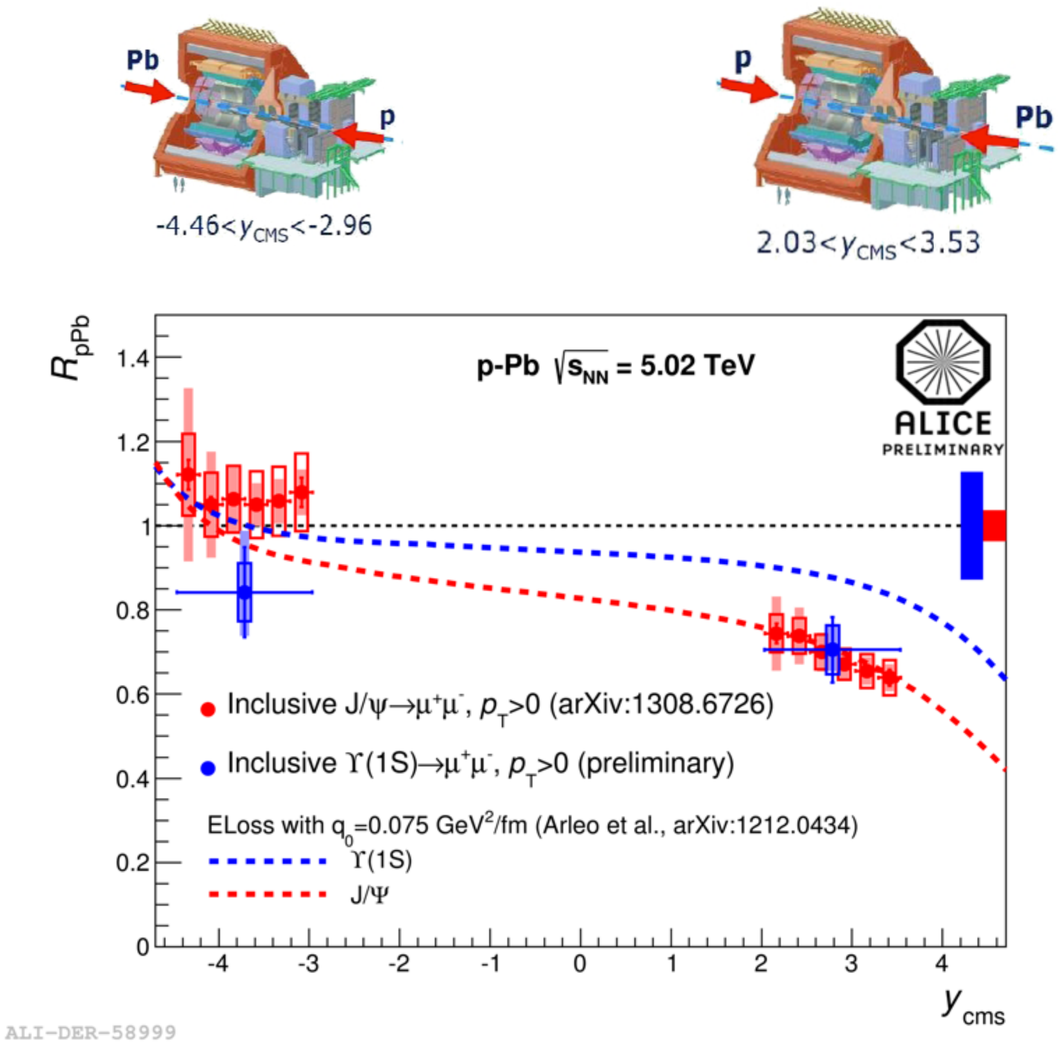

Nuclear absorption effects are small at the LHC. Data allows quantitative comparison with theory. New: measurement of Y(1s)

Theoretical predictions based on nuclear shadowing (EPS09 + NLO by R. Vogt) are in fair agreement with the J/ψ data. They reproduces trend the for Y(1s), but with slightly larger values.

Similarly for models including in addition partonic energy loss.

Quarkonia in p-Pb

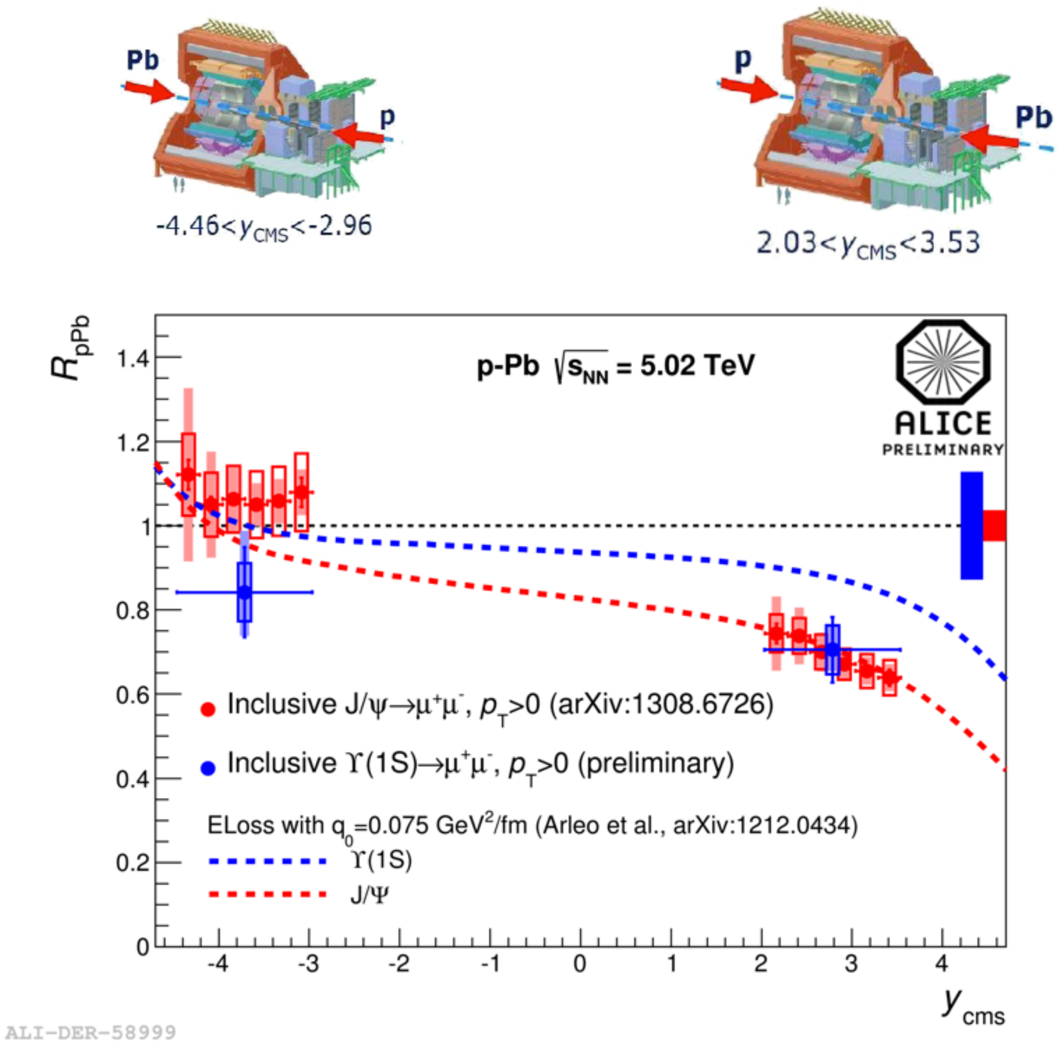

Nuclear absorption effects are small at the LHC. Data allows quantitative comparison with theory. New: measurement of Υ(1s)

Theoretical predictions based on nuclear shadowing (EPS09 + NLO by R. Vogt) are in fair agreement with the J/ψ data. They reproduces trend the for Υ(1s), but with slightly larger values.

Similarly for models including in addition partonic energy loss.

Number of models describe the forward-backward ratio within uncertainties: Υ(1s) favor low shadowing, high shadowing better for J/ψ data.

Jets in Pb-Pb and p-Pb

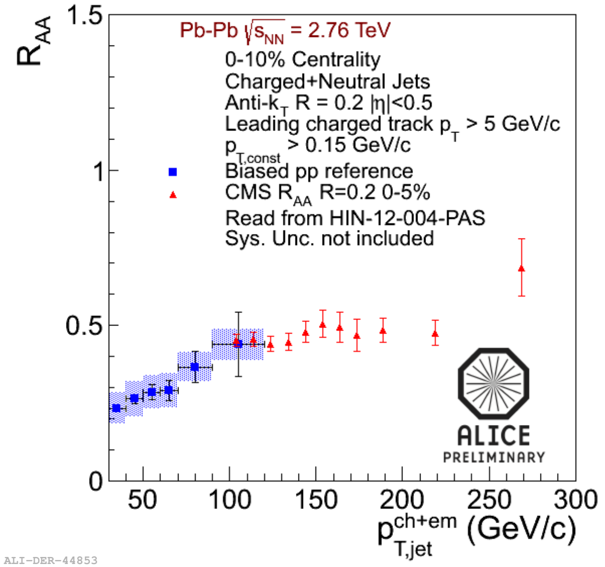

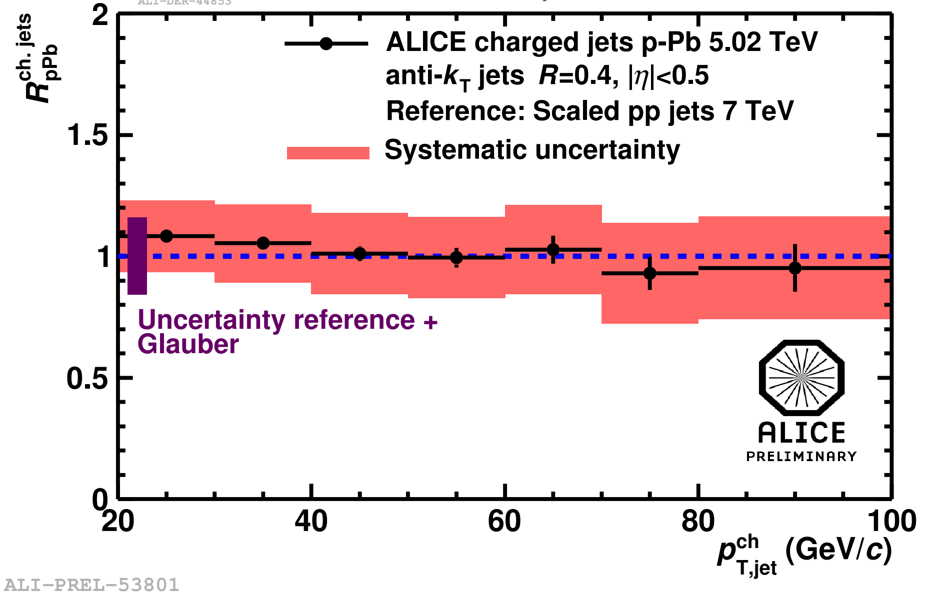

Jets in Pb-Pb and p-Pb

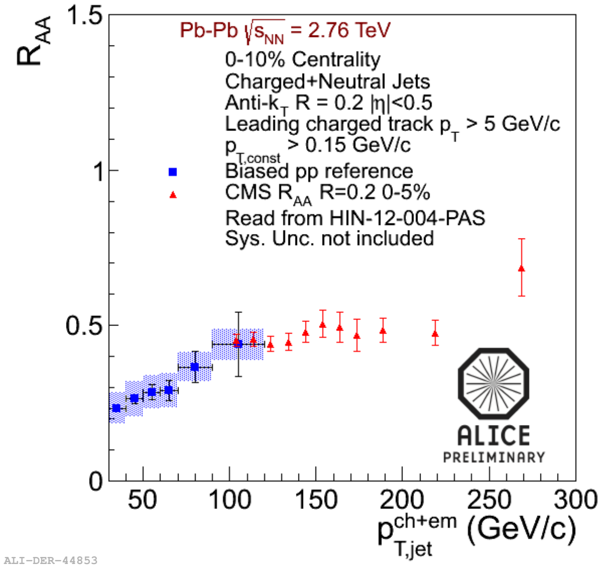

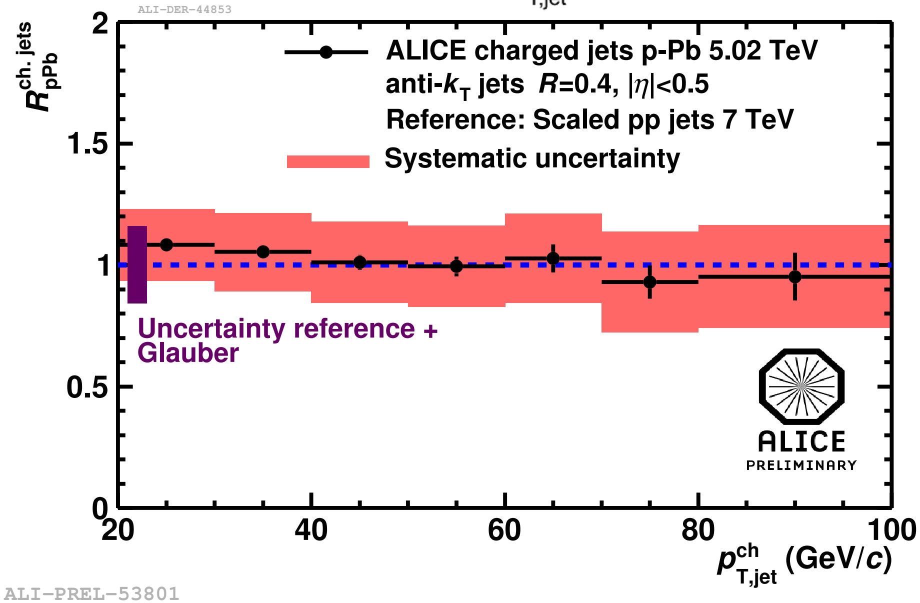

Jet R_{AA} measured down to 40 GeV/c.

Jets in Pb-Pb and p-Pb

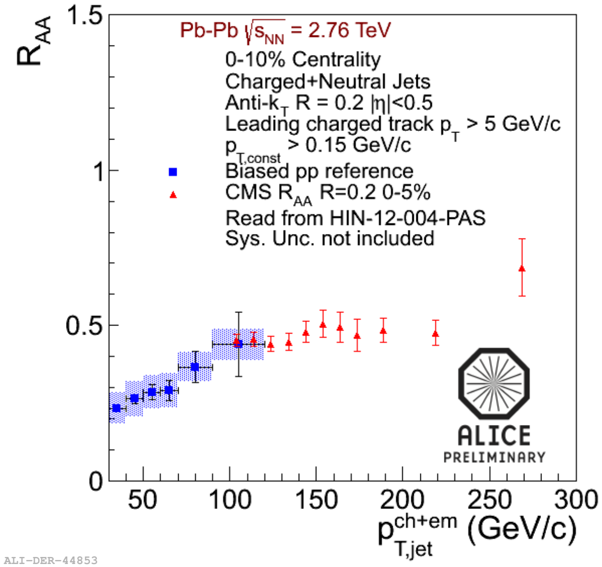

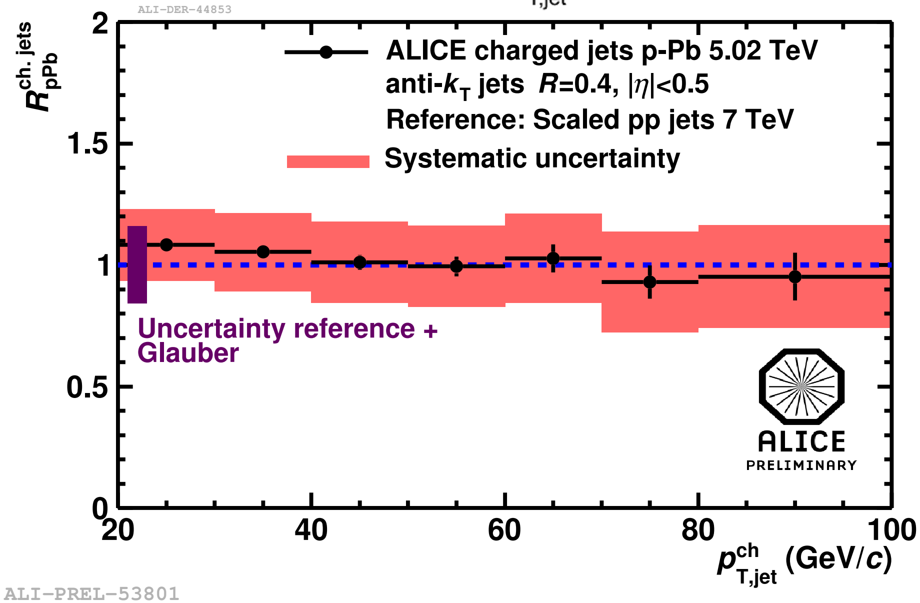

Jet R_{AA} measured down to 40 GeV/c.

Jets strongly suppressed in central Pb-Pb collisions

Jets in Pb-Pb and p-Pb

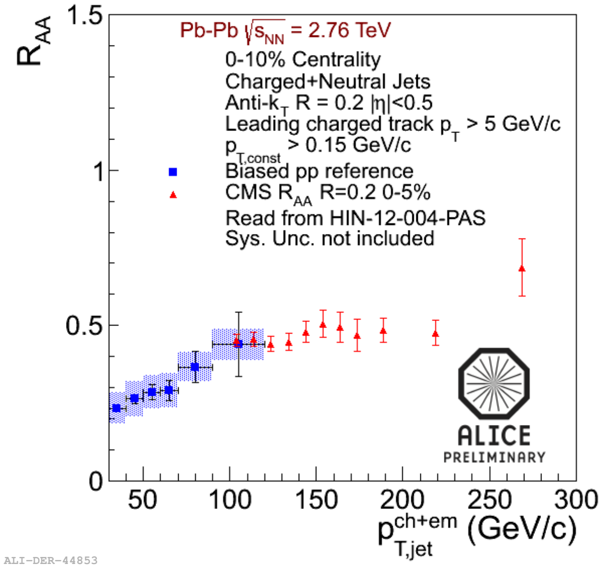

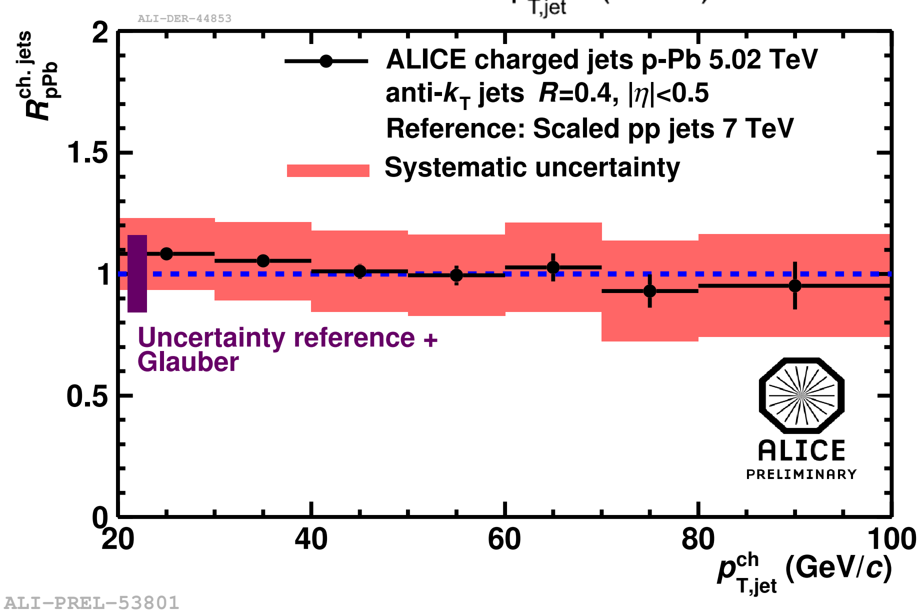

Jet R_{AA} measured down to 40 GeV/c.

Jets strongly suppressed in central Pb-Pb collisions

No suppression in p-Pb collisions.

Jets in Pb-Pb and p-Pb

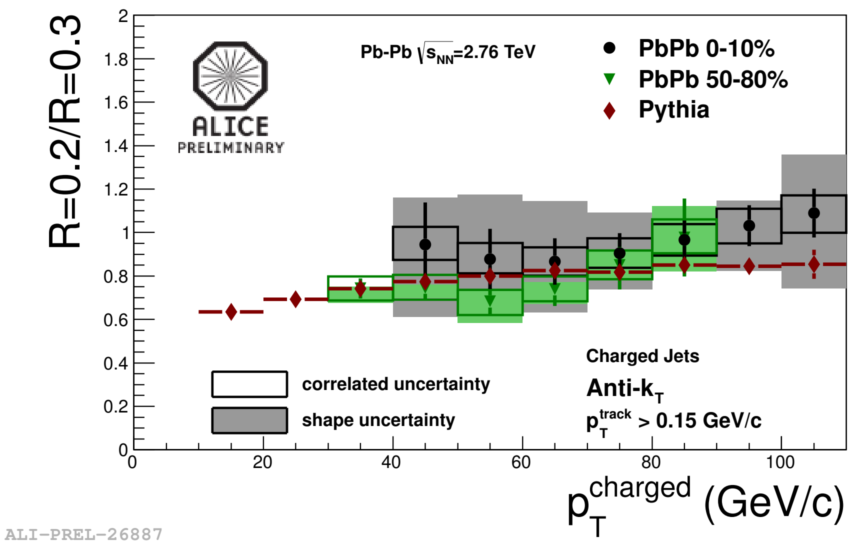

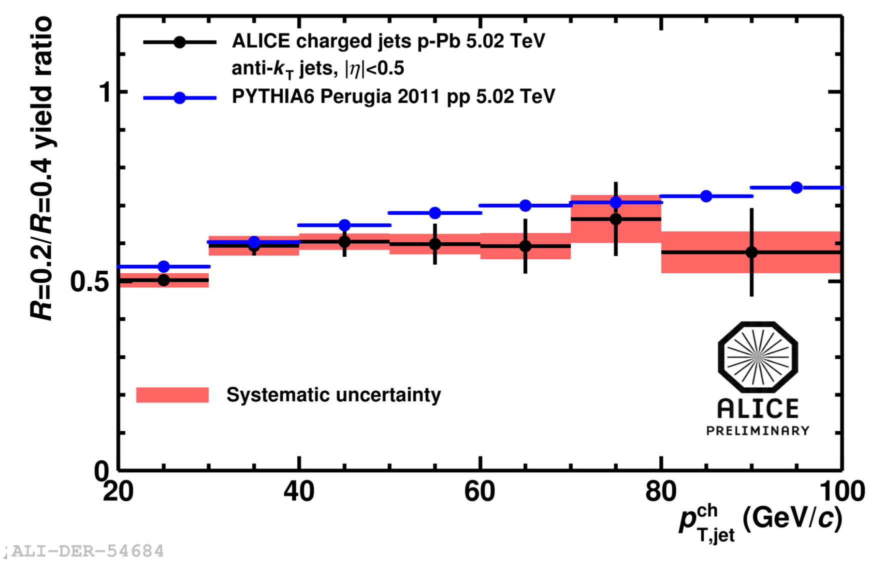

Jet R_{AA} measured down to 40 GeV/c.

Jets strongly suppressed in central Pb-Pb collisions

No suppression in p-Pb collisions.

Jets in Pb-Pb and p-Pb

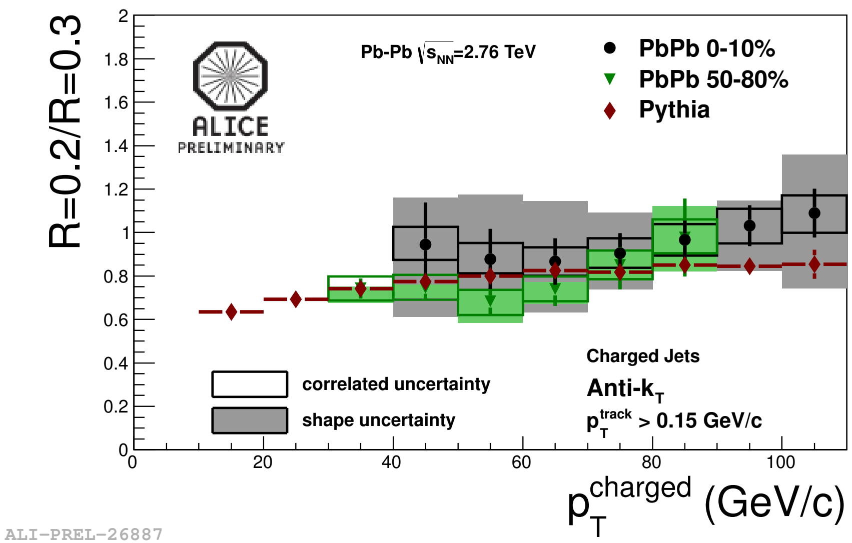

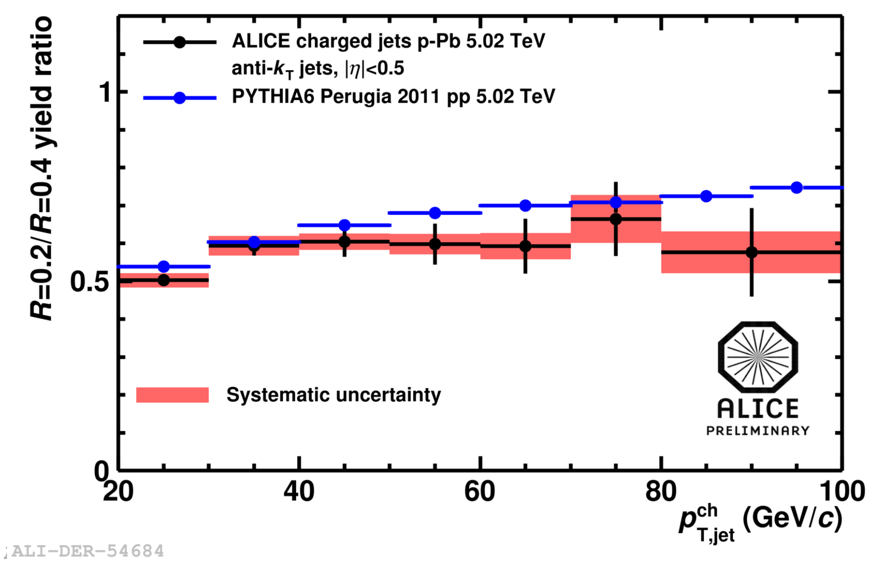

Jet R_{AA} measured down to 40 GeV/c.

Jets strongly suppressed in central Pb-Pb collisions

No suppression in p-Pb collisions.

Jet cross-section ratios (R=0.2/R=0.3) in Pb-Pb and p-Pb (R=0.2/R=0.4) are compatible with pp within uncertainties.

Detector status
(current LS1 activities)

LS1 plans and progress

Main activities planned for LS1:

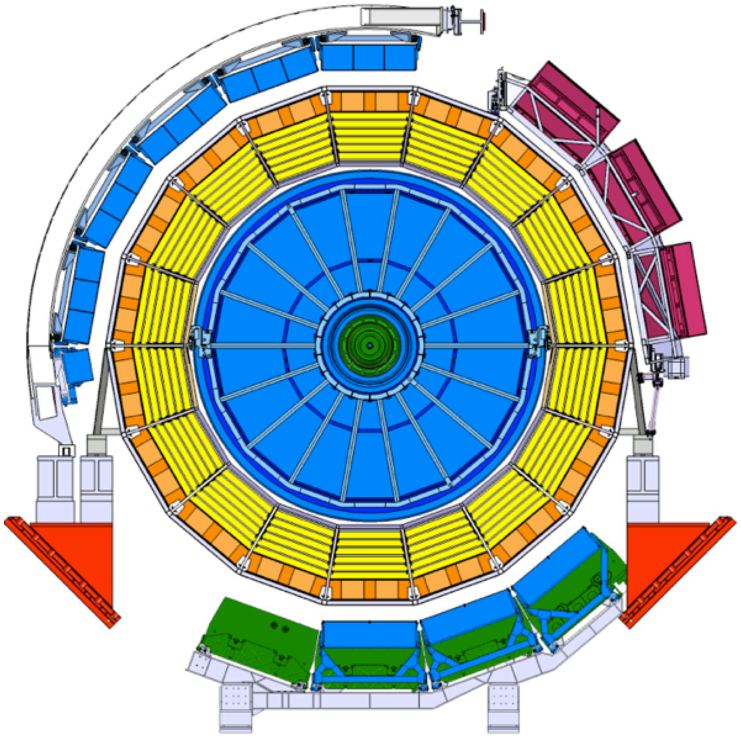

- Complete TRD (+5 supermodules)
- Install DCal calorimeter (8 supermodules)
- Install 1 PHOS supermodule
- Numerous detector consolidation efforts
- EN-EL: UPS replacement and electrical infrastructure consolidation
- EN-CV: P2 chilled water upgrade (+60% power)
- EN-CV: L3 magnet ventilation upgrade (+60% flow)

LS1 plans and progress

Main activities planned for LS1:

- Complete TRD (+5 supermodules)
- Install DCal calorimeter (8 supermodules)
- Install 1 PHOS supermodule
- Numerous detector consolidation efforts
- EN-EL: UPS replacement and electrical infrastructure consolidation
- EN-CV: P2 chilled water upgrade (+60% power)
- EN-CV: L3 magnet ventilation upgrade (+60% flow)

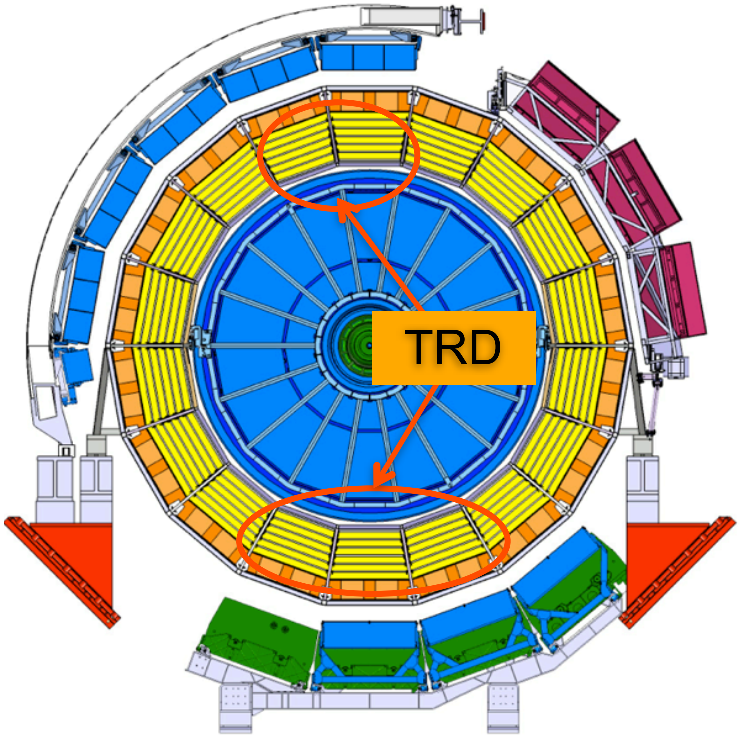

LS1 plans and progress

Main activities planned for LS1:

- Complete TRD (+5 supermodules)
- Install DCal calorimeter (8 supermodules)
- Install 1 PHOS supermodule
- Numerous detector consolidation efforts
- EN-EL: UPS replacement and electrical infrastructure consolidation
- EN-CV: P2 chilled water upgrade (+60% power)
- EN-CV: L3 magnet ventilation upgrade (+60% flow)

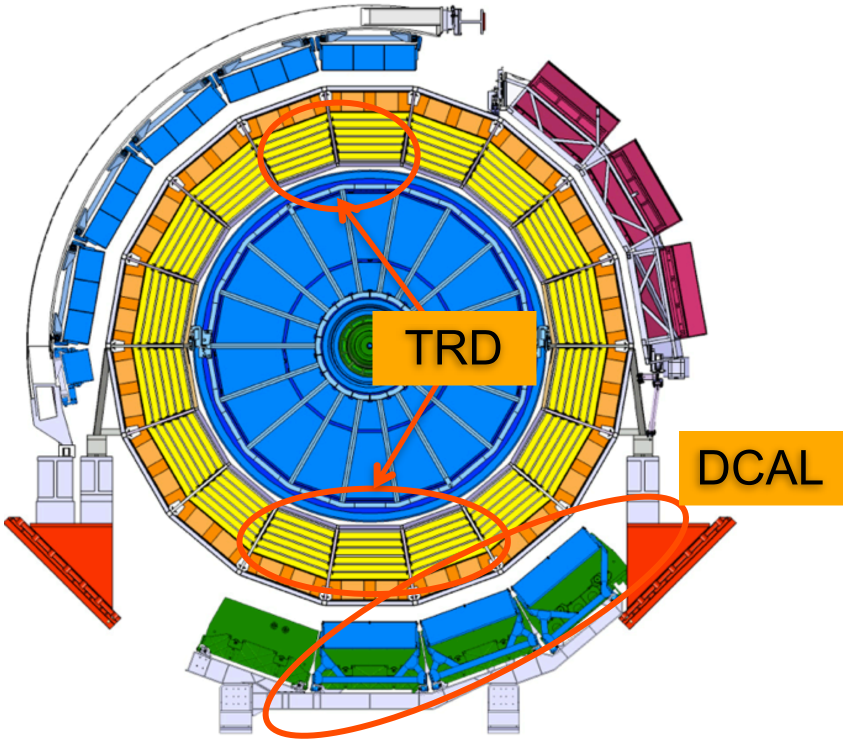

LS1 plans and progress

Main activities planned for LS1:

- Complete TRD (+5 supermodules)
- Install DCal calorimeter (8 supermodules)
- Install 1 PHOS supermodule
- Numerous detector consolidation efforts
- EN-EL: UPS replacement and electrical infrastructure consolidation
- EN-CV: P2 chilled water upgrade (+60% power)
- EN-CV: L3 magnet ventilation upgrade (+60% flow)

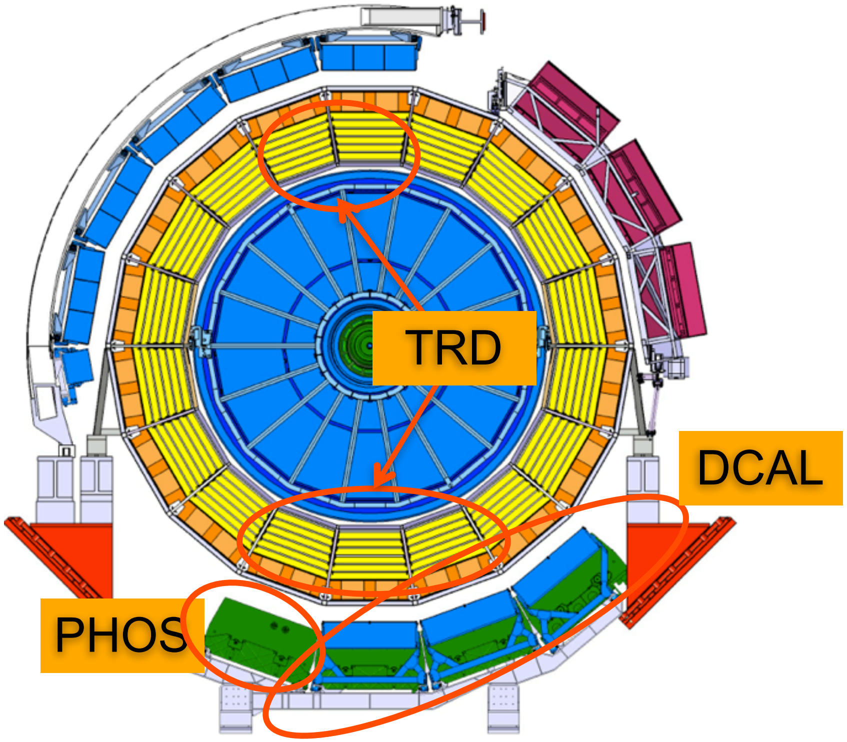

LS1 plans and progress

Main activities planned for LS1:

- Complete TRD (+5 supermodules)
- Install DCal calorimeter (8 supermodules)
- Install 1 PHOS supermodule
- Numerous detector consolidation efforts
- EN-EL: UPS replacement and electrical infrastructure consolidation
- EN-CV: P2 chilled water upgrade (+60% power)
- EN-CV: L3 magnet ventilation upgrade (+60% flow)

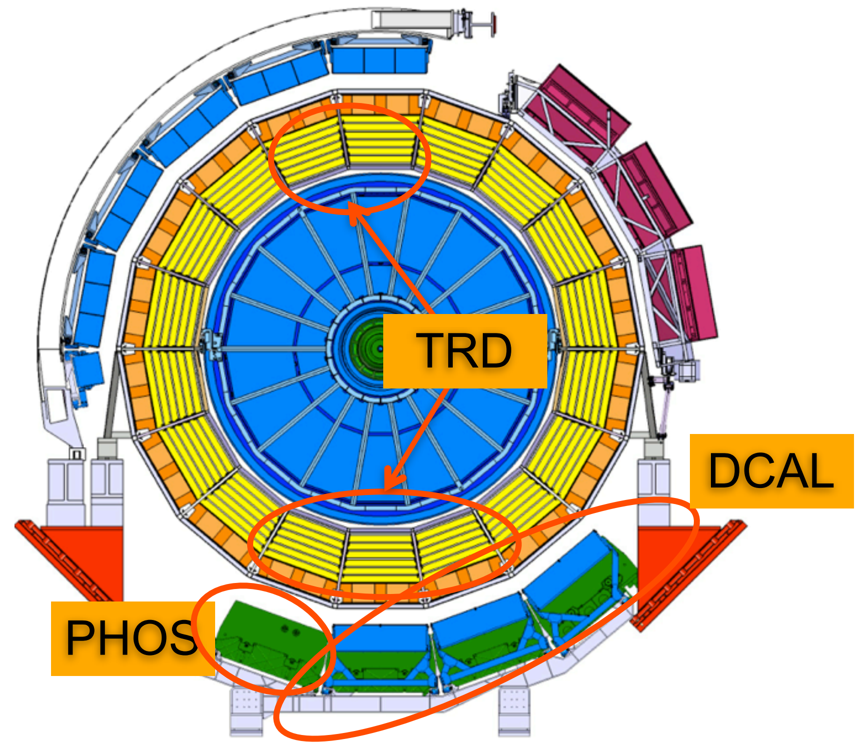

On track with LS1 schedule, but still a lot of work ahead.

LS1 plans and progress

Main activities planned for LS1:

- Complete TRD (+5 supermodules)
- Install DCal calorimeter (8 supermodules)
- Install 1 PHOS supermodule
- Numerous detector consolidation efforts
- EN-EL: UPS replacement and electrical infrastructure consolidation
- EN-CV: P2 chilled water upgrade (+60% power)
- EN-CV: L3 magnet ventilation upgrade (+60% flow)

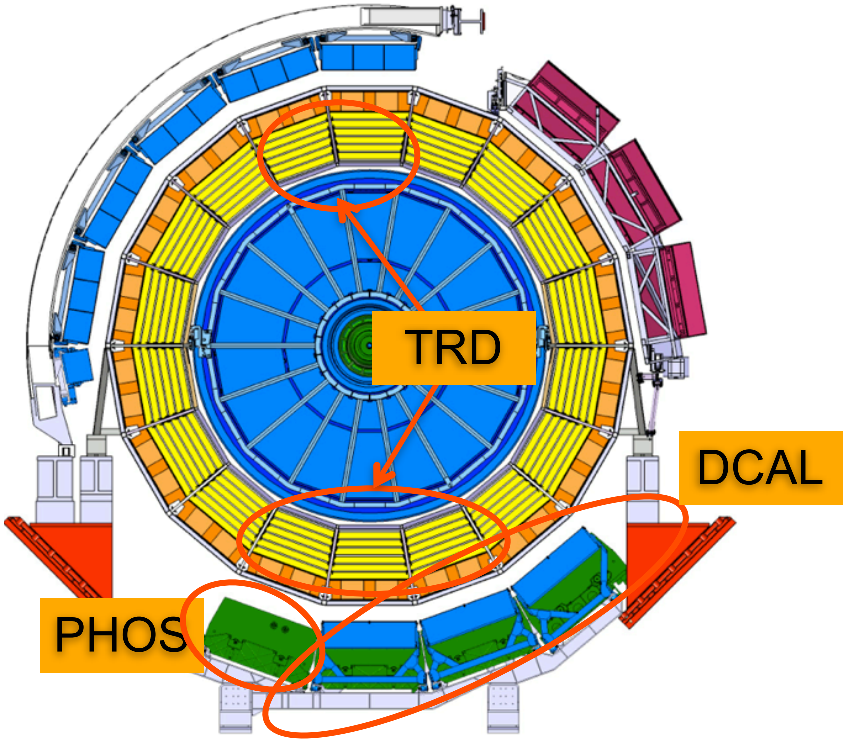

On track with LS1 schedule, but still a lot of work ahead.

A lot of activities ongoing at P2 with deep involvement of several CERN groups (EN-EL, EN-CV,..)

Detector and services consolidation

Detector and services consolidation

TRD de-installation

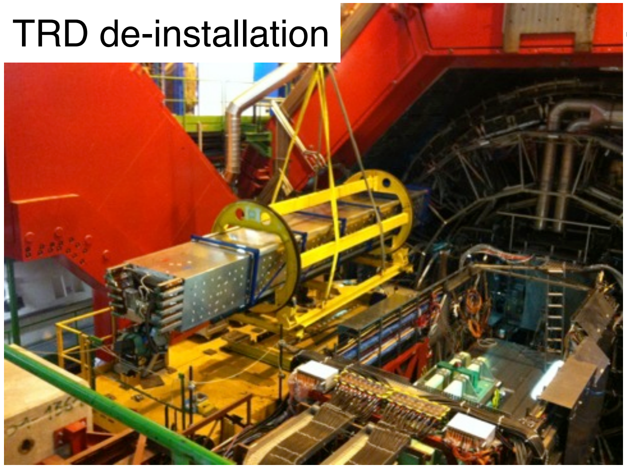

TRD LV rework:

- LV issue: hot connections due to not proper tightening of cables on patch-panel
- Fix: de-install 7 TRD SMs, rework LV distribution and re-install them in LS1
- Progress: 50% done – will be complete by end November

Detector and services consolidation

TRD de-installation

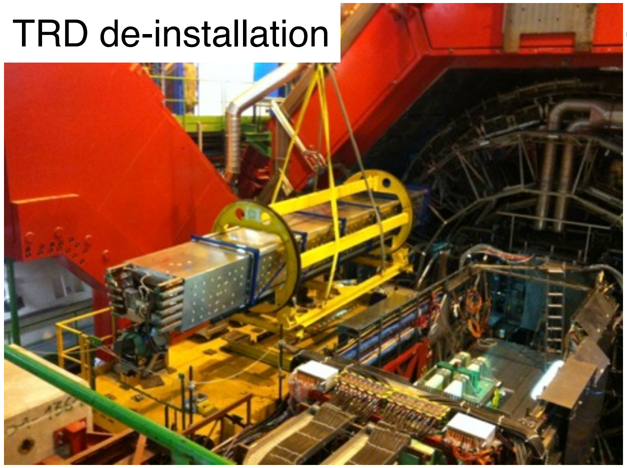

TRD LV rework:

- LV issue: hot connections due to not proper tightening of cables on patch-panel
- Fix: de-install 7 TRD SMs, rework LV distribution and re-install them in LS1
- Progress: 50% done – will be complete by end November

UPS upgrade:

UPS replaced and electrical infrastructure consolidation completed

Detector and services consolidation

TRD de-installation

TRD LV rework:

- LV issue: hot connections due to not proper tightening of cables on patch-panel
- Fix: de-install 7 TRD SMs, rework LV distribution and re-install them in LS1
- Progress: 50% done – will be complete by end November

UPS upgrade:

UPS replaced and electrical infrastructure consolidation completed

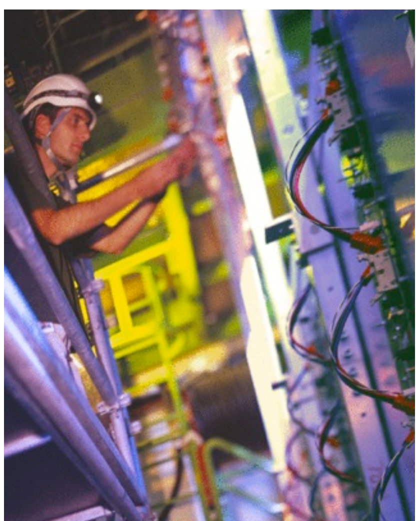

Muon Tracker LV rework:

- Almost 90 chambers (slats) to be repaired (re-solder LV busbar connection), in order to fix the occupancy problem
- Activity started in week 1 of LS1. Will take the whole 2013

Detector and services consolidation

TRD de-installation

TRD LV rework:

- LV issue: hot connections due to not proper tightening of cables on patch-panel
- Fix: de-install 7 TRD SMs, rework LV distribution and re-install them in LS1
- Progress: 50% done – will be complete by end November

UPS upgrade:

UPS replaced and electrical infrastructure consolidation completed

Muon Tracker LV rework:

- Almost 90 chambers (slats) to be repaired (re-solder LV busbar connection), in order to fix the occupancy problem
- Activity started in week 1 of LS1. Will take the whole 2013

CR1 (DAQ) renovation:

- All DAQ infrastructure dismantled, CR1 emptied
- Replacement old racks (LEP times) with new ones, with more powerful cooling
- Replacement of central router and installation of new LDCs

Low voltage rework

TRD-TPC-TOF cables in the back-frame

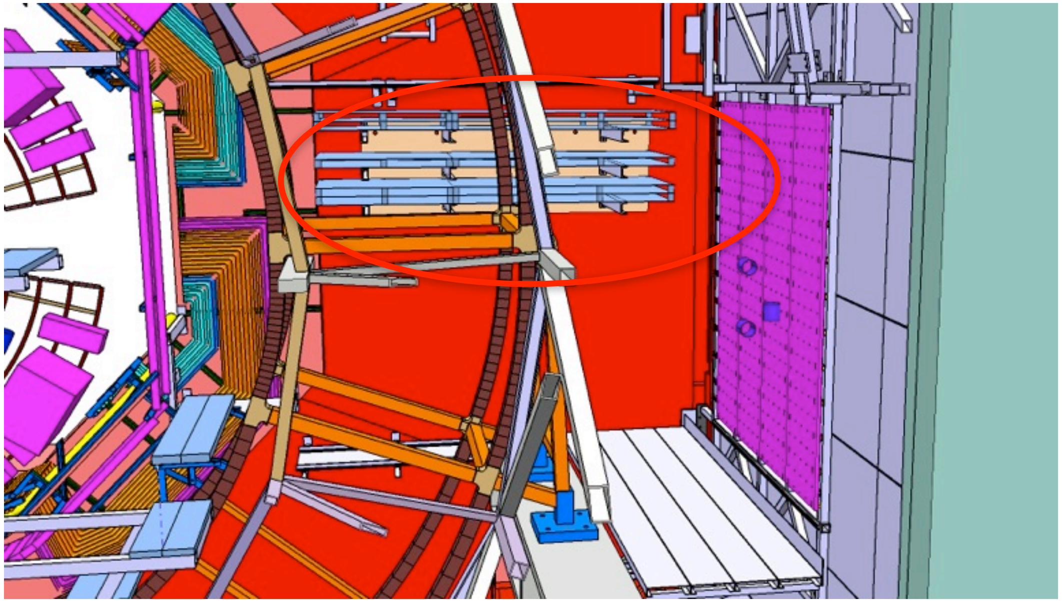

Low voltage rework

TRD-TPC-TOF cables in the back-frame

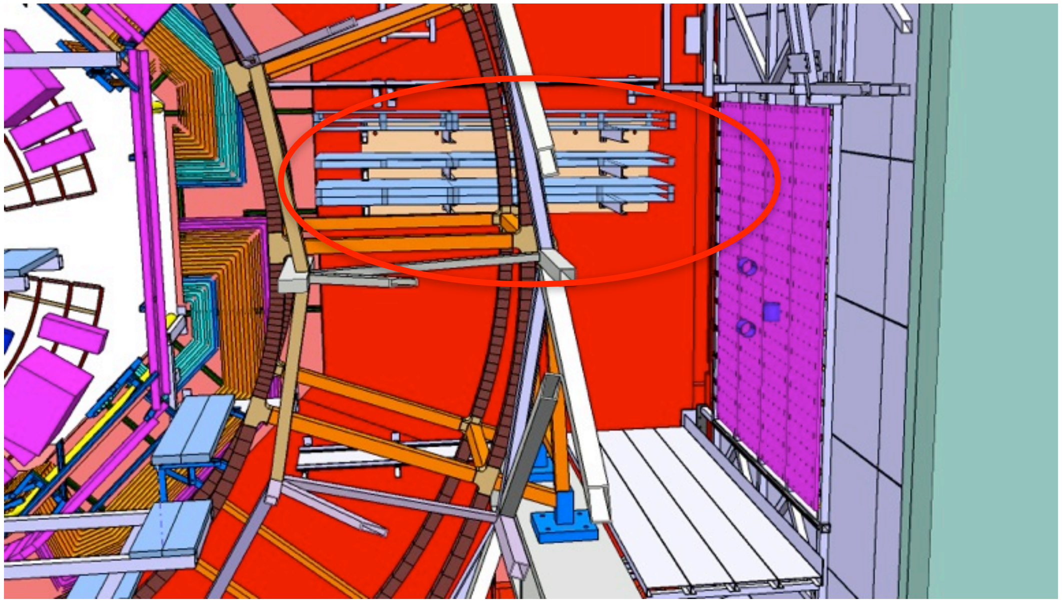

Rework of thick LV cables started beginning of June (O-side).

Low voltage rework

TRD-TPC-TOF cables in the back-frame

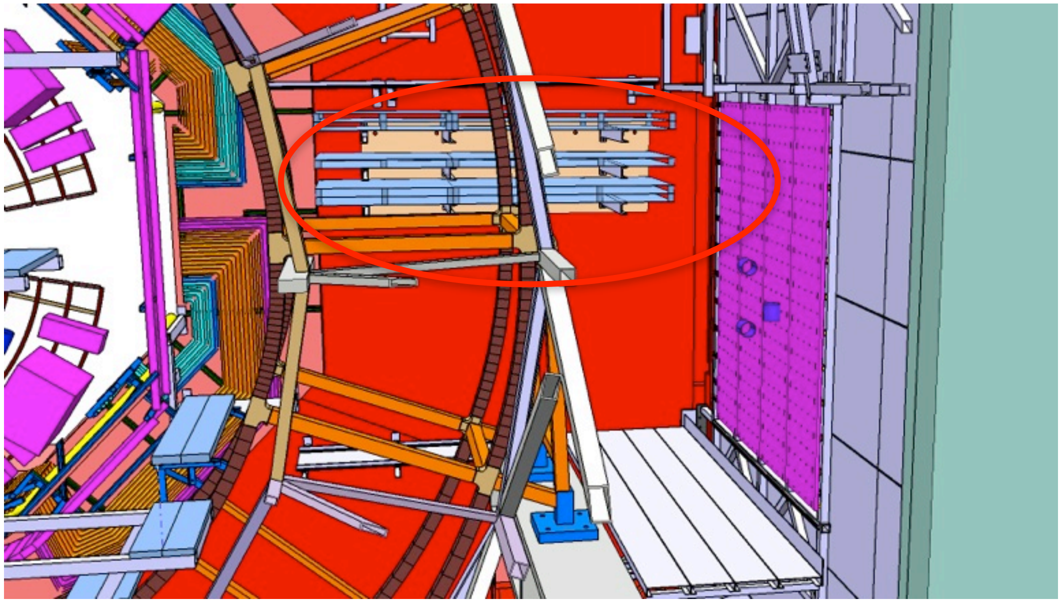

Rework of thick LV cables started beginning of June (O-side).

Plan to complete the intervention by mid November.

DCal installation

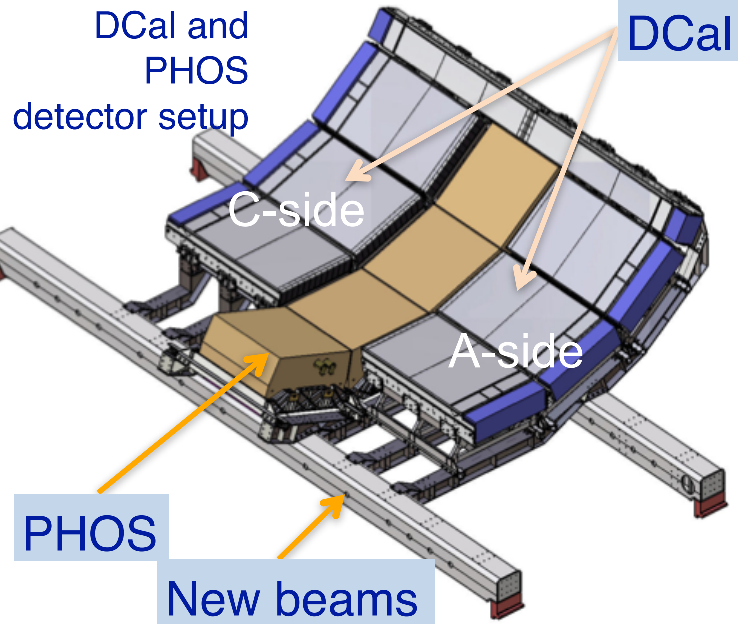

DCal installation

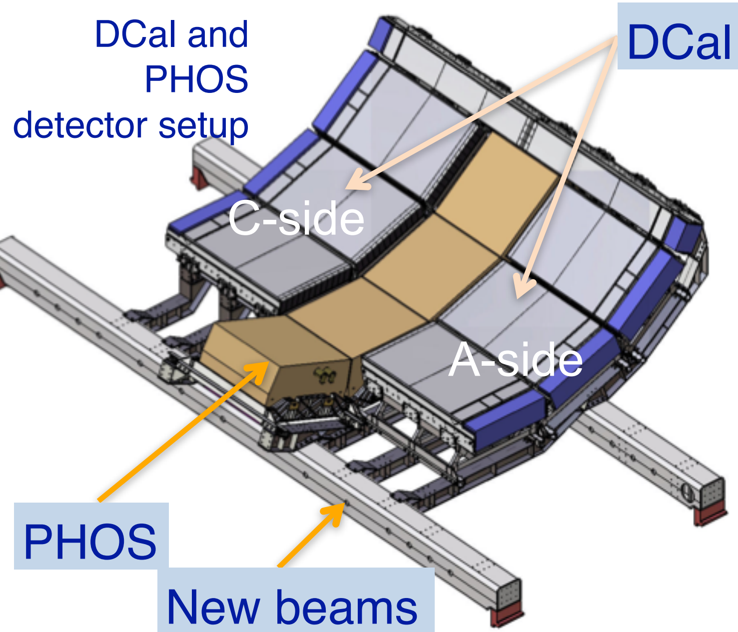

New beams installed
L3 in June

DCal installation

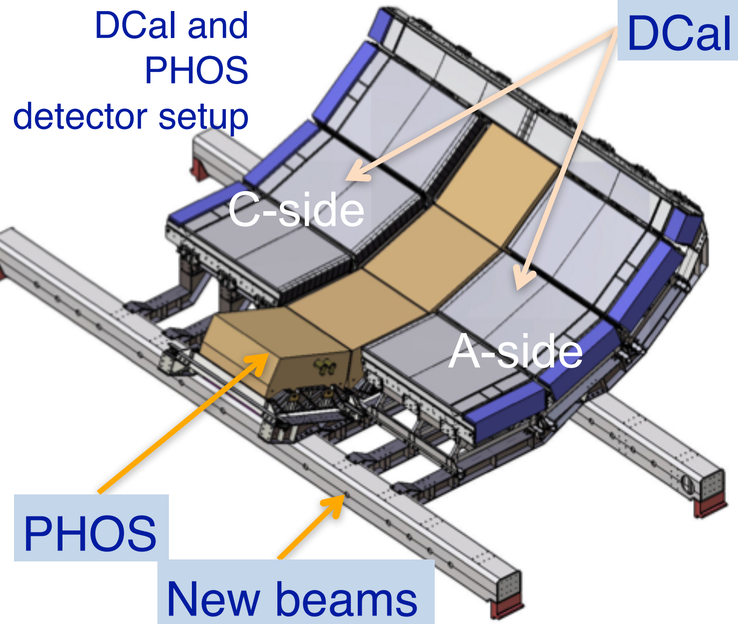

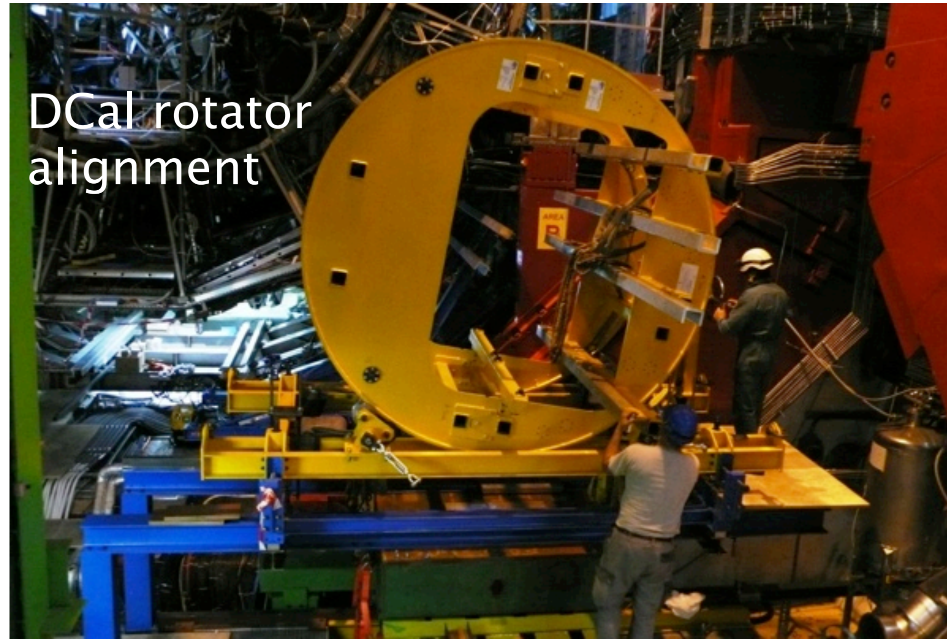

New beams installed
L3 in June

DCal installation

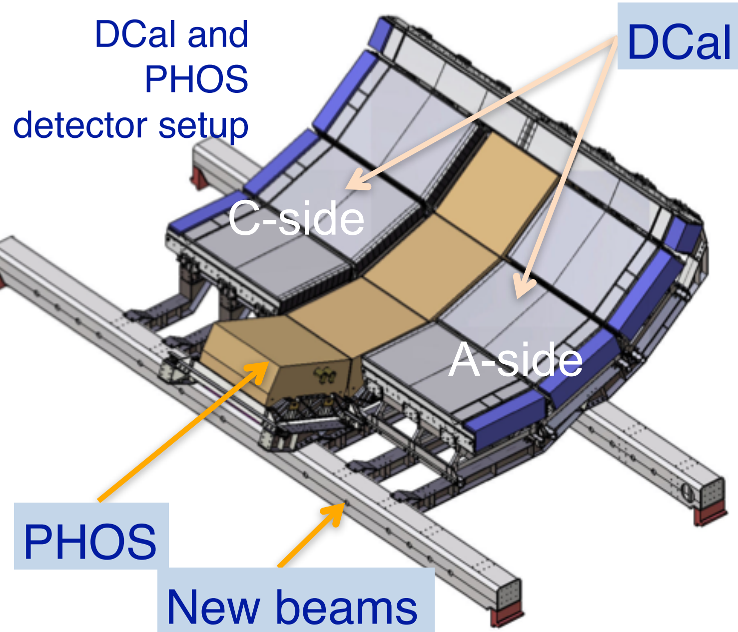

New beams installed
L3 in June

DCal installation

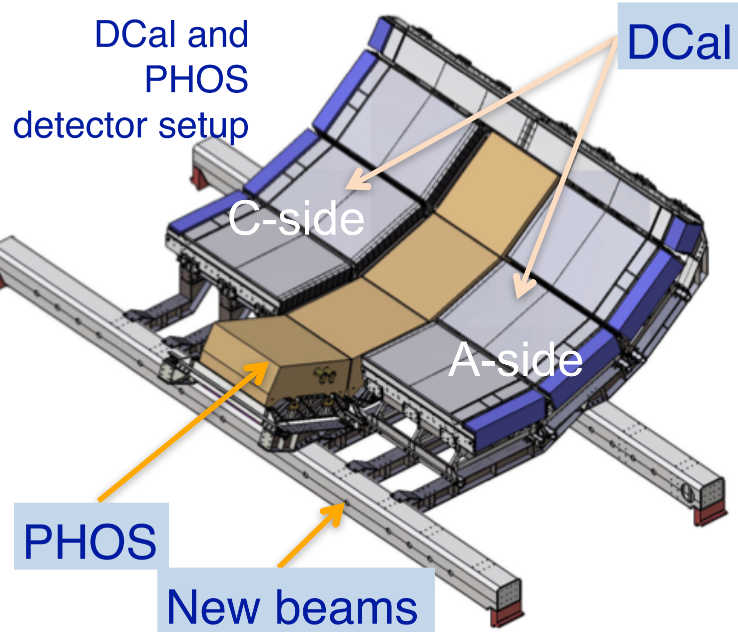

New beams installed L3 in June

C-side DCal SM installation in October

DCal installation

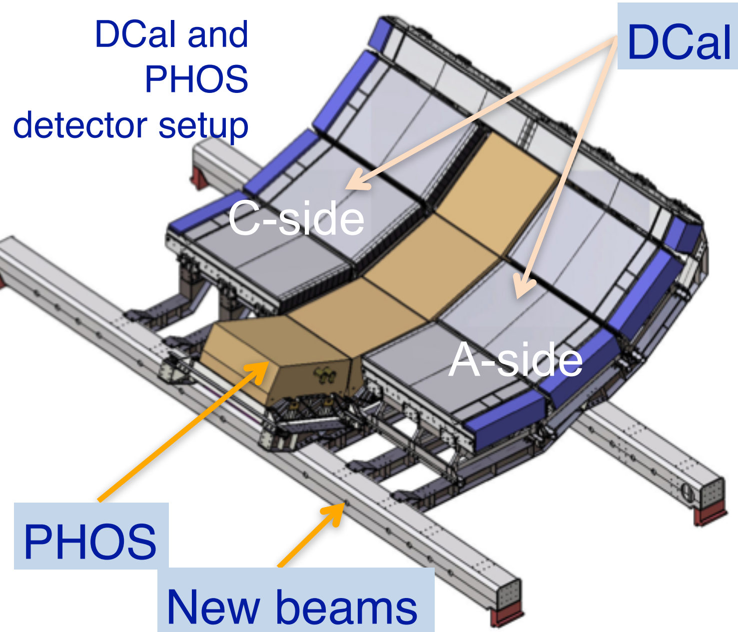

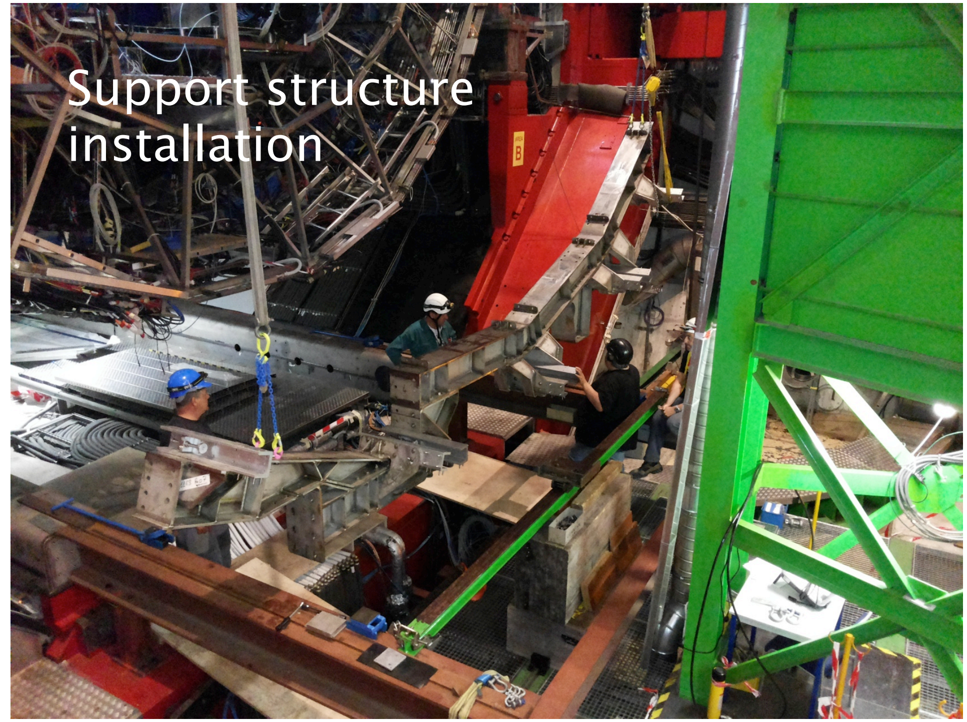

New beams installed L3 in June

C-side DCal SM installation in October

DCal installation

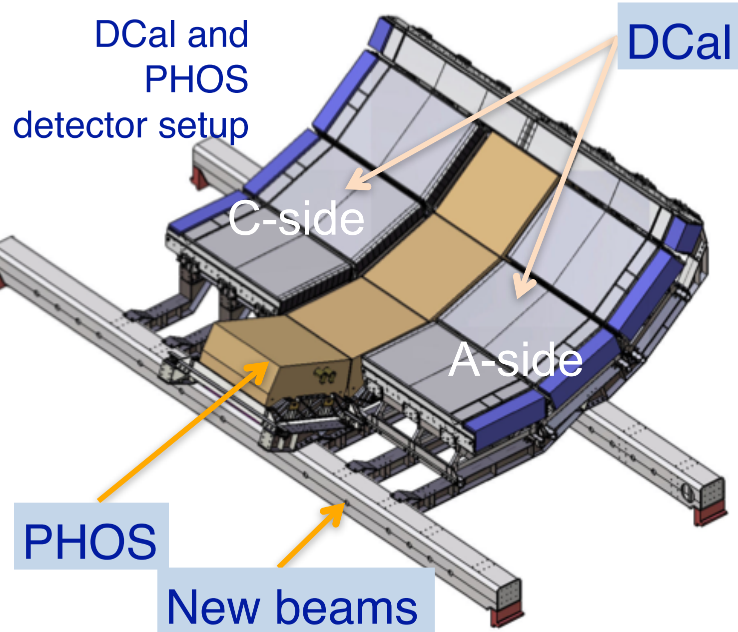

New beams installed L3 in June

C-side DCal SM installation in October

PHOS and A-side DCal installation later next year.

Upgrade

The ALICE upgrade

Detailed characterization of the Quark-Gluon-Plasma

- Measurement of heavy-quark transport parameters:
  - diffusion coefficient (QGP eq. of state, η/s) → R_{AA} and azimuthal anisotropy of HF
- Measurement of low-mass and low-p_T di-electrons:
  - chiral symmetry restoration → ρ spectral function
  - γ production from QGP (temp.) → low mass di-lepton continuum
- J/ψ, ψ', and possibly X_C states down to zero p_T
  - statistical hadronization vs. dissociation/recombination scenario
- Jets
  - Heavy-flavor tagged jets (gluon vs. quark induced jets and charm fragmentation)

The upgrade plan entails

- New, high-resolution, low-material ITS
- Upgrade of TPC with replacement of MWPCs with GEMs and read-out electronics.
- New forward silicon tracker for the muon arm: MFT
- Run ALICE at 50 kHz with O^2 project (currently 500 Hz max)
- Preparations of all other detectors for readout at 50kHz (TRD, TOF, EMCAL, MCH, MTR, ZDC, V0/T0, PHOS) → "ALICE High Rate Detector Upgrade" TDR (Dec. 2013 LHCC)

Target: 2018/19 (2nd long LHC shutdown). ~ 18 months to complete

New Inner Tracking System

See talk by L. Musa in yesterday's LHCC upgrade session for all details.

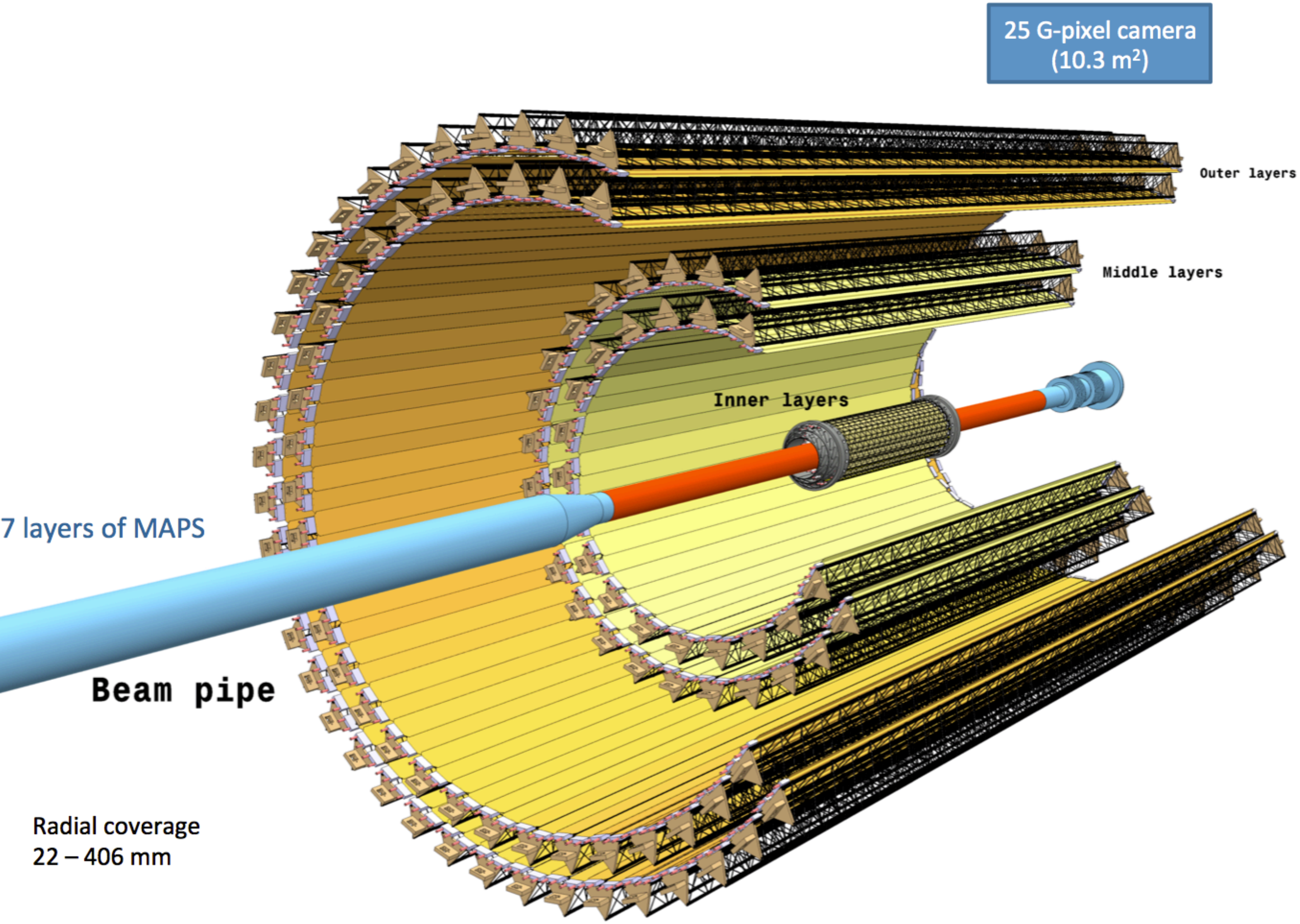

New Inner Tracking System

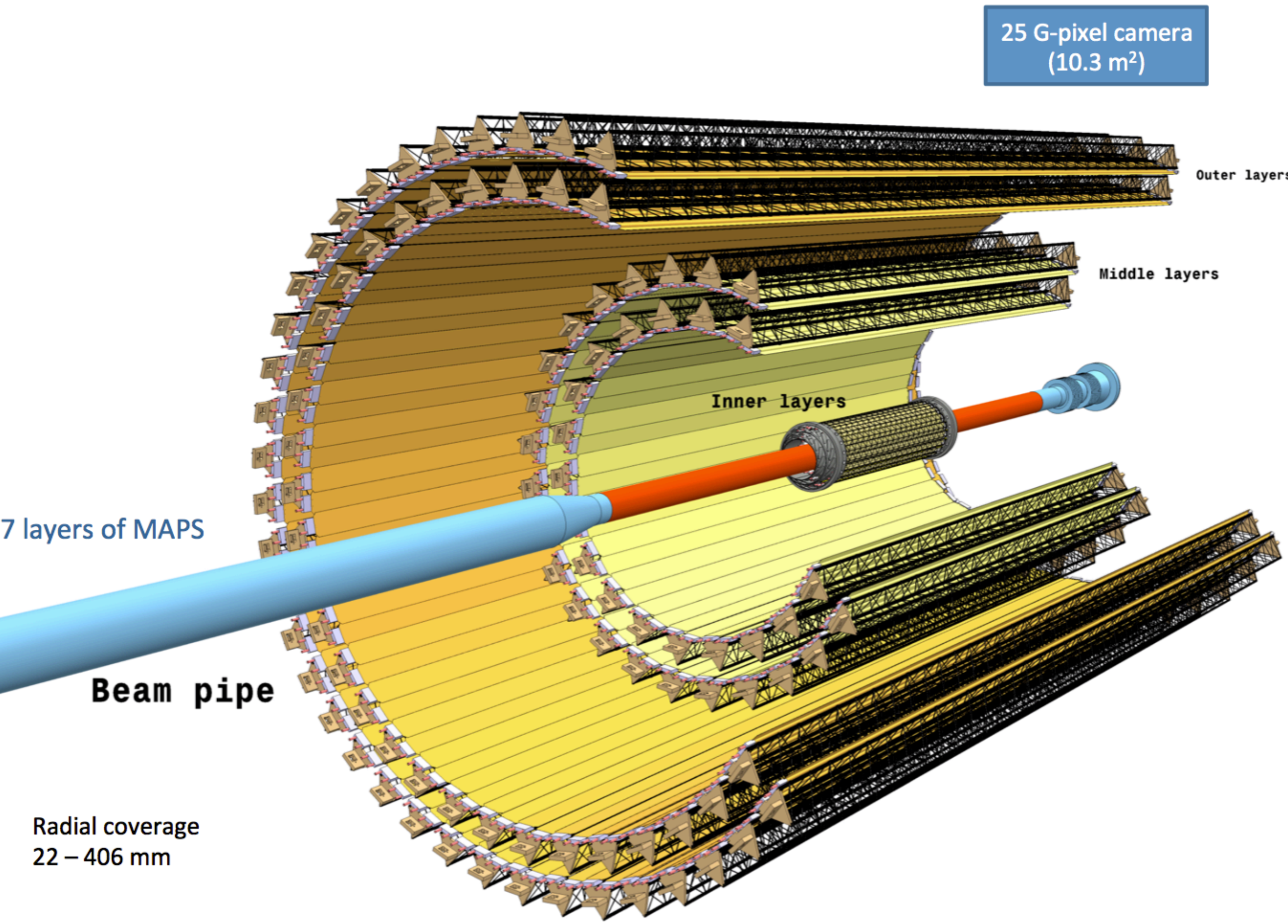

See talk by L. Musa in yesterday's LHCC upgrade session for all details.

Detector overall layout and technologies for main components defined.

New Inner Tracking System

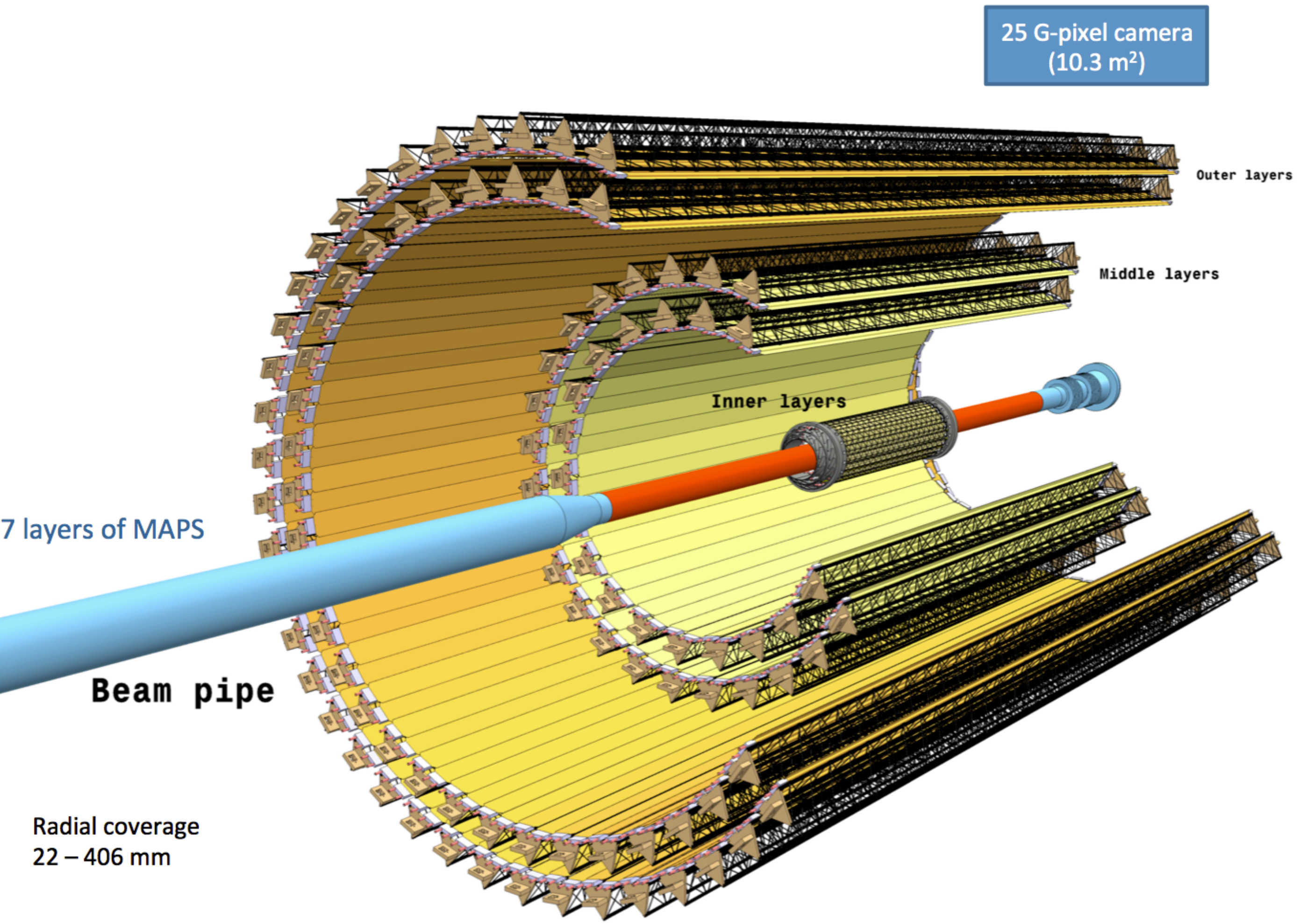

See talk by L. Musa in yesterday's LHCC upgrade session for all details.

Detector overall layout and technologies for main components defined.

Technical feasibility of main components demonstrated.

New Inner Tracking System

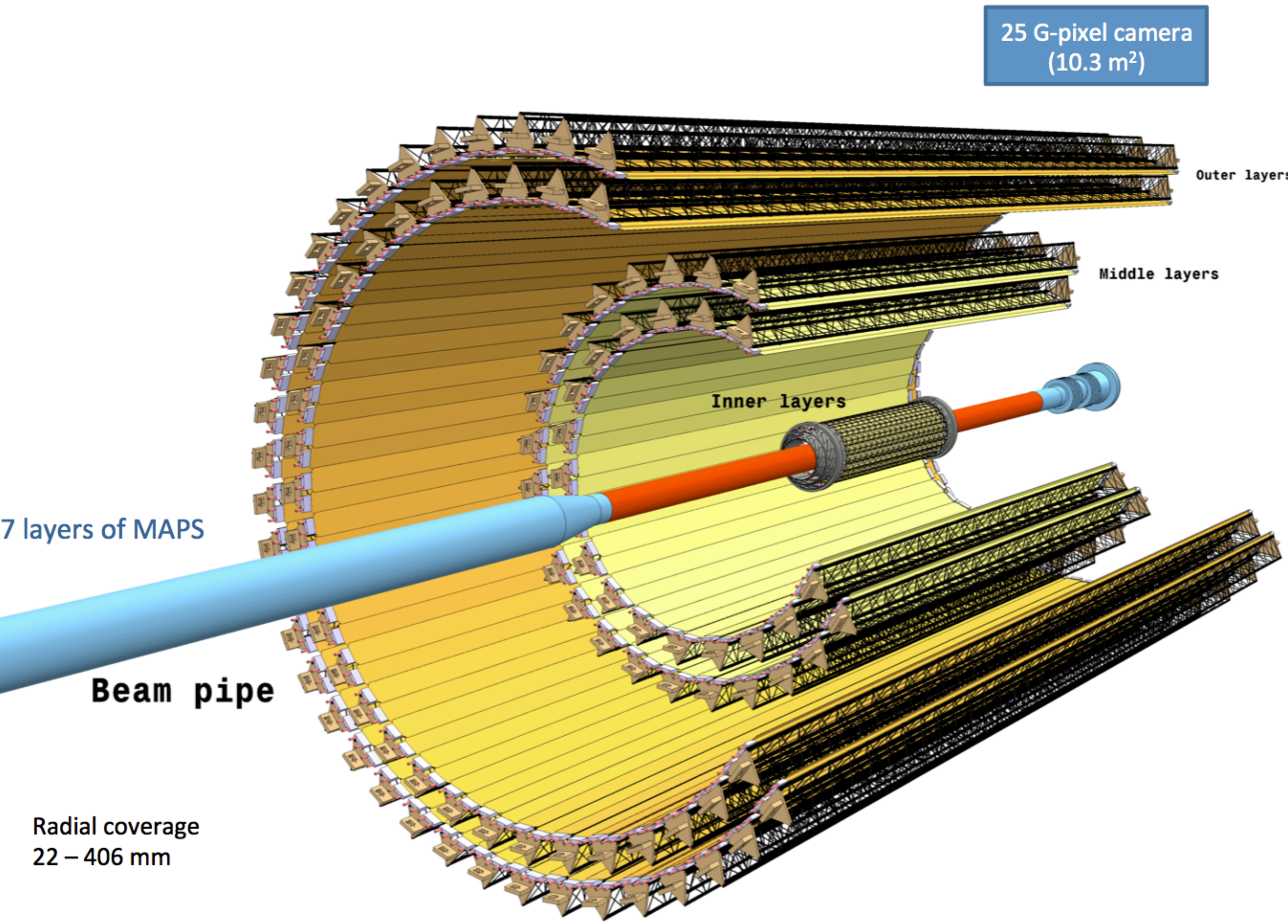

See talk by L. Musa in yesterday's LHCC upgrade session for all details.

Detector overall layout and technologies for main components defined.

Technical feasibility of main components demonstrated.

TDR being finalized and will be submitted to LHCC in about one month.

TPC: Upgrade with GEMs

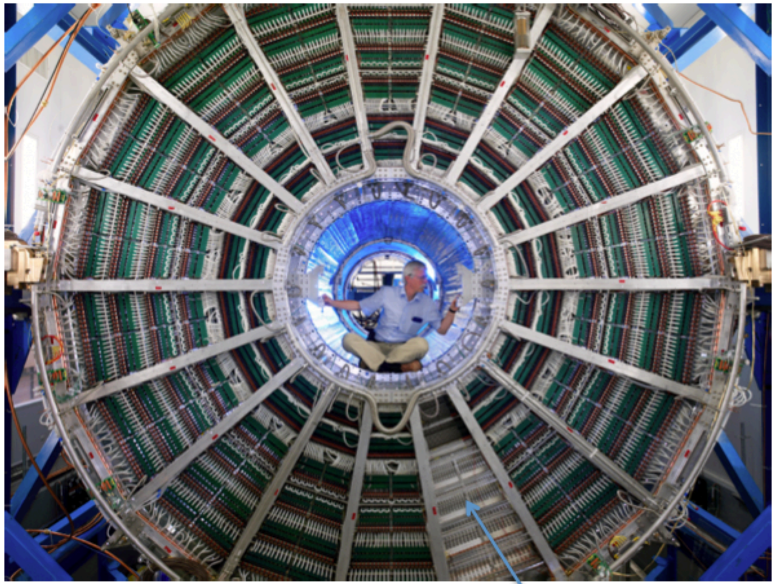

TPC readout at full min. bias rate of 50kHz in Pb-Pb requires a significant upgrade

→ readout chambers
→ frontend electronics
→ online calibration and reconstruction scheme

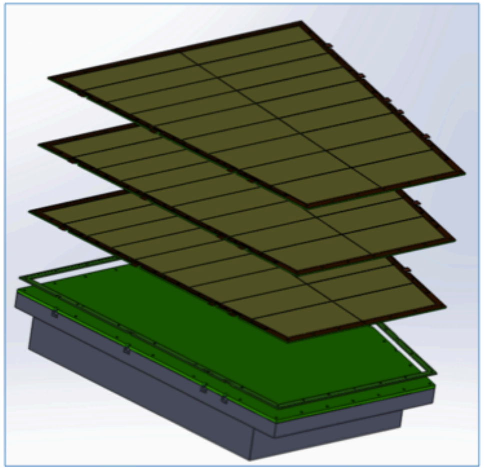

Replace wire chambers with GEMs

TPC: Upgrade with GEMs

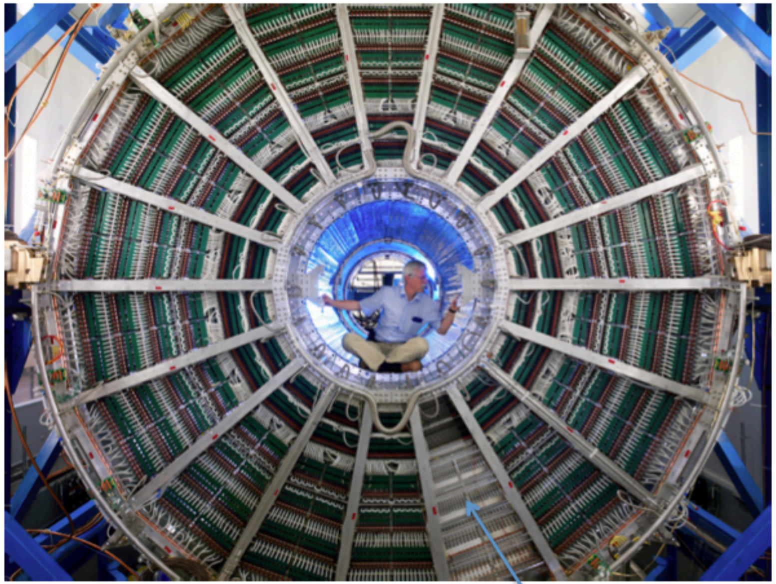

TPC readout at full min. bias rate of 50kHz in Pb-Pb requires a significant upgrade

→ readout chambers
→ frontend electronics
→ online calibration and reconstruction scheme

Replace wire chambers with GEMs

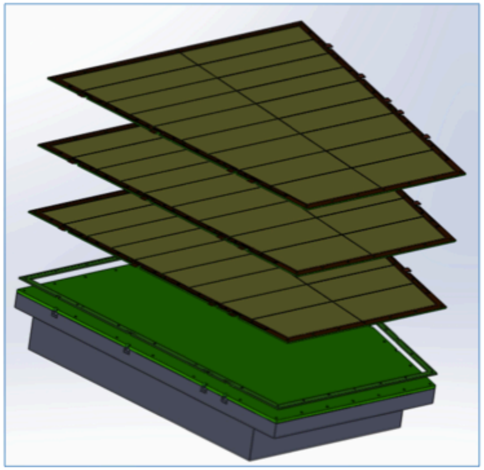

Extensive R&D and simulations ongoing through 2012 and 2013

TPC: Upgrade with GEMs

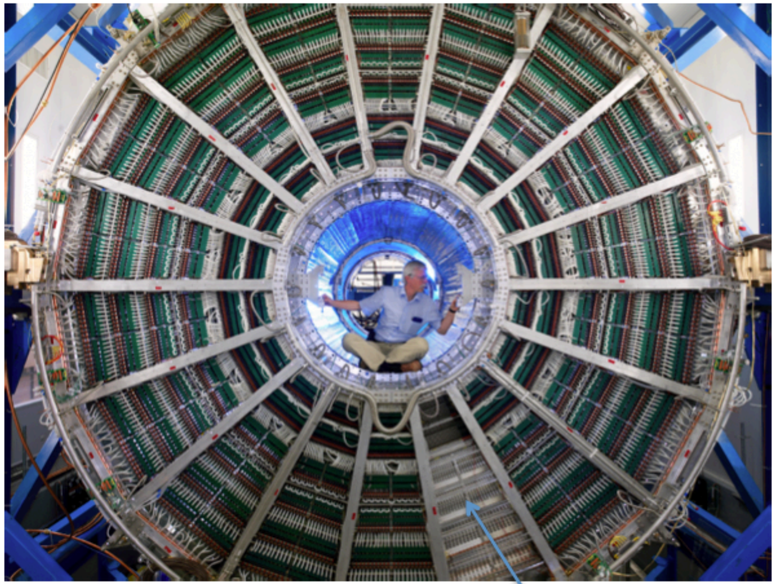

TPC readout at full min. bias rate of 50kHz in Pb-Pb requires a significant upgrade

→ readout chambers
→ frontend electronics
→ online calibration and reconstruction scheme

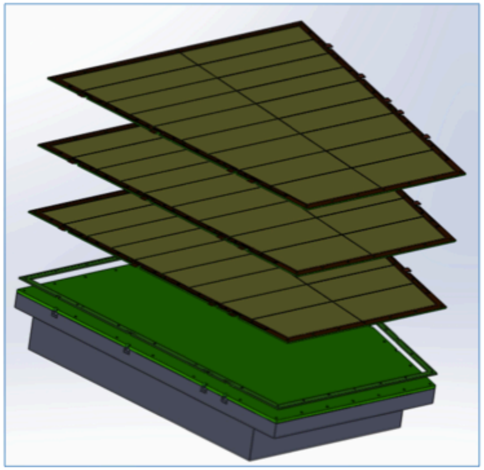

Replace wire chambers with GEMs

Extensive R&D and simulations ongoing through 2012 and 2013

Production schedule: 2014 to 2017

TPC: Upgrade with GEMs

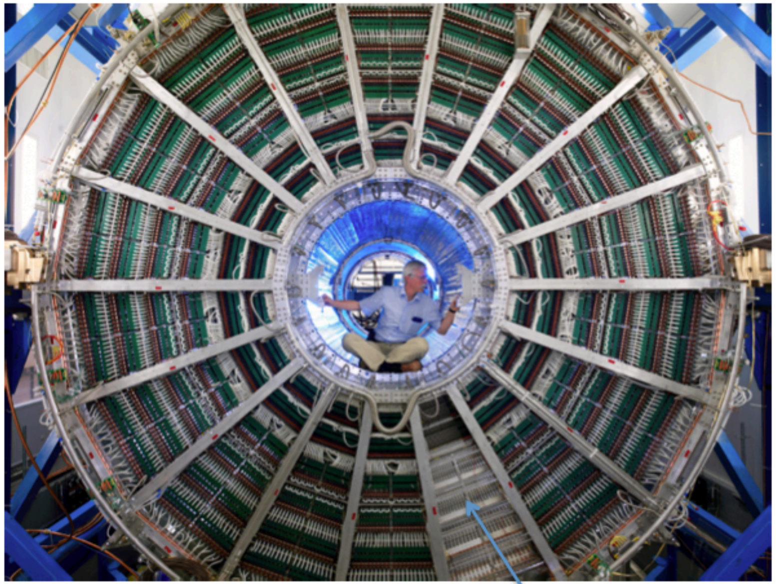

TPC readout at full min. bias rate of 50kHz in Pb-Pb requires a significant upgrade

→ readout chambers
→ frontend electronics
→ online calibration and reconstruction scheme

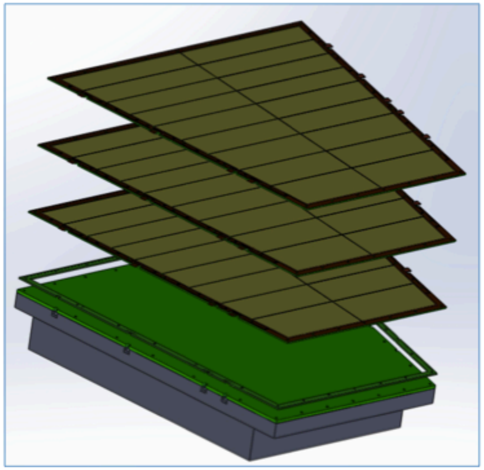

Replace wire chambers with GEMs

Extensive R&D and simulations ongoing through 2012 and 2013

Production schedule: 2014 to 2017

TDR under preparation for submission to LHCC in Dec. 2013

Muon Forward Tracker

- Matching of muon tracks with MFT clusters to improve pointing accuracy (discrimination between prompt and displaced muons) and inv. mass resolution at low masses.

- 5 planes of CMOS silicon pixel sensors covering most of the muon spectrometer acceptance.

- Monolithic Active Pixel Sensors (MAPS) as for new ITS with a pixel pitch as low as 25 μm.

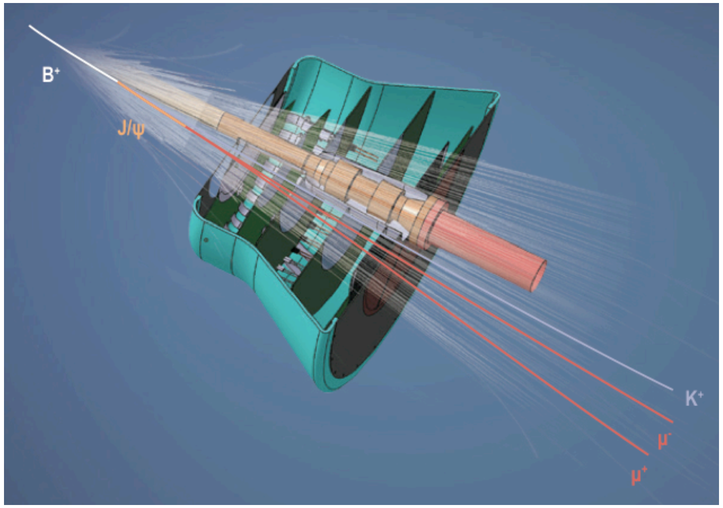

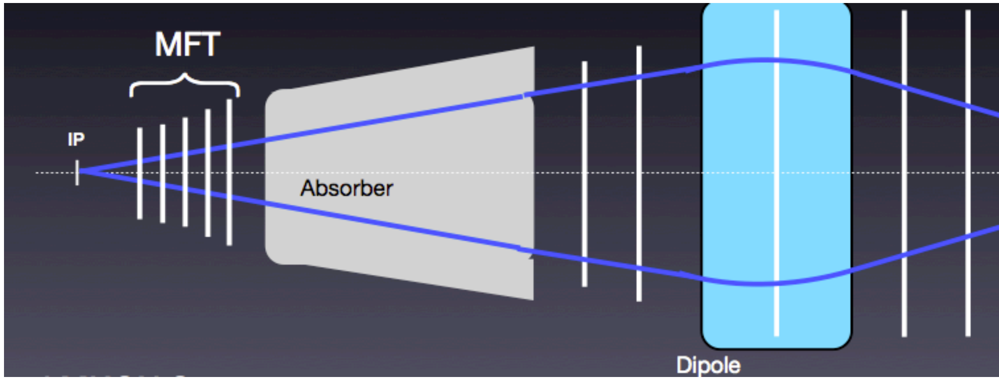

Muon Forward Tracker

- Matching of muon tracks with MFT clusters to improve pointing accuracy (discrimination between prompt and displaced muons) and inv. mass resolution at low masses.
- 5 planes of CMOS silicon pixel sensors covering most of the muon spectrometer acceptance.
- Monolithic Active Pixel Sensors (MAPS) as for new ITS with a pixel pitch as low as 25 μm.

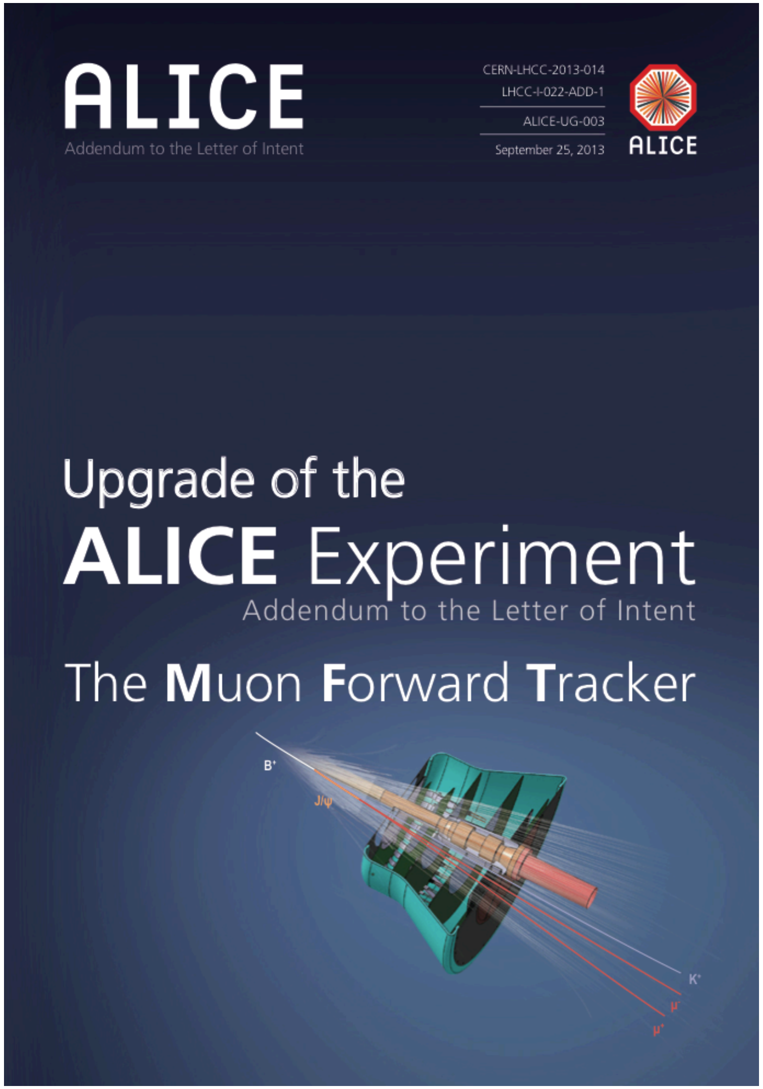

O^2 project

- Teams of HLT, DAQ, and OFFLINE form together the combined O^2 (offline&online) project to record and process Pb-Pb data taking at 50kHz
- Timeline
  - Sep 2012: ALICE Upgrade LoI
  - Jan 2013: Report of DAQ-HLT-OFFLINE software panel on "ALICE software framework for LS2 upgrade"
  - Mar 2013: O2 Computing working groups (CWGs) are set up

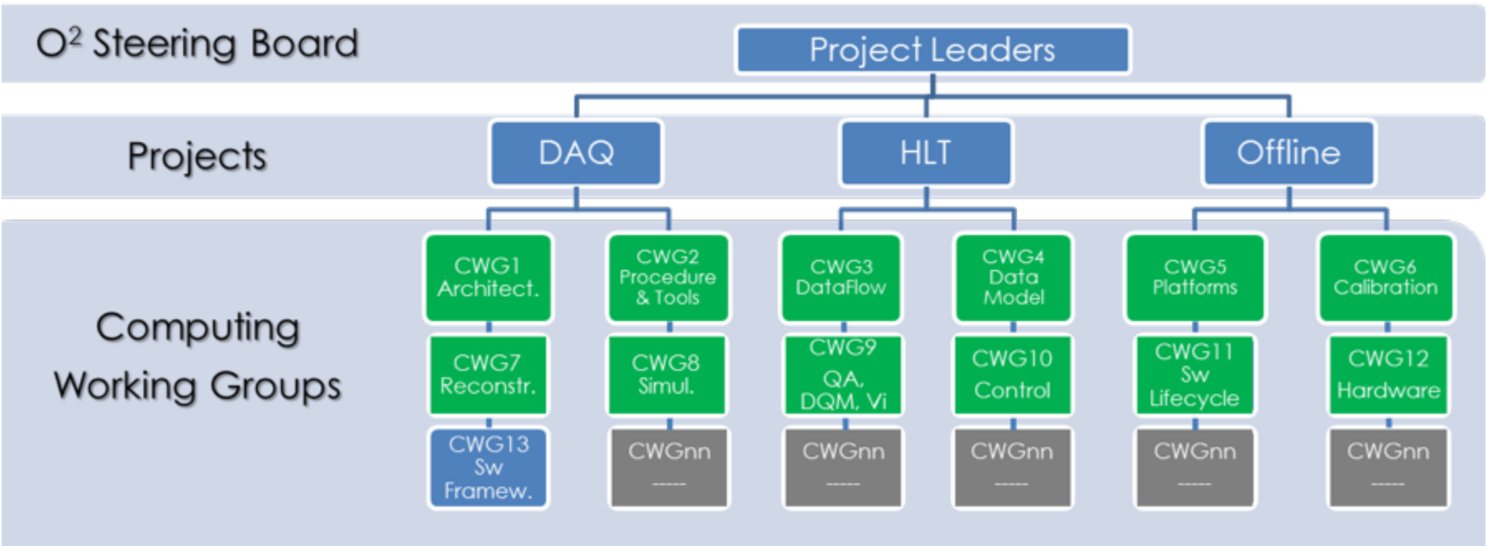

  - Sep 2014: Delivery of O^2 Technical Design Report

Summary and conclusion

Summary and conclusion

- Since the last LHCC: 8 papers were submitted
  → 3 Pb-Pb, 3 p-Pb, 2 pp
- Complete dataset of all collisions systems (pp, p-Pb, Pb-Pb) allows fantastic systematic comparisons within ALICE. Clear separation between initial and final state effects.
- Intriguing phenomena observed in p-Pb collisions. They cannot be explained by an incoherent superposition of nucleon-nucleon collisions. This might hint at collective behavior, but other explanations are also possible.
- Many ongoing activities at Point 2 during LS1 and preparations for the upgrade after LS2.

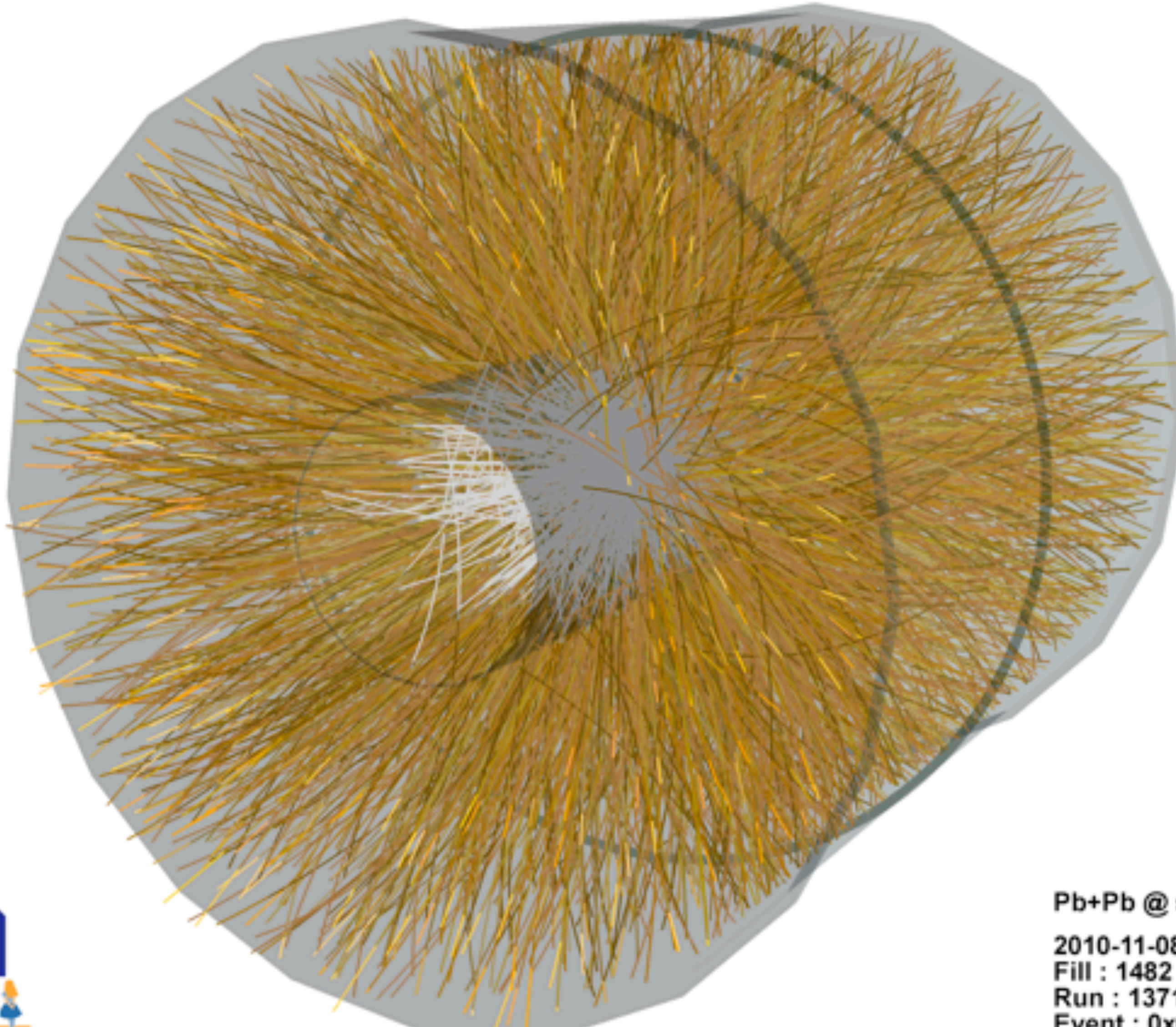

ALICE

Pb+Pb @ sqrt(s) = 2.76 ATeV

2010-11-08 11:30:46
Fill : 1482
Run : 137124
Event : 0x00000000D3BBE693

Supporting slides

J/ψ regeneration and initial state effects

(Re-)generation of J/ψ from deconfined charm quarks in the medium

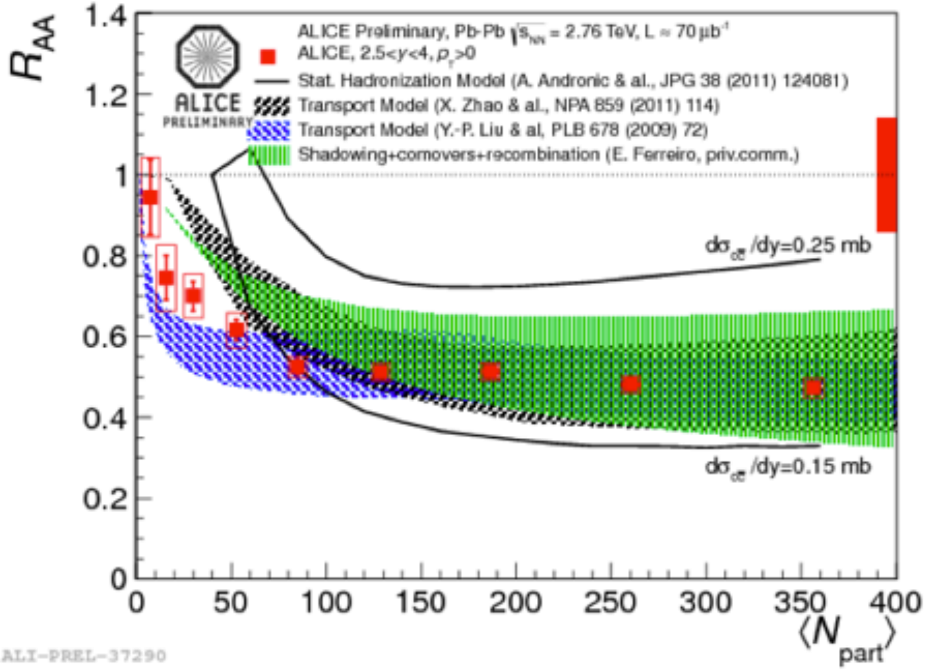

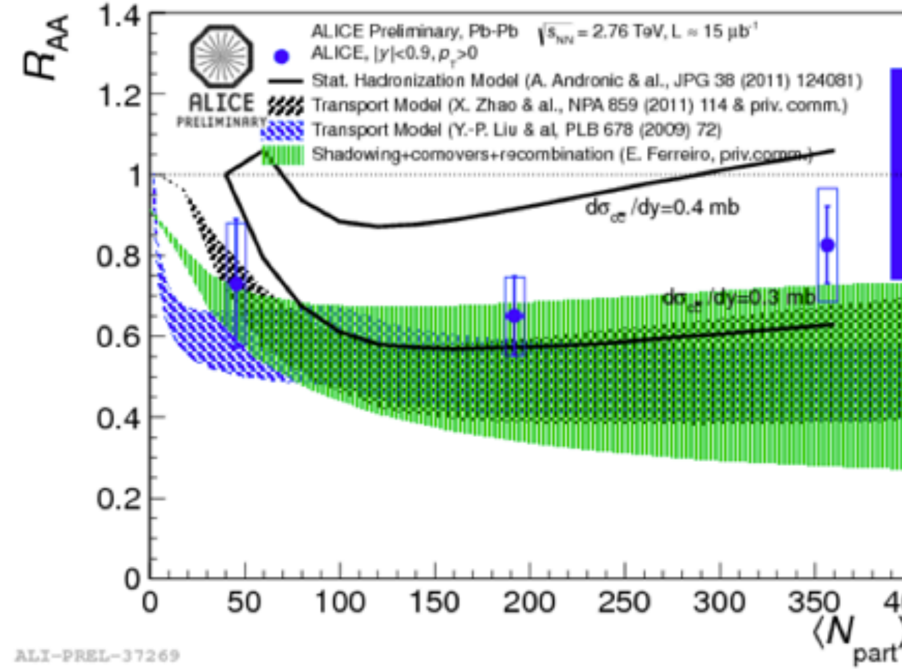

Still missing ingredients to estimate quantitatively the final state effects:

- Cold Nuclear Matter effects: nuclear absorption likely to be negligible
- Shadowing
- Charm production cross section
- Beauty feed-down (order of ~ 10%)

} **p-Pb run!!** (Cold Nuclear Matter effects, Shadowing)

B/M ratio in recombination picture

from: M. Floris

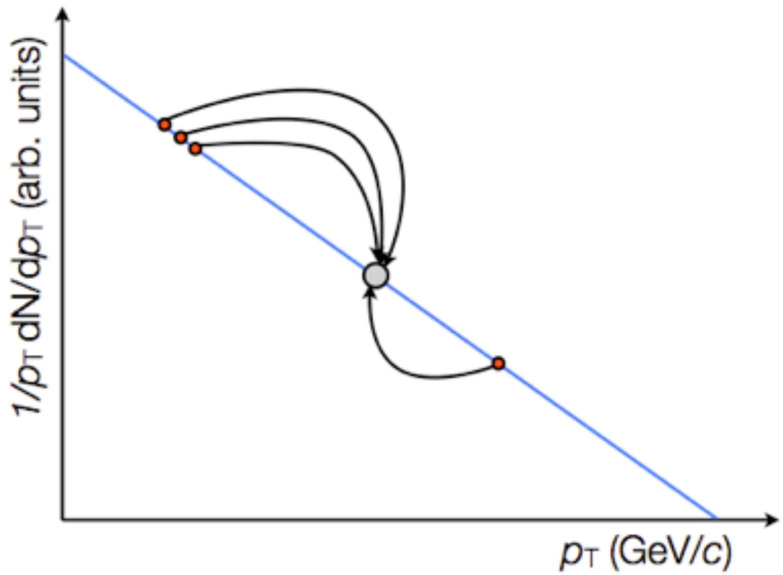

Fragmentation: single parton with $p_T > p_T^{[hadron]}$

Recombination: 2(3) partons with $p_T \sim p_T^{[hadron]}/2(3)$

$\Rightarrow$ enhances B/M

In some models: thermal + minijet recombination

recent review: Greco, Fries, Sorensen, Annu. Rev. Nucl. Part. Sci. 2008.58:177-205.

O² project (some selected highlights)

CWG1 - Architecture

→ Setting up System Requirements Specifications document.

→ Investigation of asynchronous reconstruction.

CWG7 - Reconstruction

→ Concept of calibration/ reconstruction with continuous read-out and expected space-charge distortions demonstrated with a toy model.

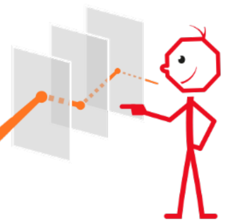

CWG8 - Simulation

→ Integration of NLO generators (ongoing)

→ Revival of barrel tracking parameterisation for fast simulation.

→ Update of FLUKA VMC interface for radiation studies related to ALICE upgrade

CWG12 - Hardware

→ Investigation of the usage of graphic cards.

→ What will be the performance in a few years.

→ GPU memory throughput increasing linearly year-by-year while single precision performance increases in steps.

FB ratio of Quarkonia in p-Pb

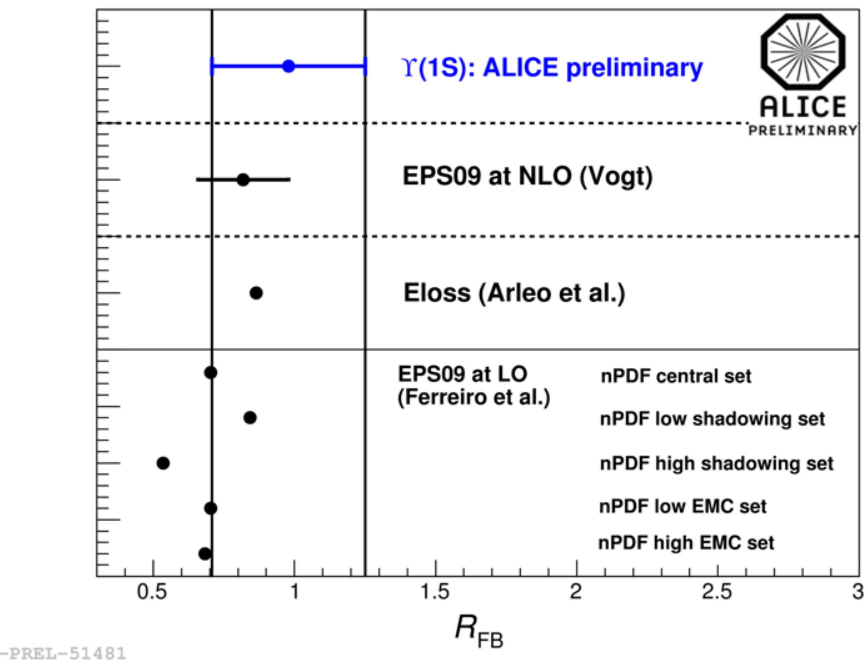

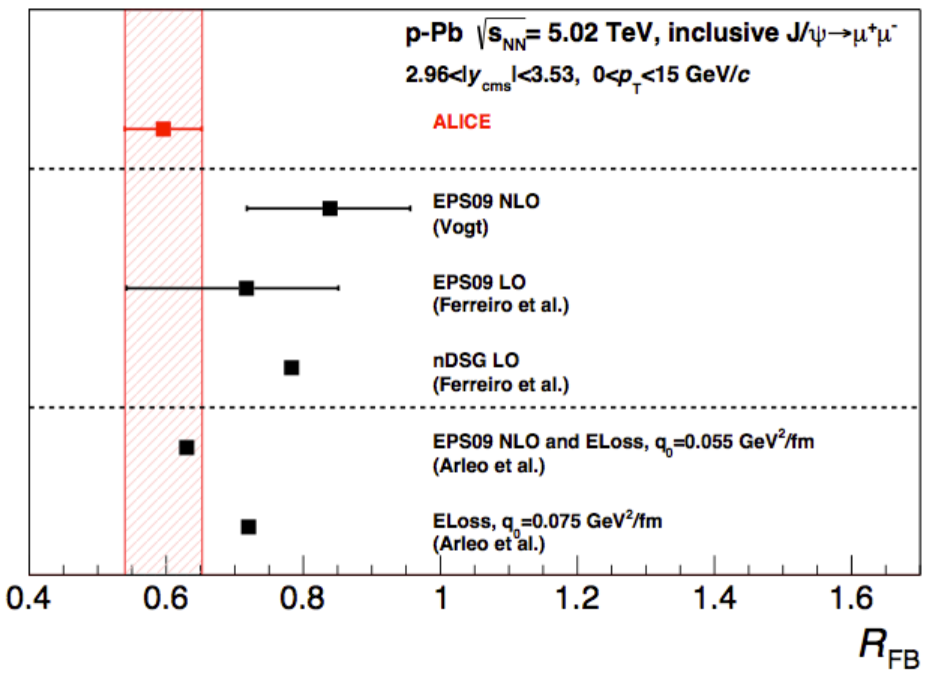

Color reconnection

- Picture from: G. Gustafson, Acta Phys. Polon. **B40**, 1981 (2009).
- See also: A. Ortiz et al. Phys. Rev. Lett. 111, 042001 (2013)

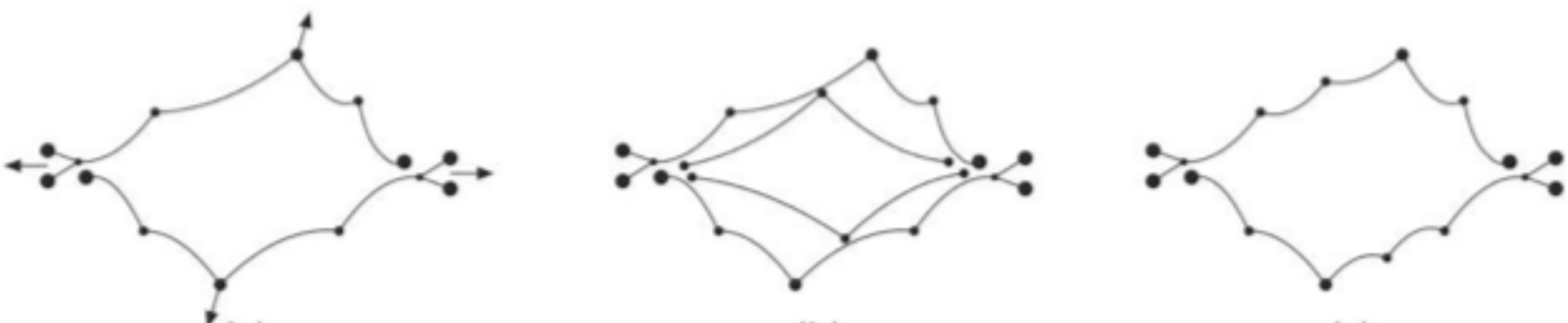

(a) (b) (c)